

**ELECTRICITY GENERATION AS A BENEFICIAL POST CLOSURE LAND  
USE OPTION FOR DORMANT TAILINGS STORAGE FACILITIES**

SJ VAN EEDEN

A dissertation submitted in partial fulfilment of the requirements for the degree of

MASTER OF ENGINEERING (GEOTECHNICAL ENGINEERING)

In the

FACULTY OF ENGINEERING

UNIVERSITY OF PRETORIA

January 2015

## DISSERTATION SUMMARY

# ELECTRICITY GENERATION AS A BENEFICIAL POST CLOSURE LAND USE OPTION FOR DORMANT TAILINGS STORAGE FACILITIES

SJ VAN EEDEN

Supervisor: Professor SW Jacobsz  
Department: Civil Engineering  
University: University of Pretoria  
Degree: Master of Engineering (Geotechnical Engineering)

As a result of the mining that has taken place over the last century in South Africa, many towns and cities have developed around mining hubs, the most significant of these being the city of Johannesburg. Over the years, residential areas have grown around these mine sites, even well after decommissioning of the mining activities. The mining activities left a lasting legacy of derelict mining infrastructure with negative effects on the surrounding environment and community, such as dormant mine shafts, sterilised land and abandoned Tailings Storage Facilities (TSFs). Due to lack of funds, commitment from mine owners and regulators these facilities are often left unrehabilitated, posing negative environmental impacts, including potential health hazards to the surrounding community. This legacy of problems posed by abandoned mines encountered in South Africa is probably unique in scale compared to any country in the world.

A significant problem South Africa currently faces is an electricity shortage, especially during the high demand season from the start of June to end of August, when it is winter in South Africa. This period is occasionally associated with so called controlled “load shedding”, i.e. managed power interruptions to prevent overload and subsequent collapse of the electricity supply and distribution network. South Africa is highly reliant on coal-fired power stations for the majority of electricity consumed, which has detrimental effects on the environment due to high carbon emissions. However, a global shift towards renewable energy, as well as South Africa’s energy

shortage, has forced the National Energy Regulator of South Africa to encourage greener alternatives.

This study is aimed at finding an opportunity to generate more electricity, which is sustainable and with reduced carbon emissions. This study was conducted to determine the financial and practical feasibility of generating energy from the ERGO TSF, near Brakpan Johannesburg, as a post closure land use option. The following options were investigated:

- Solar Photovoltaic electricity generation
- Pump storage scheme development
- A combinations of the above

In addition, rainwater harvesting and wind power generation were also considered, but were abandoned early on in the study.

From the study it was concluded that a Solar PV plant on top of the ERGO TSF will achieve the highest possible IRR of 10.70% and a power generation capacity of 471.9 MWp. Developing a pump storage scheme at the ERGO TSF can achieve an IRR of 10.27% and generation capacity of 78.2 MW. Combining the two options independently on the same site will result in an IRR of 10.61% and a combined peak generation capacity of 550 MW. If the combined system is required to be independent of the surplus electricity available in the grid an IRR of 10.32% and a combined generation capacity of 550 MW is achievable.

From a financial and technical perspective it is considered to be most beneficial to implement *only* the solar PV plant on top of the ERGO TSF. Construction of a pump storage scheme on TSF is considered to be a challenging undertaking and seeing that its generation capacity is only 17% of that of the solar PV facility on the same ERGO site, it is probably not the optimal solution for utilisation. Solar panels are light weight structures that can easily be installed in large numbers on TSFs with little engineering challenges.

**ABSTRACT**

**Title:** Electricity generation as a beneficial post closure land use option for dormant tailings storage facilities

**Author:** SJ van Eeden

**Supervisor:** Professor SW Jacobsz

**Department:** Civil Engineering

**University:** University of Pretoria

**Degree:** Master of Engineering (Geotechnical Engineering)

A global shift towards renewable energy over the last decade has forced the National Energy Regulator of South Africa to pursue greener alternatives. In addition, dormant tailings storage facilities (TSFs) have negative effects on the surrounding environment and communities.

This study is aimed at determining the financial and practical feasibility of generating energy from the ERGO TSF, near Brakpan, Johannesburg, as a post closure land use option. Solar photo voltaic and pump storage scheme options, as well as a combination thereof were investigated.

It was found that a 472 MWp Solar PV plant on top of the ERGO TSF will provide the best solution both from a practical and financial point of view, with an IRR of 10.70% over 50 years. With a pump storage scheme an IRR of 10.27% can be achieved, with a generation capacity of 78.2 MW. A combination of the above might provide the ideal uninterrupted electricity supply solution.

## DECLARATION

I, the undersigned hereby declare that:

I understand what plagiarism is and I am aware of the University's policy in this regard;

The work contained in this dissertation is my own original work;

I did not refer to work of current or previous students, lecture notes, handbooks or any other study material without proper referencing;

Where other people's work has been used this has been properly acknowledged and referenced;

I have not allowed anyone to copy any part of my dissertation;

I have not previously in its entirety or in part submitted this thesis at any university for a degree.

---

SJ van Eeden

Student number 27314759

Date 5 January 2015

## ACKNOWLEDGEMENTS

I wish to express my appreciation to the following organisations and persons who made this dissertation possible:

- a) Dr. Martin Rust for this opportunity and for bestowing his trust in me to make a success of this project.
- b) My supervisor, Professor S.W. Jacobsz for his support, guidance and patience throughout the project and his example of humility.
- c) The Green Fund which provided the funding for this project. The Green Fund is an environmental programme implemented by the Development Bank of Southern Africa (DBSA) on behalf of the Department of Environmental Affairs (DEA). Opinions expressed and conclusions arrived at are those of the author and are not attributed to the Green Fund, DBSA or DEA.
- d) DRDGold Limited, specifically Mr Louis Kleynhans, who kindly provided the background information of the site.
- e) The South African Weather Service for supplying the weather data for the study.
- f) Last but not least, my loving fiancé (editor in chief) for all the encouragement and continuous support throughout.

All the glory to God.

## TABLE OF CONTENTS

		PAGE
<b>1</b>	<b>INTRODUCTION</b>	<b>1-1</b>
1.1	Background	1-1
1.2	Objectives of the study	1-2
1.3	Scope of the study	1-2
1.4	Methodology	1-3
1.5	Organisation of research project report	1-4
<b>2</b>	<b>LITERATURE REVIEW</b>	<b>2-1</b>
2.1	Introduction	2-1
2.2	Legacy of mining	2-1
2.2.1	Closure of mine sites	2-3
2.2.2	Mining process and infrastructure	2-5
2.2.3	Extent of gold mining in South Africa	2-7
2.3	Lack of renewable energy	2-10
2.4	Productive use of dormant TSFS	2-13
2.5	Solar Photo Voltaic power generation	2-15
2.5.1	Brief principles of operation	2-15
2.5.2	Determining the available solar resource	2-20
2.5.3	Factors influencing a solar PV plant's production	2-27
2.5.4	Cost of solar PV	2-27
2.5.5	Examples of solar power plants	2-29
2.5.6	Alternative forms of solar power generation	2-30
2.6	Pump Storage Scheme power generation	2-32
2.6.1	Brief principle of operation	2-32
2.6.2	Determining the available water resource	2-34

2.6.3	Determining the generating capacity and associated electricity production of a pump storage scheme	2-36
2.6.4	Determining the pump capacity required and associated electricity consumption	2-38
2.7	Summary of findings from literature review	2-40
<b>3</b>	<b>FEASIBILITY ANALYSIS OF ELECTRICITY GENERATION OPTIONS ON DORMANT TSFS</b>	<b>3-1</b>
3.1	Introduction	3-1
3.2	Site identification	3-1
3.3	Common factors	3-4
3.3.1	Life of the facility	3-4
3.3.2	Assessment of financial return	3-4
3.3.3	Determining the income with Megaflex tariffs	3-6
3.3.4	Default option	3-7
3.4	Other renewable energy options considered	3-8
3.4.1	Wind power generation at the ERGO site	3-8
3.4.2	Rain water harvesting from the ERGO site	3-9
3.5	Evaluation of Solar Photo Voltaic power generation potential	3-10
3.5.1	Determination of the solar resource at ERGO	3-11
3.5.2	Verification of resource calculations with NASA data	3-12
3.5.3	Determining the size of the solar plant	3-13
3.5.4	Determination of the plant output	3-16
3.5.5	Allocation of construction costs	3-17
3.5.6	Determination of potential income and IRR	3-18
3.5.7	Optimisation of the plant to generate maximum return on investment	3-19
3.5.8	Reliability of daily plant production and associated income	3-19
3.5.9	Sensitivity analysis	3-20
3.6	Evaluation of pump storage scheme development potential	3-20
3.6.1	Determination of the water resource available for power generation	3-20

3.6.2	Determining the flow between the upper and lower reservoirs	3-30
3.6.3	Determining the electricity generation potential and production	3-32
3.6.4	Determining the pump capacity required and associated electricity consumption	3-34
3.6.5	Allocation of construction costs	3-35
3.6.6	Determination of potential income and IRR	3-38
3.6.7	Optimisation of the pump storage scheme system	3-38
3.6.8	Reliability of daily plant production and associated income	3-39
3.6.9	Sensitivity analysis	3-39
3.6.10	Determining the effect of lining the TSF basin	3-41
3.7	Combination of Solar PV and Pump storage scheme options	3-41
3.7.1	Combination 1 - Optimising the release rate of the pump storage scheme in a combined system	3-43
3.7.2	Combination 2 - Financial feasibility of a combined solar PV and pump storage scheme option on the same site	3-43
3.7.3	Combination 3 - Assessing financial feasibility of a combined solar PV and pump storage scheme to be independent of Eskom's surplus electricity supply	3-44
<b>4</b>	<b>RESULTS</b>	<b>4-1</b>
4.1	Solar Photo Voltaic power generation	4-1
4.1.1	Solar resource at ERGO	4-1
4.1.2	Verification of calculated data	4-2
4.1.3	Optimisation of the plant	4-6
4.1.4	Determination of the size of the solar plant	4-8
4.1.5	Daily plant output	4-10
4.1.6	Daily electricity production	4-13
4.1.7	Financial implications	4-15
4.1.8	Reliability analysis	4-17
4.1.9	Sensitivity analysis results	4-20
4.2	pump storage scheme development	4-25

4.2.1	Determination of the water resource available for power generation	4-25
4.2.2	Results of the optimisation of the pump storage scheme system	4-26
4.2.3	Reliability analysis	4-29
4.2.4	Sensitivity analysis results	4-32
4.2.5	Determining the effect of lining the TSF basin	4-40
4.3	Combination of Solar PV and pump storage scheme options	4-43
4.3.1	Combination 1 - Optimising the release rate of the pump storage scheme in a combined system	4-43
4.3.2	Combination 2 - Financial feasibility of a combined solar PV and pump storage scheme option on the same site	4-44
4.3.3	Combination 3 - Assessing financial feasibility of a combined solar PV and pump storage scheme to be independent of Eskom's surplus electricity supply	4-44
<b>5</b>	<b>CONCLUSIONS</b>	<b>5-1</b>
5.1	Solar photo Voltaic power generation	5-1
5.2	Pump storage scheme	5-2
5.3	Combination of Solar PV and pump storage scheme	5-5
5.4	Summary	5-6
<b>6</b>	<b>LIST OF REFERENCES</b>	<b>6-1</b>

## LIST OF TABLES

Table 3-1: Performance and corresponding efficiencies for various panels (Yingli Solar, 2012)	3-18
Table 3-2: Catchment areas and allocated runoff factors (PBA International SA, 2011)	3-25
Table 3-3: Formulas used to calculate cost of electrochemical equipment as a function of generating capacity and head (Saini and Singal, 2008, adapted by Van Vuuren et al., 2011):	3-36
Table 3-4: Formulas used to calculate cost of civil works as a function of generating capacity and head (Saini and Singal, 2008, adapted by Van Vuuren et al. (2011):	3-36
Table 3-5: Percentages making up the operation and maintenance costs as a function the cost of works (Van Vuuren et al. 2011):	3-37
Table 3-6: Summary of combinations investigated	3-45
Table 4-1: Summary of optimal solar plant on top of the ERGO TSF	4-15
Table 4-2: Performance and corresponding efficiencies for various panels (Yingli Solar, 2012)	4-21
Table 4-3: Summary of sensitivity analysis	4-24
Table 4-4: Particulars of a system with a release capacity of 230 000 m <sup>3</sup> /h (63.9 m <sup>3</sup> /s)	4-27
Table 4-5: Comparison of indicative prices by European turbine manufacturers	4-28
Table 4-6: Particulars of a system with a release capacity of 1 400 000 m <sup>3</sup> /h	4-41
Table 4-7: Summary of results for combinations investigated	4-45
Table A-1: Weather data (SAWS, 2014)	6-2

## LIST OF FIGURES

Figure 2-1: Extent of mining activity across the city of Johannesburg (Google Earth copyright acknowledged)	2-8
Figure 2-2: Extent of mining activity in the Welkom area (Google Earth copyright acknowledged)	2-8
Figure 2-3: Extent of mining activity in the Orkney area (Google Earth copyright acknowledged)	2-9
Figure 2-4: Scale of TSFs relative to a national sports stadium and close proximity of these structures to residential areas (Google Earth copyright acknowledged)	2-9
Figure 2-5: Variation in electricity demand in South Africa (Dames, 2014)	2-11
Figure 2-6: Composition of a solar cell (Zweibel, 1990)	2-20
Figure 2-7: Illustration of the earth revolving around the sun (adapted from Masters (2004) for Southern Hemisphere conditions)	2-23
Figure 2-8: Illustration of altitude and azimuth angles of the sun (adapted from Masters (2004) for Southern Hemisphere)	2-23

Figure 2-9: An example of a sun path diagram for a site in the Northern Hemisphere with a latitude angle of 40° (Masters, 2004)	2-24
Figure 2-10: Combination of insolation striking a surface (Masters, 2004)	2-25
Figure 2-11: An example of a 10 MW CSP in USA (Image courtesy of NREL)	2-31
Figure 2-12: Graph plotting efficiency of three different types of turbines against flow rates	2-38
Figure 2-13: Graph plotting efficiency of pumps against specific speed for various flow rates (Jones et.al, 2008).	2-39
Figure 3-1 Location of ERGO relative to some of the large suburbs in Johannesburg	3-2
Figure 3-2: Lidar photograph of the current 800 ha ERGO footprint	3-3
Figure 3-3: AutoCAD drawing of the planned extension to 1 500 ha footprint	3-3
Figure 3-4: Megaflex tariffs (Eskom, 2014f)	3-7
Figure 3-5: Region for which the NASA solar data is applicable	3-13
Figure 3-6: Placement of panels in arrays	3-14
Figure 3-7: Determination of the spacing of arrays	3-15
Figure 3-8: Layout of a block of arrays	3-15
Figure 3-9: Illustration of pump storage scheme configuration on a TSF	3-22
Figure 3-10: Water balance diagram for a pump storage scheme at the ERGO TSF	3-22
Figure 3-11: Illustration of envisaged TSF catchment area at closure	3-26
Figure 3-12: Typical distorted cross-section of a TSF (Chamber of Mines of South Africa, 1996)	3-27
Figure 3-13: Example of the variation of permeability with distance down the beach of a <i>diamond</i> TSF (Chamber of Mines of South Africa, 1996)	3-27
Figure 4-1: Sun path diagram for the ERGO TSF	4-3
Figure 4-2: Illustration of the shadow line	4-4
Figure 4-3: Comparison of calculated and recorded average daily solar radiation on a horizontal surface	4-5
Figure 4-4: Optimisation of the array azimuth angle	4-7
Figure 4-5: Optimisation of the array tilt angle	4-7
Figure 4-6: Illustration of incidence angles of the sun and direction of the solar array	4-8
Figure 4-7: Spacing of arrays	4-9
Figure 4-8: Layout of blocks	4-9
Figure 4-9: Sun path diagram for the ERGO site	4-11
Figure 4-10: The sun's daily clear sky radiation at different times of day	4-11
Figure 4-11: Variation of output of a single solar panel during the day (dimensions 990 mm x 1650 mm, 15% efficiency)	4-12
Figure 4-12: Output of the plant at various times of day	4-12
Figure 4-13: Comparison of daily solar radiation on a horizontal surface and the amount converted to electricity by a tilted panel	4-13

Figure 4-14: Daily electricity production over a calendar year	4-14
Figure 4-15: Degradation of plant performance over the operational life of the plant	4-14
Figure 4-16: Increase of cumulative plant production over the life of plant	4-16
Figure 4-17: Increase in annual and cumulative income over the life of the plant	4-16
Figure 4-18: Progressive increase in IRR over life of the plant	4-17
Figure 4-19: Reliability of daily electricity generation and associated income	4-19
Figure 4-20: Distribution of daily production	4-19
Figure 4-21: Distribution of daily income	4-20
Figure 4-22: Sensitivity of the IRR and total plant production to change in efficiency	4-21
Figure 4-23: Sensitivity of the IRR and total plant production to change in degradation rate	4-22
Figure 4-24: Sensitivity of the IRR and total plant production to change in degradation rate	4-23
Figure 4-25: Sensitivity of the IRR and total plant production to change in available area	4-24
Figure 4-26: Volume of water in the TSF pond available for power generation	4-25
Figure 4-27: Profit and IRR for various release rates	4-28
Figure 4-28: Profit and IRR for various release rates (plotted on a log scale)	4-29
Figure 4-29: Reliability of daily electricity generation and associated daily operational profit	4-31
Figure 4-30: Distribution of daily electricity production during the peak hours of week days	4-31
Figure 4-31: Distribution of daily operational profit on week days	4-32
Figure 4-32: Sensitivity of the IRR and overall efficiency to a change in catchment area contributing to rainfall runoff	4-33
Figure 4-33: Sensitivity of the IRR and overall efficiency to a change in flow velocity during release	4-34
Figure 4-34: Sensitivity of the IRR and overall efficiency to a change in final height of the facility	4-35
Figure 4-35: Sensitivity of the IRR and overall efficiency to a change in turbine efficiency	4-36
Figure 4-36: Sensitivity of the IRR and overall efficiency to a change in pump efficiency	4-37
Figure 4-37: Sensitivity of the IRR and overall efficiency to a change in Eskom peak/off-peak tariff differential	4-38
Figure 4-38: Sensitivity of the IRR to change in high demand season release rate	4-39
Figure 4-39: Volume of water in the lined TSF pond available for power generation	4-41
Figure 4-40: Profit and IRR for various release rates when the TSF basin is lined	4-42
Figure 4-41: Profit and IRR for various release rates when the TSF basin is lined (plotted on a log scale)	4-42
Figure A-6-1: Locations of the respective weather stations relative to the ERGO TSF (Google Earth Copyright Acknowledged)	6-3

**NOMENCLATURE****General**

DMR	Department of Mineral Resources
DRD	Durban Roodepoort Deep Gold Limited
DWS	Department of Water and Sanitation
EMM	Ekurhuleni Metropolitan Municipality
FAT	Fraser Alexander Tailings Pty Ltd
FWA	Fritz Wagener and Associates
GWh	Gigawatt-hour
IRR	Internal Rate of Return
kWh	Kilowatt-hour
LHWP	Lesotho Highlands Water Project
MAE	Mean annual evaporation
MAP	Mean annual precipitation
MWh	Megawatt-hour
NERSA	National Energy Regulator of South Africa
NPV	Net present value
NREL	National Renewable Energy Laboratory
PV	Photo voltaic
SAGNA	South African Government News Agency
SAWS	South African Weather Service
TSF	Tailings Storage Facility
TWh	Terawatt-hour

**Solar Photo Voltaic**

$m$	Air mass ratio
$\beta$	Altitude angle
$\Phi_c$	Azimuth angle of the collector
$\Phi_s$	Azimuth angle of the sun
$n$	Day number of the year
$I_{DC}$	Diffused radiation on collector surface
$I_B$	Direct beam radiation
$I_{BC}$	Direct beam radiation on collector surface
$CCF$	Cloud cover factor
$\eta_{SP}$	Efficiency of Solar Panel
$A$	Extraterrestrial flux
$H$	Hour angle
$\theta$	Incidence angle
$L$	Latitude of site
kWp	Kilowatt-peak
$k$	Optical depth
$C$	Sky diffuse factor
$\delta$	Solar declination
$SP$	Sun's potential
STC	Standard test conditions
$\Sigma$	Tilt angle of collector surface

**Pump storage scheme**

$\rho$	Density of the fluid to be released through a turbine or pumped
$\mu$	Dynamic viscosity of the fluid being released or pumped
$E_P$	Electricity consumed by pumping by a turbine
$E_T$	Electricity generated by a turbine
$Q_T$	Flow rate of water through the turbine
$Q_P$	Flow rate at which water is pumped
$v_T$	Flow velocity in outlet pipe during release of water
$h_f$	Friction losses in the outlet pipe
$g$	Gravitational acceleration, assumed to be $9.81\text{m/s}^2$
$k_s$	Internal roughness of outlet pipe
$t_T$	Time duration of water release
$t_P$	Time duration of pumping
$h_L$	Local losses in the outlet pipe.
$H_T$	Net head of the water upstream of the turbine
$H_P$	Net head that has to be overcome to pump the water to the upper reservoir
$D$	Outlet pipe diameter
$L$	Outlet pipe length
$\lambda$	Outlet pipe friction factor
$P_T$	Power of a turbine
$P_P$	Power of a pump
$\eta_P$	Pump efficiency
$Re$	Reynolds' number
$H_S$	Total static head

$\eta_T$	Turbine efficiency
$V_P$	Volume of water pumped
$V_T$	Volume of water released

# 1 INTRODUCTION

This chapter provides an introduction to the research study, the background of the research and the research methodology.

## 1.1 BACKGROUND

As a result of the mining that has taken place over the last century in South Africa, many towns and cities have developed around mining hubs, the most significant of these being the city of Johannesburg. Over the years, residential areas have grown around these mine sites, even well after decommissioning of the mining activities. The mining activities left a lasting legacy of derelict mining infrastructure with negative effects on the surrounding environment and community, such as dormant mine shafts, sterilised land and abandoned Tailings Storage Facilities (TSFs). Due to lack of funds, commitment from mine owners and regulators these facilities are often left unrehabilitated, posing negative environmental impacts, including potential health hazards to the surrounding community. This legacy of problems posed by abandoned mines encountered in South Africa is probably unique in scale compared to any country in the world.

A significant problem South Africa currently faces is an electricity shortage, especially during the high demand season, from the start of June to end of August, when it is winter in South Africa. This period is occasionally associated with so called controlled “load shedding”, i.e. managed power interruptions to prevent overload and subsequent collapse of the electricity supply and distribution network. South Africa is highly reliant on coal-fired power stations for the majority of electricity consumed, which has detrimental effects on the environment due to high carbon emissions. However, a global shift towards renewable energy, as well as South Africa’s energy shortage, has forced the National Energy Regulator of South Africa (NERSA) to encourage greener alternatives.

This study is aimed at finding an opportunity to generate electricity, which is sustainable and with reduced carbon emissions. A desktop study was conducted to determine the financial and practical feasibility of generating electricity from dormant TSFs as a beneficial post closure land use option. The following options were investigated:

- Solar Photovoltaic electricity generation
- Pump storage scheme development
- A combination of the above

In addition, rainwater harvesting and wind power generation were also considered as potential post closure land use options, but were abandoned early on in the study.

The aim of this research was to find methods to alleviate the negative environmental legacy posed by historical TSFs, whilst providing additional electricity. It is believed that this research can make a valuable contribution towards a greener future for cities with significant mining legacy problems in South Africa.

## **1.2 OBJECTIVES OF THE STUDY**

The main objective of this study is to find an optimal use of the available TSF land area, which is currently underutilised. Some of the other objectives that are aimed to be achieved include:

- To find a post closure land use option, which can generate sufficient income to offset the closure cost, in order to:
  - Transform these mining infrastructure liabilities into sustainable resources.
  - Present a land use for the facilities that could benefit nearby cities and surrounding residents.
  - Contribute to the establishment of greener cities.
- To achieve the highest possible return on investment in order to attract investors to the project.
- To supplement the supply of electricity, by constructing the largest possible electricity generating capacity on the available space (only if the return on investment is not influenced by the capacity).

## **1.3 SCOPE OF THE STUDY**

This study investigates beneficial post closure land use options for dormant gold tailings storage facilities commonly found in mining areas in South Africa. Two post closure options are investigated, i.e. the generation of electricity using solar photo voltaic panels placed on the TSF or by means of converting the TSF to a pump storage scheme. A combination of the two systems was also investigated. Two other options, i.e. rain water harvesting and wind power generation were also investigated but abandoned at an early stage.

The study aimed to define the respective electricity generation systems in such detail to allow a preliminary construction cost to be estimated. This, in combination with the expected income to

be generated from the sale of electricity over the life of the facility, was used to assess the financial feasibility in terms of an internal rate of return (IRR) for the system.

The following did *not* form part of the scope of the study and were specifically excluded:

- Assessment of the electricity grid infrastructure at the identified site.
- Other renewable energy options, such as biogas, concentrated solar arrays etc.
- Chemical analysis to determine whether the chemicals in the tailings will have any effect on the proposed structures.
- Geotechnical stability of the TSF on which the study is based.
- Design of any components mentioned in the study.

This study was limited to only one site. Feasibility of one site does *not* imply feasibility of all sites.

## 1.4 METHODOLOGY

The following methodology was followed during the execution of this study:

1. Literature review aimed at describing the mining legacy in South Africa and define the potential green electricity generation options, including solar Photo Voltaic (PV) technology and small scale hydro electrical power generation.
2. Identification of a suitable TSF to base the study on.
3. Feasibility analysis of solar PV electricity generation as a potential post closure land use option, including:
  - a. Quantifying the solar resource available for power generation at the identified site.
  - b. Determining the optimal layout and orientation of the solar plant.
  - c. Quantifying the maximum output capacity and associated income.
  - d. Quantifying construction costs.
  - e. Determining and assessing the return of investment.
4. Feasibility analysis of a pump storage scheme to store energy and generate electricity generation as a potential post closure land use option, including:
  - a. Quantifying the water resource available for power generation at the identified site.
  - b. Determining the optimal release rate of the pump storage scheme.
  - c. Quantifying the maximum output capacity and associated income.
  - d. Quantifying construction costs.

- e. Determining and assessing the return of investment.
5. Feasibility analysis of combining the solar and pump storage scheme options.

## **1.5 ORGANISATION OF RESEARCH PROJECT REPORT**

This research report is organised as follows:

- Chapter 1 provides an introduction to the research report.
- Chapter 2 contains a literature review of the knowledge available in the field of study.
- Chapter 3 describes the feasibility analysis conducted to assess the various energy options.
- Chapter 4 provides a discussion of the results.
- Chapter 5 provides the conclusion and recommendations for further work based on the outcomes of the study.

## **2 LITERATURE REVIEW**

This section provides a review of the literature available on the topics relevant to this study. The literature study provides background information on the study. The general topics covered in this literature review include:

- The legacy of mining in South Africa
- The lack of renewable energy in South Africa
- Productive use of dormant mine sites to generate energy
- The principles of solar photo voltaic power generation
- The principles of pump storage scheme power generation

### **2.1 INTRODUCTION**

This research project investigates the feasibility of generating alternative energy from dormant mine sites as a post closure land use option. In this literature review the two pertinent challenges mentioned below are discussed, namely:

- The lasting negative effect of mining activities and associated abandoned infrastructure on the surrounding environment and community.
- The global problem of the lack of renewable green energy resources.

Later in this literature review more in-depth technical information is provided for the potential post closure land use options that were investigated during the study.

The project covers a wide range of topics and although it was attempted to cover each of the topics in detail, the literature review is not exhaustive.

### **2.2 LEGACY OF MINING**

South Africa is a world leader in the mining sector, that has earned its fame for its abundance of mineral resources, with an estimated worth of R20.3 trillion. South Africa is estimated to have the world's fifth largest mining sector in the world, based on its Gross Domestic Product (GDP) (Kearney, 2012).

Since the discovery of gold in 1886, on a farm in the Highveld, 47 352 tonnes of gold (or 31.4% of the world's overall gold production) has been produced from the Witwatersrand basin up until 2002.

Although gold mining has been taking place for more than a century, gold and diamond mining still remains the corner stone of the South African economy today, as there is still an estimated 36 500 tonnes of gold available in the South African reserves (Handley, 2004, Winde et al., 2010). South Africa's gold exports account for a third of the world's gold exports and South Africa's diamond mining industry is reckoned to be the fourth largest in the world. According to the Chamber of Mines of South Africa, mining contributes 18% of South Africa's annual GDP (Kearney, 2012).

With such vast resources and wealth comes vast responsibility, more specifically, environmental responsibility towards the surrounding environment and community. In an age where great emphasis is being placed on all industries to become more environmentally conscious, mines in South Africa have a massive challenge to undo the negative legacy from the past. The environmental laws and regulations are becoming increasingly stringent.

Many residential areas, towns and cities across South Africa have developed around mining hubs, during and after decommissioning of the mining activities, the most significant of these being the city of Johannesburg (Van Eeden et al., 2014). Unfortunately, these mining activities leave a lasting legacy of mining infrastructure with negative effects on the surrounding environment and community such as dormant mine shafts, sterilised land and abandoned Tailings Storage Facilities (TSFs).

Over the last century, mines relied heavily on imported (migrant) labour. Although some of these people were housed in the hostels located on the mines, many of the labourers flocking to the mines for work had to settle in the local townships, like Mohlakeng, Toekomsrus, Bekkersdal and others. Unfortunately, this urban sprawl did not end when the mining activities ceased and therefore these suburbs are encroaching onto hazardous abandoned mine sites. In some cases this entails building informal housing ("shacks") directly onto the existing tailings facilities (Winde et al., 2010).

With the amount of mining that has taken place in South Africa over the last century, these legacy problems are unique in scale compared to any country in the world, making this a very relevant problem in South Africa.

This infrastructure presents a continuous negative impact on the surrounding communities in terms of:

- Air pollution (Van Wyk et al., 2014),
- Groundwater contamination in the form of Acid Mine Drainage (DWA, 2012) and leachate from TSFs,
- Threat to safety both in terms of potential TSF failure and uncontrolled access to steep slopes and polluted ponds,
- Danger of uncontrolled access to dormant mine shafts (DMR, 2013) and
- Negative aesthetic impact resulting in lower property values.

According to the Chamber of Mines of South Africa (1996) preparation for eventual closure should be started as soon as possible and the costs of closure should be regarded as an integral part of the cost of production. However, this has not often been the case. The mines do not allocate enough funds during operation to allow for proper closure of these facilities at the decommissioning phase of the life of the mine. Therefore, an alternative method of funding for the proper rehabilitation and closure of such facilities is required.

### **2.2.1 Closure of mine sites**

The subject of mine closure has been of considerable international interest for a number of decades. Hence, the Sixth International Conference on Mine Closure was held in Alberta, Canada from 18 to 21 September 2011.

According to Butler et al. (2011) for a mine site to be “relinquished”, closure must be achieved to such an extent that the mining company can return the land to a land owner and walk away completely, transferring all future risks and liabilities to the following land owner. The main reasons argued of why this situation has seldom been achieved at any mines across the world are according to Butler et al. (2014):

- The absence of guidance from a regulatory authority as far as closure is concerned and therefore also an absence of closure guidelines and criteria.
- Difficulty in proving that closure criteria have been met and the reluctance of future land owners to accept responsibility of unknown risk.
- Some of these relinquishment activities can take long periods of time to incorporate. An example of this is the Contact Lake Gold Mine, in the Saskatchewan Province in Canada, which was operated for only three and a half years. Reclamation activities, however, took more than 10 years, including placement of engineered caps over surface openings and covering tailings under a permanent water cover.

- There are no guarantees for the mining company that the land will be relinquished once they have spent a lot of money on closure, even if the pre-determined closure criteria has been met.
- The concern that successful closure/relinquishment (often associated with large capital expenditure) may create a precedent with the regulator of how closure can be done. This is a concern that was also identified by the project team of a solar project constructed on top of the Questa Mine TSF in the USA (Gulde et al., 2011)
- In the end it comes down to the uncertainty of the quantification of the risks and liability over a long period of time because there is limited data to base the predictive models on.
- Due to the constantly changing expectations of the stakeholders with regard to closure. If closure is not an integral part of the life of mine operational cost (which in most cases it is not, because of the long term duration of the mining activity), and if the closure plan is not being update regularly, there are bound to be unforeseen costs incurred during closure (Butler et al., 2011).

The situation in South Africa is similar. Due to the unpredictability of liability, risk and costs associated with mine closure, South African mining companies are reluctant to spend a lot of time and money on closure of facilities after its successful operation.

One of the risks that are difficult to quantify is the expectation of the environmental regulator. The majority of mining infrastructure is designed to operate for an extended life (of the order of a few decades, depending on the size of the resource), based on this best practice available at the time. These structures are designed, constructed, commissioned and operated according to the environmental legislation, regulations and specifications applicable at that time. Over the years, where necessary, alterations are made to the existing designs and sometimes new infrastructure is added to adapt to changes in the life of mine plan. These additions will then comply with the best practice standards applicable at the time of design. The point is that mining is an ongoing activity that can take place over decades, for as long as there is a resource that can be feasibly mined. Legislation, regulations, standards and specifications, however, change frequently and therefore staying on the right side of the environmental agency regulator is often an ongoing battle.

A large part of the current mining infrastructure was constructed many decades ago when environmental laws were not as stringent. If mining activities are to continue, these mines have to bear the legacy of the previous mining generations. A TSF, for example, can be operated for up to 50 years or even longer, depending on the deposition rate. During the 50 year operation of such a TSF, environmental legislation might be revised numerous times. It is difficult to predict

what the future generations of environmental regulators would require as the minimum standard. Therefore, the current mining generation has to act based on the best knowledge available at the time, but also remain accommodating to any changes that might take place in future.

The same logical principle applies to the previous mining generations. When they constructed the legacies which we see today, they did not know what effects it would have on the environment decades into the future. Therefore, it is now the current generation's responsibility to rectify their mistakes by taking care of the environment using the best practice known today. This applies to construction of new infrastructure, rectification of existing infrastructure, but most importantly, the closure of dormant mining infrastructure.

This study is specifically focussed on the mining infrastructure legacy of abandoned TSFs that were inherited by the current generation. The following section discusses the mining process and how TSFs are constructed.

### **2.2.2 Mining process and infrastructure**

In order to engage into more in-depth discussion of the problems associated with TSFs, it is important to establish a basic understanding of the mining process and where these legacy structures fit in.

When mining for metalliferous minerals, blasted rock (containing the precious minerals) is removed from underground, either by underground or opencast mining methods. Once the mineral containing rock, called ore, has been blasted underground, it is hoisted to the surface to the process plant, where it is milled to a fine powder. This fine powder is often mixed with chemicals to extract the valuable minerals contained within depending on the extraction process being used. Once the precious minerals are extracted from the powder, the residue (often toxic) is then mixed with process water, to achieve slurry-like consistency to form a substance referred to as tailings, slimes or residue (Chamber of Mines of South Africa, 1996). In limited cases some of this tailings material is thickened (removal of excess water) and placed back underground to fill some of the underground voids where the rock originated from (Chamber of Mines of South Africa, 1996).

Most often the tailings are pumped to the location where it will be disposed of above ground at a TSF. TSFs are also referred to as residue deposits or slimes dams. Pumping is the cheapest mode of transport of this type of mine waste. At the TSF the tailings is deposited of in a specific way that the solids remain behind and the excess water can be recovered. The excess water runs down the beach to the TSF pond. It is then either contained in the TSF pond or extracted (usually via

an outlet pipe, also referred to as a penstock) to a return water dam. When required, this water can then be pumped back to the plant to be reused in the tailings circuit (Chamber of Mines of South Africa, 1996).

The average TSF is a massive structure, containing many millions of tons of finely crushed rock. Such a facility can have a footprint of a few square kilometres and can reach heights in excess of 60 m. If a TSF is properly designed, correctly operated, water carefully managed and its stability is regularly reassessed, these facilities can be operated for long periods of time, in excess of 50 years and will outlast the careers of numerous design/surveillance teams.

If a TSF reaches its final design height, or the mine reaches the end of its life, or the TSF can no longer be constructed to remain stable for future deposition, the TSF is decommissioned. All the operating equipment is removed from the facility and the facility is then abandoned. Some of the most significant threats that these abandoned TSFs pose to the environmental and surrounding communities include:

- Air pollution in the form of dust clouds originating from these facilities (Van Wyk et al., 2014),
- Groundwater contamination from seepage of these toxic facilities (Copeland, 2014),
- Threat to the safety of the surrounding community both in terms of potential TSF failure and uncontrolled access to steep slopes and polluted ponds,
- Unused land will soon be used for grazing or crop generation, which could lead to serious consequences (plants rooted in toxic waste can cause ill health or even death),
- Vast tracts of sterilised, stripped and exposed land that has limited post-closure land use options,
- Negative aesthetic impact resulting in lower property values in the area.

From this introduction to the mining process, it is to be noted that this displaced rock (deposited on TSFs) will remain in place for a very long time after the mining activity has ceased. During this time these facilities are causing and will continue to cause many challenges in future. These are the negative legacies referred to in the introduction of this section.

Although the majority of these problems were caused by previous mining generations, it is now the current generation responsibility to provide for future generations. Due to the development of modern technology and advances in science, the modern mining generation is better educated in environmental conservation and ignorance is no longer an excuse.

It is therefore the current generation's responsibility to mitigate, or at least minimise, the environmental effects as far as possible. This includes proper closure/rehabilitation of abandoned TSFs.

### **2.2.3 Extent of gold mining in South Africa**

As mentioned in the introduction, many towns and cities around South Africa have grown around mining hubs, the most significant of these being the city of Johannesburg. The extent of gold mining development across the city of Johannesburg is indicated with the white outline on the satellite image in Figure 2-1. There are more than 80 different TSFs of different shapes and sizes located within the outlined area. Satellite images of the areas around the gold mining towns of Welkom and Orkney, located on the Freestate Gold Fields of South Africa, are shown in Figure 2-2 and Figure 2-3 respectively.

Figure 2-4 shows a satellite image of Soccer City, located just outside Soweto, Johannesburg and the adjacent TSF's. Note the scale of these structures relative to the national football stadium. The location of Figure 2-4 can be seen as the square in Figure 2-1. Also note the close proximity of these TSFs (now left dormant) to the residential areas of Soweto. A major opportunity associated with these abandoned TSFs located so close to these residential areas is the availability of good supporting infrastructure development, such as access roads, the proximity of the electricity grid and water reticulation services.

This project, i.e. investigating the productive use of abandoned TSFs, was focussed on gold mines in the Johannesburg region, as Johannesburg is probably the city that is worst affected and will benefit the most from such a research study.

The rationale behind this research project was to investigate potential uses for the dormant TSFs in order to:

- Alleviate or eliminate the negative impact on the surrounding community
- Present beneficial land uses for these facilities that could benefit the city, surrounding residents and contribute to the establishment of green cities.

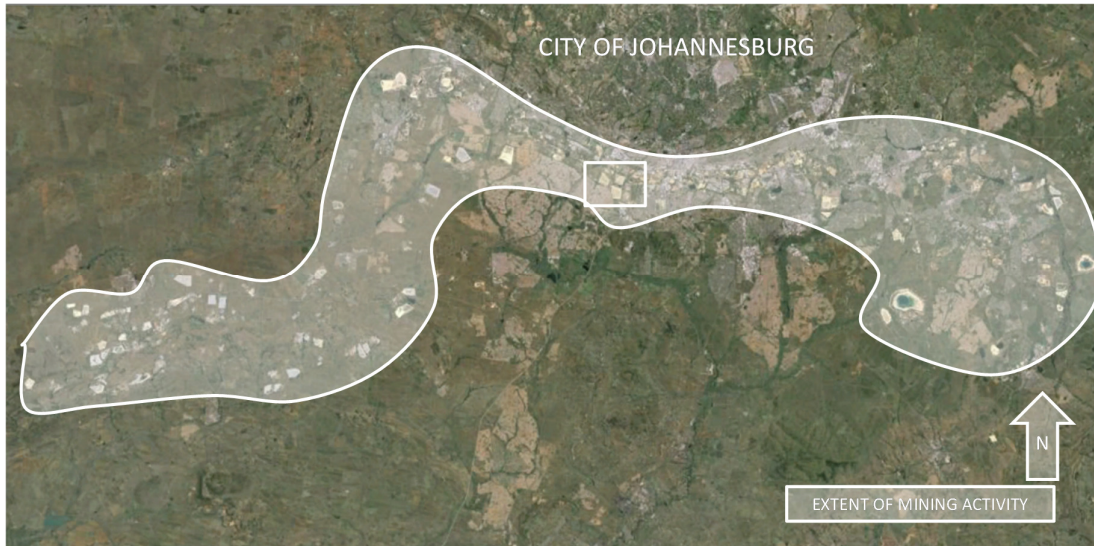


Figure 2-1: Extent of mining activity across the city of Johannesburg (Google Earth copyright acknowledged)



Figure 2-2: Extent of mining activity in the Welkom area (Google Earth copyright acknowledged)



Figure 2-3: Extent of mining activity in the Orkney area (Google Earth copyright acknowledged)

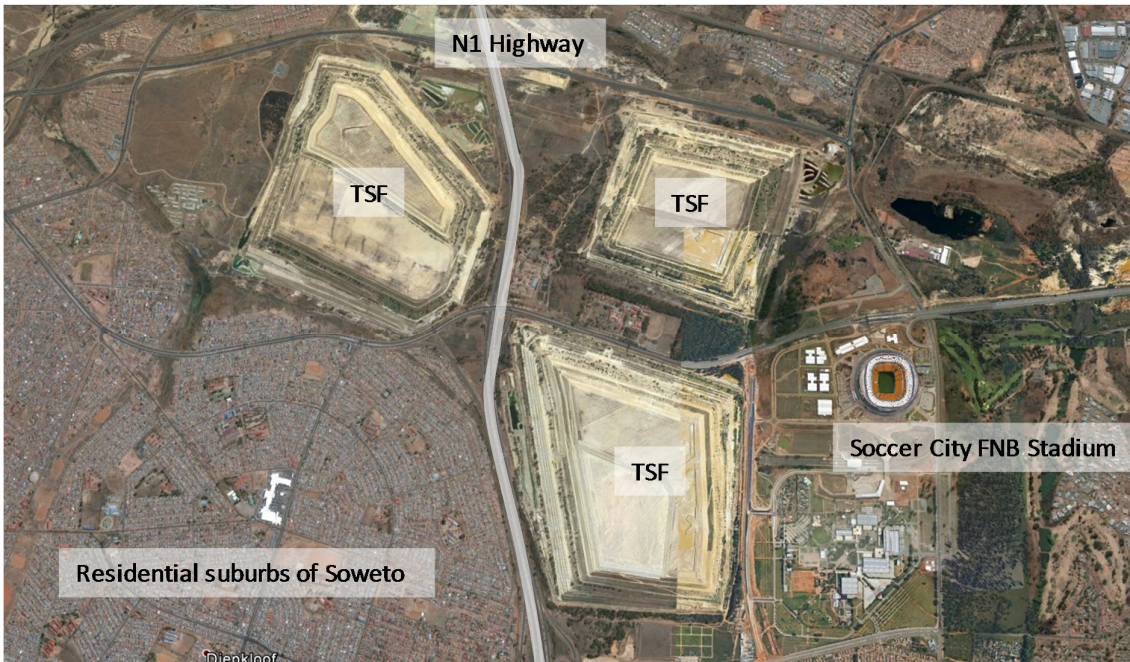


Figure 2-4: Scale of TSFs relative to a national sports stadium and close proximity of these structures to residential areas (Google Earth copyright acknowledged)

## 2.3 LACK OF RENEWABLE ENERGY

In the previous section the legacy of dormant TSFs were discussed. Renewable energy generation might pose a productive post closure land use option for these dormant TSFs.

South Africa has a major need for renewable energy resources. The Electricity Supply Commission of South Africa (Eskom) owns and operates the national electricity grid. They generate approximately 95% of the electricity used in South Africa and approximately 45% of the electricity used in Africa (Eskom, 2014c). They control electricity supply and transmission in South Africa. Therefore, it is deemed important to provide a basic background of their operations.

Of the 95% of electricity generated by Eskom 93% is generated by coal fired power stations. Eskom operates thirteen coal fired power stations and one nuclear power station that makes up their base load generation. Their generation capacity also includes two conventional hydro power stations, two pumped storage schemes and four gas fired stations that are used to supply electricity during peak demand. They also invested in number of wind farms which demonstrates their commitment to finding sustainable renewable energy generation solutions and more are under development. Eskom has a total generation capacity of 44 GW. They are currently constructing two new coal fired power stations, one pumped storage scheme and another wind farm which are to be commissioned soon to meet the ever growing electricity demand (Eskom, 2011).

Electricity cannot be stored in large quantities and has to be used as it is generated. Eskom therefore generates electricity based on a supply demand requirement (Eskom, 2014a). The demand is however not constant and varies throughout the day, but also seasonally, as can be seen from the graph in Figure 2-5 (Dames, 2014).

The electricity demand in the low demand season (September to May), when it is summer in South Africa, is shown by the “Table Mountain profile” in Figure 2-5. The demand increases between 5:00 and 23:00. During the high demand season (June to August), when it is winter in South Africa, the overall demand is higher than in summer, due to the effect of domestic heating appliances. Again, the demand increases between 5:00 and 23:00, but the highest demand is taking place early in the morning (7:00 to 10:00) and in the evening from 18:00 to 20:00. These consumption patterns as shown in Figure 2-5 are the motivation behind Eskom’s tariff structure, which is discussed in greater detail later on in Section 3.3.3. The amplitude of these demand patterns also increases annually due to economic growth and social development in South Africa.

Due to the variation in demand Eskom has an array of power stations that supply energy when required to match this fluctuating demand. All of these power stations fall into one of two categories, base load stations and peak load stations (Eskom, 2014a).

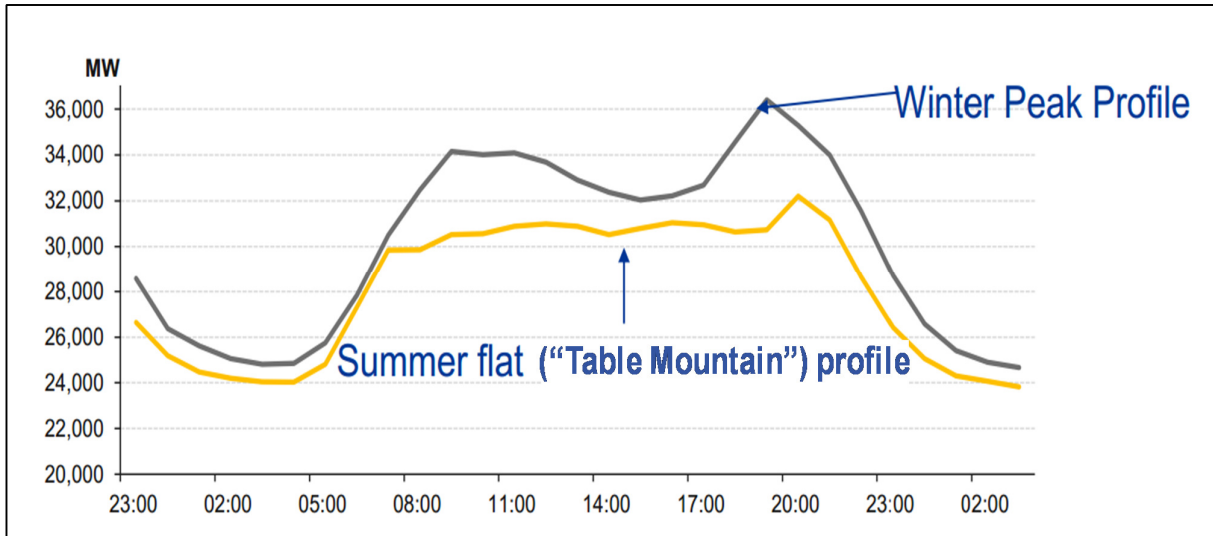


Figure 2-5: Variation in electricity demand in South Africa (Dames, 2014)

Base load stations supply electricity all day and night at a steady load. These stations take a minimum of 8 hours from cold start-up to reach full load generating capacity and the start-up process is very expensive. These plants are only shut down for maintenance and emergency repairs. The majority of the base load power is supplied from coal fired power stations, because of South Africa's abundant coal supply (Eskom, 2014a).

Peak load stations only supply electricity when additional power is required, above the normal base load requirements. These stations can react rapidly to an increase in power demand (Eskom, 2014a).

Eskom's national control centre can control each of these stations to balance the supply and demand. The electricity network in South Africa is maintained at a frequency of 50 Hz. If demand exceeds supply, this frequency decreases and if supply exceeds demand this frequency increases. This change in frequency can damage electrical equipment. Therefore, Eskom applies load shedding measures when demand becomes too high in order to maintain the 50 Hz frequency (Eskom, 2014a).

Eskom operates 23 power plants across South Africa with a total installed capacity of 44 084 MW. Thirteen of these power plants are coal fired power plants that generate 37 748 MW

(86% of the Eskom's total generation capacity) of base load electricity. Two more of these plants (Medupi and Kusile) are to be commissioned soon. Eskom operates one nuclear power station at Koeberg north of Cape Town to make up the remainder of the base load of electricity demanded throughout South Africa. Two conventional hydro power stations and two existing pumped storage schemes, with a third (the Ingula pump storage scheme) to be commissioned soon, are used to supply additional electricity during high demand periods. They also operate four gas fired stations that are only used during extreme emergency demand periods due to their high operating costs. The cost of a gas fired station is 16 to 18 times more than coal fired power stations, depending on the oil price (Eskom, 2011, Eskom, 2013c, Eskom, 2014d).

South Africa's abundant and relatively cheap low-grade coal makes coal-fired power stations an attractive base load option, but the associated emissions have a detrimental effect on the environment. However, a global shift towards renewable energy, as well as South Africa's energy shortage, has forced the National Energy Regulator of South Africa (NERSA) to encourage greener alternatives. This feasibility study is one of many seeking for opportunities to generate more green electricity, which is sustainable and with reduced carbon emissions. Eskom CEO, Brian Dames, stated that the South African government has set a target of 10 000 GWh per annum of renewable energy by 2013 (SAGNA, 2009). It could not be established whether this has been achieved.

Another factor that has contributed to the transformation from conventional coal fired power plant supply to more renewable energy sources, is the fact that coal resources are not renewable. Twenty five per cent of South Africa's coal is exported annually. The remainder of the coal is distributed as follows:

- 53% electricity generation, mostly Eskom
- 33% petro chemical industry, predominantly Sasol
- 12% metallurgical industries
- 2% domestic heating and cooking.

This emphasizes South Africa's dependency on our coal reserves. However, South Africa's coal reserves are limited and will eventually become depleted. South Africa's coal reserve is estimated at 53 billion tonnes and at the current extraction rate will only last another 200 years (Eskom, 2014b).

It is interesting to note that Eskom is operating a 3 MW wind farm (consisting of 3 turbines) at Klipheuwel in the Western Cape. Although this wind farm is the only renewable energy source currently in their repertoire, it shows Eskom's commitment and undertaking to sustainable

development and to move towards a greener future by reducing its dependence on coal. Their new Sere wind farm (100 MW capacity) is expected to be in full commercial operation by March 2015 (Eskom, 2013d).

A shortage of sustainable renewable energy is not unique to South Africa. In fact, it is a global problem, which has been solved in numerous ways in other countries all over the world. The majority of these countries are however first world countries and can afford expensive infrastructure. Worldwide there has been a shift of energy generation to renewable energy resources such as wind and solar, which is energy which goes to waste if not utilised. This is largely due to the over exploitation of other mineral resources such as coal, which is not renewable as well as the damage caused to the environment by conventional power generation methods, such as the Acid rain in the 1980's, the Chernobyl disaster, global warming etc. (Breeze, 2005).

## **2.4 PRODUCTIVE USE OF DORMANT TSFS**

As discussed in the previous two sections, South Africa, and specifically Johannesburg, has two challenges namely the legacy of abandoned TSFs and a lack of renewable energy. This study is aimed at assessing the possibility of generating energy from dormant TSFs in the Johannesburg region.

Four different beneficial land use options were considered in this study as potential post closure options land use options for a dormant TSF. These include:

- Electricity generation from photovoltaic solar power generation
- Electricity from wind power generation
- Electricity from pump storage scheme power generation
- And harvesting of rain water from the TSF catchment for raw water supply.

However, both the wind power generation and rain water harvesting options were abandoned at an early stage of the study, with reasons discussed in Section 3.4.

Whitbread-Abrutat et al. (2001) presented a number of innovative ideas regarding renewable energy sources from mine sites. They also listed a number of case studies where such developments have been successfully implemented. However, none of the case studies listed are located in South Africa (or Africa).

Dormant mine sites are often more favourable locations for the generation of renewable energy resources than green field sites. The following are a few reasons why this is the case (Whitbread-Abrutat et al., 2011):

- Vast tracts of land, some thousands of hectares, that has limited post closure land use potential. Therefore, renewable energy generation will have little further environmental impact and opposition. In fact, the application of renewable energy infrastructure might decrease environmental effects.
- Existing infrastructure, such as electricity transmission systems and roads are in close proximity, therefore less capital expenditure is required.
- Concession of land is easier as it is often owned by less stake holders than green fields of a similar size owned by numerous farmers.
- Dormant mine sites provides an opportunity to reemploy a skilled labour force from the local community that use to work for the mine.
- TSFs specifically are denuded and exposed, making them suitable for solar or wind power plants.

Gulde et al. (2011) stated numerous lessons learnt during the planning, design, permitting and construction of a solar plant on top of a dormant TSF. Some of the most prominent lessons were:

- Identify all the stakeholders involved and revise the stakeholder engagement plan frequently as different stakeholders are involved in different stages of the project.
- Engage with the local community by involving them in the project and educate and explain to them how they will benefit from the project.
- Because this is new technology and new way of exploiting an opportunity, approval is required from a higher level (often at government level), because at agency level there is uncertainty around decision making.
- Identify the correct agencies to be approached for permits, as early as possible. A local construction team can be instrumental in getting this section of the project addressed.
- Get agreement in writing. This principle applies to any business in the modern age. In Gulde et al.'s case, some construction permits were verbally agreed, but was later required in writing.
- Involve someone with experience in the design of similar systems. Involve consultants familiar with the alternative energy technology to be constructed on site, as well as someone who is familiar with the terrain.
- Spend money to characterise the site properly, as part of the design phase of the project. This can save significant costs at the construction and implementation phases of the

project. Topographical surveys, geotechnical investigations and contaminant surveys are essential.

- Involve the contractor with the design as early as possible. If the envisaged contractor has prior experience of similar construction projects, their opinion is invaluable and can save cost during construction.

In the previous three sections the reason for utilising electricity generation as a beneficial post closure land use option for dormant TSFs has been motivated. The following two sections are aimed at providing a background from literature focussed on solar photo voltaic and pump storage scheme power generation respectively.

## **2.5 SOLAR PHOTO VOLTAIC POWER GENERATION**

Electricity from photo voltaic (PV) solar cells is solely dependent on the energy provided by the sun, as PV cells require the energy of the sunlight to generate electricity.

The following topics are discussed in this section:

- A brief history of where solar PV started and how it operates
- Quantifying the available solar resource
- Factors influencing a solar PV plant's production
- Cost of solar PV
- Applicable examples
- Alternative forms of solar power generation

### **2.5.1 Brief principles of operation**

The discovery of the photo voltaic effect dates back to 1893, when a French scientist called Edmund Becquerel placed two electrodes in a fluid. When the fluid was exposed to sunlight, a spontaneous current flowed. Although the scientific reason and its potential was not realised at the time, it was the birth of an alternative energy source that would benefit mankind for years to come (Zweibel, 1990).

Even before the discovery made by Becquerel, an American, Charles Frits, speculated that “the supply of solar energy is both without limit and without cost” (Zweibel, 1990). Not only is the sun's energy essential to existence on earth, but it is an inexhaustible source of energy. Therefore, solar energy can be classified as a renewable energy source, unlike conventional methods of fossil fuel energy generation.

The PV cell shares a history with the microchip, transistor and diode (Breeze, 2005). The first PV module was built in the Bell laboratories in 1954 (Eskom, 2013e).

In the 1950s the development of PV technology was halted due to its cost, compared to conventional power generation. However, NASA took interest in PVs due to its relative weight to energy generation potential. In their applications fuel driven energy sources does not suffice. NASA has adopted solar energy on almost all their satellites. Although the investment for solar energy is expensive, it was a small component of NASA's overall project cost. What NASA was after was reliability, as they could not afford an unreliable power source. Since then solar PV has become synonymous with reliability (Zweibel, 1990).

The science behind PV has improved significantly since its inception and is still improving rapidly. With the changes in science and technology, comes a decrease in cost. The more competitive it becomes to produce solar cells, the lower the initial required investment becomes. From 1973 till 1990 the cost of global PV has reduced about 20 times, and will continue to reduce in future (Zweibel, 1990).

Solar cells (or PV cells) are powered by sunlight. Sunlight consists of a whole spectrum of colours, each with its own level of energy and wavelength. Not all of these can be converted to electricity. In fact only about 15% of this energy can be converted by a normal solar cell. At around midday on a cloudless day the sunlight provide between 1.0 kW and 1.4 kW of power on every exposed square meter. During an average day the sun produces between 5 to 9 kWh of energy for every square meter of exposed area (Zweibel, 1990; Breeze, 2005).

A solar cell consists of a sandwich of different layers of material, each with its own function. The top layer, as can be seen in Figure 2-6, is a cover glass layer, intended to protect the cell against the elements of the surrounding environment. The next layer is called an anti-reflective layer, which minimises the amount of sunlight that is reflected by the cell, as the output of the cell is directly proportional to the sunlight it absorbs.

The core of each cell consists of two contacts (a bottom and top contact) with two layers of semiconductors (the n-type and the p-type) which are placed between them. The operation is explained below (Zweibel, 1990, Breeze, 2005):

- The two contacts are essential bridges to the external circuit. The bottom contact, a metal sheet that can convey electrons to the cell, is usually made of a conductive metal such as aluminium or silver.
- The top contact is there to convey electrons away from the cell. The top contact can either consist of a grid or fingers made of silver or aluminium. The closer the fingers are

spaced, the shorter the distance an electron has to travel, resulting in less resistance and therefore a higher efficiency. However, the closer the spacing of the fingers, the more shadow is cast on the semi-conductors. In some of the more advanced solar cell designs the top contact is made of metal oxides, such as zinc oxide or tin oxide. The metal oxides have the advantage that they are transparent, but just as effective in conducting electricity.

- The two layers semi-conductor layers have two important functions. The first is that a semi-conductor material expels electrons when photons of radiation in the visible spectrum of the electromagnetic spectrum (what sunlight consists of at an atomic scale) with sufficient energy is absorbed. The second is that a fixed electric field is induced when two dissimilar semi-conductors are joined. The bottom semi-conductor, usually the p-type, expels electrons when exposed to sun light, becoming positive (hence the name p-type). The n-type conductor accepts the electrons, driven by the induced electric field between the two semi-conductors, becoming negative. This flow of electrons causes an imbalance in the cell. This imbalance drives the electrons through an external circuit to provide the electrical power that is required from the cell. The flowing current is produced at a fixed voltage, called the cell voltage. The cell voltage is a function of the semi-conductor material and for silicon it is usually around 0.6 V.

The semiconductor most often used in solar cells today is silicon. Silicon is one of the most abundant elements on earth, the main constituent of silica sand, also known as beach sand (Zweibel, 1990). However, although silicon is widely available and therefore cheap, the production of pure silicon which is used in solar cells, is energy intensive, up to 90 kWh for every kilogram of silicon. Therefore, a solar cell has to be operational for 2 years to produce the electricity required to produce the cell itself (Breeze, 2005).

Experimentation with other semiconductors, such as cadmium telluride, copper indium selenite and gallium arsenide has proved successful. Some of these alternative semiconductors include toxic elements such as cadmium and can pose an environmental risk, especially at the decommissioning phase of a plant (Breeze, 2005).

The efficiency of a solar system is measured as light-to-electricity conversion efficiency (Zweibel, 1990). An efficiency of 15% implies that 150 W of electricity can be expected for every 1000 W of sunlight to which the cells are exposed. The efficiency of commercially available crystalline silicon cells are in the order of between 14 to 16% (Yingli Solar, 2012).

The efficiency of a cell is dependent on a number of variables, including the material used for the production, the structure of the cell, concentration of the sunlight, the age of the technology

etc. Efficiencies of various solar cell technologies currently under research and development (not only crystalline silicon) vary from as low as 9.2% to as high as 44.7%. The efficiency of crystalline silicon technologies varies between 20.4% and 27.6% (NREL, 2014). Note that these efficiencies are tested in laboratories under ideal conditions and will not necessarily deliver equally high efficiencies when installed in the field. In addition, not all of these cells are commercially available yet. However, it does provide a positive indication that the technology is improving and that higher efficiencies can be expected in future.

A constraint with a solar system is that PV produces Direct Current (DC) electricity. This DC current can be converted to Alternating Current (AC) using an inverter. AC current can be fed into the electricity grid, as it is the current used by the majority of household appliances (Zweibel, 1990).

A single solar cell can generate limited power. Power (in Watt) is the product of the cell voltage potential (in volts) and the current (in amperes). If the cell voltage is assumed to be 0.6 V, as mentioned earlier, a single cell can generate a current of between 3 and 5 A. Dependent on its size, the modern solar cell can generate between 2 and 3 W of power. If 36 of these cells are stringed in series an output of 20 V can easily be achieved to charge a 12 V battery (Breeze, 2005). Single solar cells are arranged into modules. These modules, also known as solar panels, are then grouped into arrays, which make them easier to install. Grouping a number of solar cells together can generate a significant amount of power.

Solar modules are rated in a unit of power (Watt) according to their performance. During the manufacturing process the cells are tested under Standard Test Conditions (STC) according to EN 60904-3. This means that the cell's output is measured (in watt-peak) while it is exposed to 1000 W/m<sup>2</sup> irradiance, at a global standard terrestrial spectrum with an air mass ratio of 1.5 (which is a function of the wavelength of light the cell is exposed to) and the cell temperature is maintained at 25 °C (Yingli Solar, 2012). Cells are then sorted into various output ranges, although they come from the same batch. Hence a whole range of potential outputs are available, with a positive power tolerance of 0 to +5 W. I.e. a panel that performs at 242.6 Wp under STC, will be sorted with other 240 Wp panels. The price of a panel is influenced by its watt-peak rating and is discussed in more detail in Section 3.5.5.

The power output capacity of plant is also rated in terms of watt-peak, calculated by multiplying the number of panels with the power output of a single panel. This output capacity is often also referred to in industry as the "nameplate" capacity.

Once a solar plant is constructed, the system has a certain output capacity. This does not remain constant with time, but degrades linearly. To accurately predict the return of investment for a

project like this an accurate prediction of decreased power output over time is required. A study by the National Renewable Energy Laboratory (NREL) showed that the median of nearly 2 000 degradation rates assessed over the last 40 years was in the order of 0.5% per year (NREL, 2012). Some of the solar panel suppliers provide a guarantee for the rate of linear degradation over time. Yingli Solar (2012) for example guarantees that their panels will perform at 80.7% of its original output capacity after 25 years (i.e. an average degradation rate of 0.8% per year).

The efficiency of solar panel, and therefore the output, is also a function of the angle at which the sunlight strikes the cell, there are three different installations of arrays that have varying degrees of efficiency, but also difference in cost, namely (Zweibel, 1990):

- There are fixed arrays, the cheapest installation, that do not follow the sun, it is installed at a fixed angle, usually towards the north in the Southern hemisphere. These are the least effective.
- Then there are single axis arrays that track the sun from east to west, from sunrise to sunset. This provides better efficiency than a fixed array system.
- Lastly, there are double axis arrays that can follow the sun in two directions, both from sunrise to sunset, but also as seasons change (between the summer and winter solstices). This installation is the most expensive, but also the most efficient. Trackers can increase the amount of intercepted sunlight by 20 to 40%, when compared to fixed arrays. However, it also requires a larger area as the arrays have to be placed further apart to avoid it casting a shadow on another array (Zweibel, 1990). Another factor to keep in mind is the complexity of installation and its maintenance requirement.

There are two different kinds of PV modules, flat plate modules and concentrators. Flat plate modules are a collection of flat solar cells. Concentrators use mirrors and reflective surfaces to concentrate sunlight onto smaller solar cell areas. Concentrators need to be tracking the sun as they can only operate when exposed to direct sunlight and are often less efficient than fixed flat plate modules (Zweibel, 1990).

In order to determine the output capacity from a solar plant at any site of interest the solar resource has to be determined for that site. Section 2.5.2 below discusses how the solar resource for any site is determined.

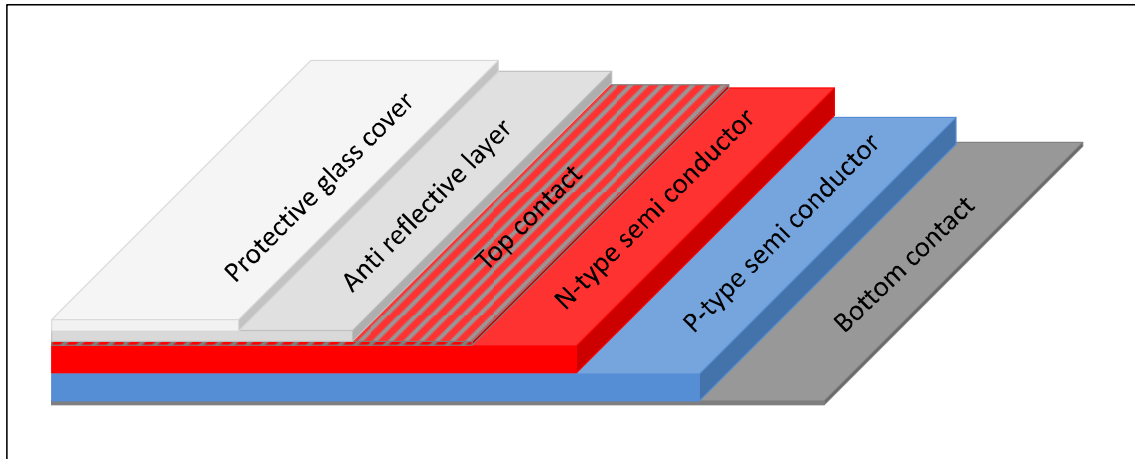


Figure 2-6: Composition of a solar cell (Zweibel, 1990)

### 2.5.2 Determining the available solar resource

Before it can be determined how much electricity can be generated by solar PV panels and allocating a potential income to it, the sun's potential (solar resource) has to be quantified.

Insolation is a term used in the solar energy industry to quantify the energy available from the sun per unit area, sometimes also referred to as solar radiation or irradiance. This energy might take on various forms, such as direct sun beam radiation, diffused light from particle matter in the earth's atmosphere, as well as reflected light. However, all these forms originate from the sun. Throughout this section solar insolation is written in unit kilowatt-hour per square meter.

The following procedure is followed to determine the total radiation provided by the sun for any site of interest:

1. Determine the position of the sun as a function of time
2. Determine the direct beam solar radiation on a horizontal surface
3. Convert the direct beam solar radiation to radiation on a Solar PV collector
4. Calculate the diffused solar radiation
5. Calculate the total solar radiation

#### 2.5.2.1 Determining the position of the sun

The earth revolves around the sun. Each revolution takes 365.25 days. The earth moves in an elliptical orbit around the sun, as illustrated in Figure 2-7. It is the furthest away from the sun (approximate distance of 152 million kilometres) on 4 July annually, called the aphelion. It is the closest to the sun on 3 January annually (approximate distance of 147 million kilometres), called

perihelion. Therefore the earth is in approximately the same position (relative to the sun) every 365.25 days.

At the same time the earth is also revolving around its own axis. The earth's axis is tilted  $23.45^\circ$  relative to the elliptical orbit plane in which it revolves around the sun. This tilt of the axis causes the four distinct seasons to take place, with the winter and summer solstices occurring annually on 21 June and 21 December respectively (for the Southern Hemisphere). The sun is directly above the equator on 21 March and 21 September, called the autumn and spring equinoxes respectively. The earth revolves around its own axis every 24 hours.

All of the abovementioned rotations have to be taken into account when determining the position of the sun relative to the site of interest at any moment in time. These rotations are fairly predictable and it can be assumed with reasonable accuracy that the sun is in the same position every 365 days. Hence the position of the sun can be predicted with a set of formulae for any day of the year and any time of day (between sun rise and sun set). The position of the sun before the sunrise and after sunset has no significance to the solar resource available for power generation at the site of interest.

The position of the sun relative to the site of interest at any time between sunrise and sunset, on any day of a calendar year can be described with two coordinate angles, called the altitude ( $\beta$ ) and azimuth ( $\Phi_s$ ) angles, respectively. The altitude angle ( $\beta$ ) can be described as the vertical angle of the centre of the sun relative to the horizon, as illustrated in Figure 2-8, and can be calculated with the following formula (Masters, 2004):

$$\sin \beta = \cos L \cos \delta \cos H + \sin L \sin \delta$$

Where:  $L$  is the latitude of site (in degrees)

$\delta$  is the solar declination (explained below) (in degrees)

$H$  is the hour angle (explained below) (in degrees)

The solar declination ( $\delta$ ) is the angle of the sun at any time relative to its position when it is directly above the equator (during the equinoxes). This angle is caused by the earth's revolving around the sun and the earth's tilt angle with respect to its elliptical movement plane, illustrated in Figure 2-7. The solar declination angle varies between  $+23.45^\circ$  during the summer solstice and  $-23.45^\circ$  at the winter solstice and can be approximated at any time of the year with the following formula (adapted from Masters (2004) for Southern Hemisphere calculations):

$$\delta = 23.45 \sin \left[ \frac{360}{365} (n + 101.5) \right]$$

Where:  $n$  is the day number of the year, i.e. for 1 January  $n=1$  and 1 February  $n=32$ .

The hour angle ( $H$ ) is how far (in degrees) the sun has to move to be directly above the local meridian (line of longitude). The hour angle at solar noon is zero degrees. Solar noon is when the sun is located directly north of the site of interest (true north). The earth rotates around its own axis  $360^\circ$  in 24 hours. Hence it appears like the sun is moving at  $15^\circ/\text{hour}$ . The hour angle is positive before solar noon and negative after solar noon and can be calculated with the following formula (Masters, 2004):

$$H = \left( \frac{15^\circ}{\text{hour}} \right) * (\text{hours before solar noon})$$

The azimuth angle ( $\Phi_s$ ) can be described as the horizontal angle of the sun (at any time) relative to its position at solar noon (true north), measured in degrees. East of north provides a positive azimuth angle. West of north provides a negative azimuth angle. The azimuth angle can be calculated with the following formula (Masters, 2004).

$$\sin \Phi_s = \frac{\cos \delta \sin H}{\cos \beta}$$

Where:  $\delta$  is the solar declination (as explained above) (in degrees)

$H$  is the hour angle (as explained above) (in degrees)

$\beta$  is the altitude angle (as explained above) (in degrees)

By calculating the altitude and azimuth angles at regular time intervals between sunrise and sunset for every day of the calendar year, it is possible to plot a sun path diagram, of which an example can be seen in Figure 2-9 (Masters, 2004).

Once the position of the sun is known, the next step is to determine the solar insolation that can be expected on a surface, be it a horizontal surface or a tilted solar panel. Determining the insolation is the objective of this section.

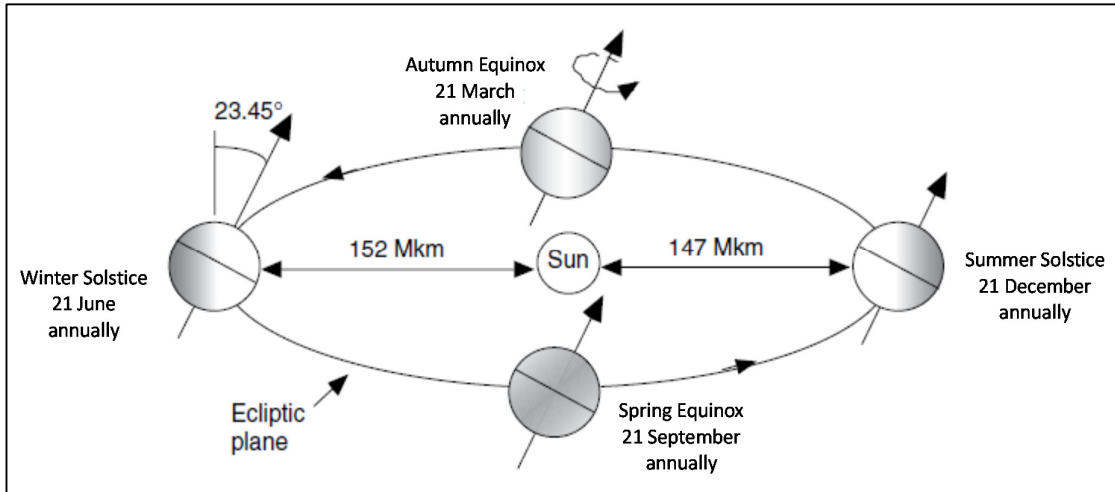


Figure 2-7: Illustration of the earth revolving around the sun (adapted from Masters (2004) for Southern Hemisphere conditions)

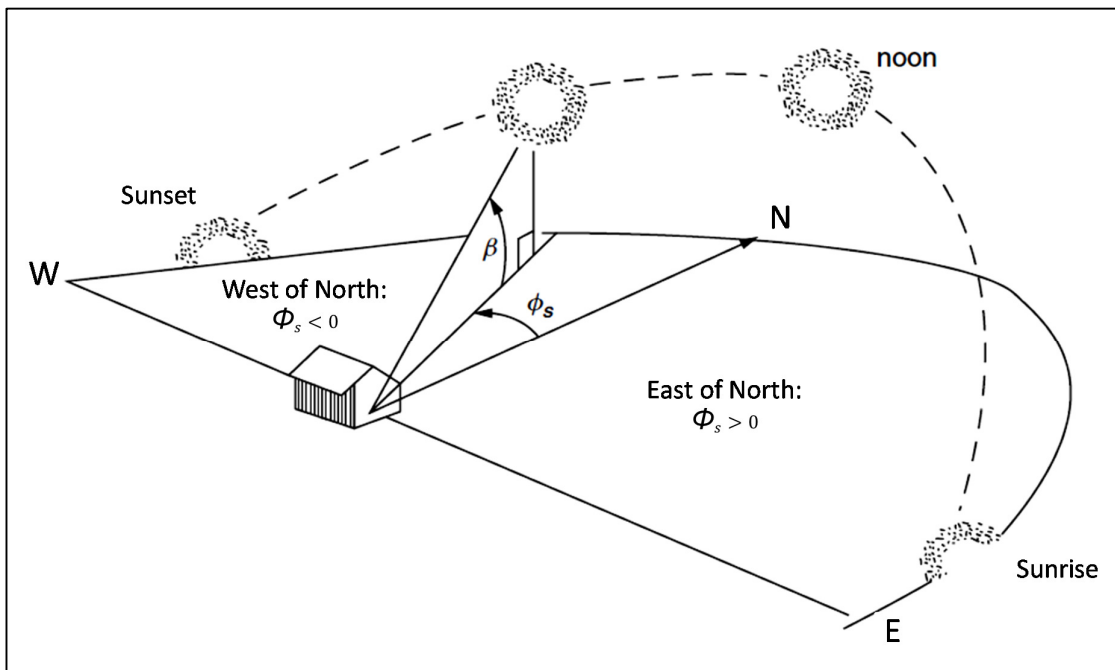


Figure 2-8: Illustration of altitude and azimuth angles of the sun (adapted from Masters (2004) for Southern Hemisphere)

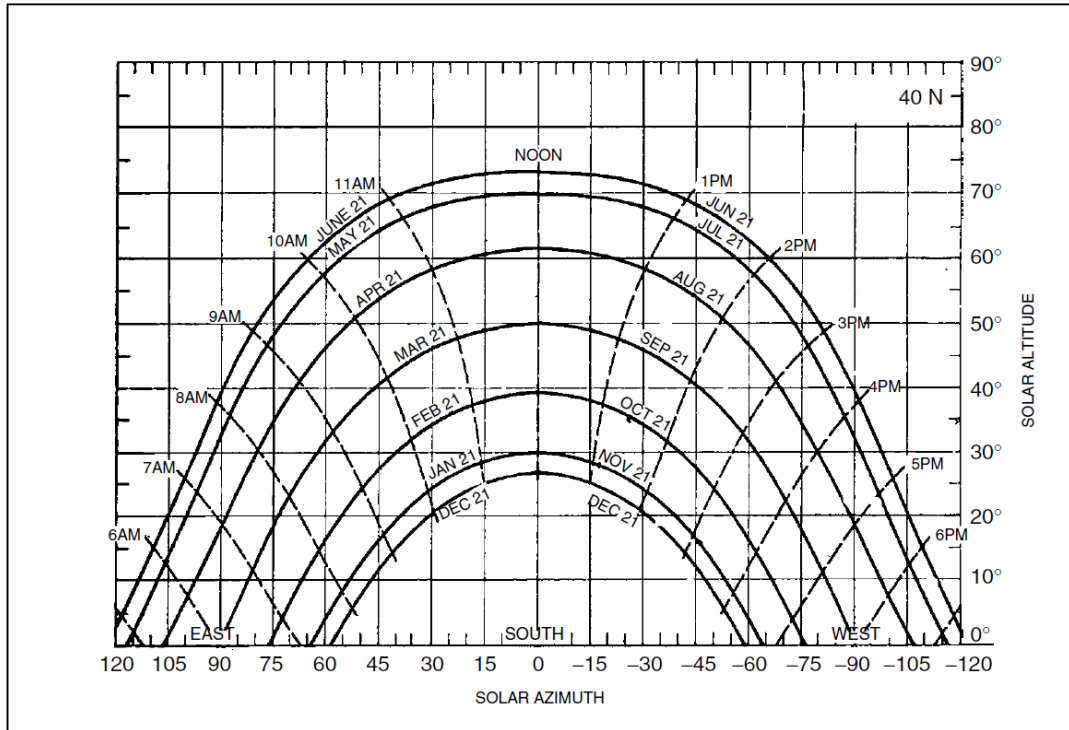


Figure 2-9: An example of a sun path diagram for a site in the Northern Hemisphere with a latitude angle of  $40^\circ$  (Masters, 2004)

### 2.5.2.2 *Determining the direct beam solar radiation on a horizontal surface*

The largest component of the total radiation is direct beam radiation. The direct beam portion of radiation on a horizontal surface can be estimated at any time of day with the formula (Masters, 2004):

$$I_B = Ae^{-km}$$

Where:  $A$  is the extraterrestrial flux ( $\text{W}/\text{m}^2$ ), calculated with:

$$A = 1160 + 75 \sin \left[ \frac{360}{365} (n - 275) \right]$$

$k$  is the optical depth (dimensionless):

$$k = 0.174 + 0.035 \sin \left[ \frac{360}{365} (n + 82.5) \right]$$

$m$  is the air mass ratio:

$$m = \frac{1}{\sin \beta}$$

Where  $n$  is the day number and  $\beta$  is the altitude angle of the sun at a specific time of day, as discussed in the previous section.

### 2.5.2.3 *Converting the direct beam solar radiation to radiation on a Solar PV collector*

To determine the direct beam radiation striking an inclined collector surface (such as a tilted solar panel), as shown in Figure 2-10) the following formula can be used (Masters, 2014):

$$I_{BC} = I_B \cos \theta$$

Where:  $\theta$  is the incidence angle, which is the angle between the incoming beam and a line drawn normal to the collector surface and can be calculated with the following formula (Master, 2014):

$$\cos \theta = \cos \beta \cos(\Phi_S - \Phi_C) \sin \Sigma + \sin \beta \cos \Sigma$$

Where  $\Phi_C$  and  $\Sigma$  are the azimuth angle and tilt angles of the collector surface respectively.

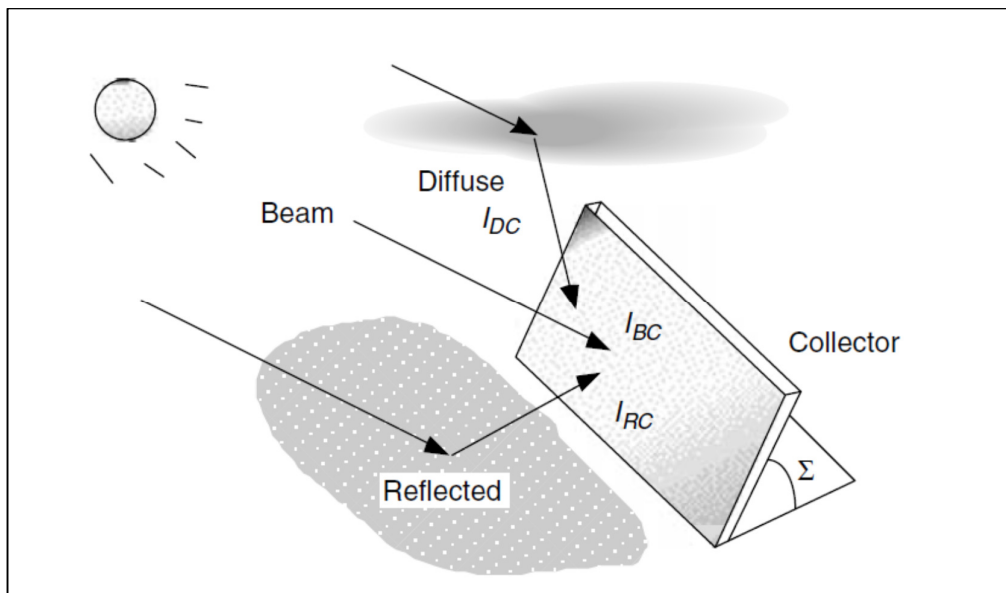


Figure 2-10: Combination of insolation striking a surface (Masters, 2004)

### 2.5.2.4 *Calculating the diffused solar radiation*

The diffuse radiation is more difficult to quantify than the clear sky direct beam radiation as it is light diffused by particulate matter in the earth's atmosphere. The best estimate is to assume the

sky is isotropic, hence with equal intensity from all directions. The diffuse radiation on an inclined collector surface can be calculated with the following formula (Masters, 2004):

$$I_{DC} = CI_B \left( \frac{1 + \cos \Sigma}{2} \right)$$

Where:  $C$  is the sky diffuse factor calculated with formula (Masters, 2004):

$$C = 0.095 + 0.04 \sin \left[ \frac{360}{365} (n + 82.5) \right]$$

Where  $I_B$  is the direct beam radiation on a horizontal surface,  $\Sigma$  is the tilt angle of the collector and  $n$  is the day number as discussed previously.

#### 2.5.2.5 ***Calculating the total solar radiation***

The only remaining portion of the total radiation shown in Figure 2-10 is the reflected radiation. Although the contribution by reflected radiation may be significant if there is a lake of water reflecting light onto the panels, most often it contributes a negligible amount, and is often conservatively ignored (Masters, 2004).

By summing each of the radiation components (each calculated at 5 minute intervals between sunrise and sunset using the site of interest's specific coordinates) it is possible to determine the total solar radiation potential for any site of interest at any time during a 365 day year, with the following formula:

$$\text{Total radiation on a tilted collector} = I_{BC} + I_{DC}$$

The total radiation potential on 1 January, for example, is expected to recur annually.

All the above mentioned calculations were based on the assumption that there are clear skies above throughout the year. Weather patterns, however, cause clouds and other particulate matter (such as dust) to diffuse some of the direct beam sunlight or even cast shadows on the panels. Therefore, using the total radiation as calculated above to determine the feasibility of a solar PV plant development, would lead to a significant overestimation of the actual solar potential.

Quantifying the reduction due to cloud cover and weather patterns is the most difficult part of the exercise, as it is as unpredictable as the weather. Therefore, site specific weather data or cloud cover data has to be used to account for this reduction. NASA (2014) has calculated solar energy data using the Pinker/Laszlo shortwave algorithm and added cloud cover data from the

International Satellite Cloud Climatology Project to produce a realistic solar energy data base. This data can be used to obtain a realistic estimation of the actual solar potential.

Calculated values can also be compared to the NASA (2014) data in order to assess whether the calculated values are in the correct order of magnitude. The NASA data is readily available on the internet and is used by reputable solar suppliers in South Africa.

### 2.5.3 Factors influencing a solar PV plant's production

From the previous sections it can be concluded that a solar plant's production at any given time is influenced by a number of factors, including (but not limited to):

- The material of which the solar cells are produced.
- Efficiency of each solar cell (influenced by the operating temperature)
- Efficiency of the system (including cables and inverters)
- Degradation (i.e. the age of the plant).
- The availability of quality sunlight, influenced by:
  - The solar declination ( $\delta$ ) of the sun at the given time
  - The coordinates of the site
  - The time (time of the day between sunrise and sunset, as well as day of the year)
- The orientation of the panels including:
  - The azimuth angle of the panels ( $\Phi_C$ )
  - The tilt angle of the panels ( $\Sigma$ )
  - Using a tracking system or not
  - Using flat plate modules or concentrators.

### 2.5.4 Cost of solar PV

Determining the cost of a solar PV plant forms a large section of this study. This section provides an introduction to the factors that influence the financial and practical feasibility of installing a solar PV plant.

Financially, there are three main components to take into account when costing a solar PV project, namely, the solar cell modules, its support structure (the tracking arrays included) and the electronic equipment and storage that make it a viable energy source (Zweibel, 1990).

To cost a solar project, the following have to be taken into consideration:

- System design costs
- Land (assumed to be negligible, as the TSF has to undergo closure anyway)
- Site preparation, such as roads and fences (some of this infrastructure might be available already, from when the site was operated as a TSF site)
- System installation.
- Array and tracking structures
- Power conditioning equipment such as inverters.
- Operation and maintenance (minimal as no storage batteries, usually the biggest maintenance item, will be installed. Occasional cleaning and servicing of the panels might be required. Operation can be controlled by a remote computer and do not even require personnel on site).
- Indirect costs (allowance for contingencies).
- Fixed costs (interest on capital expense).

The majority of the cost of a solar project is vested in the solar cells. Approximately a third of the expenses can be accounted to the cost of silicon required to manufacture the cells. A further third is spent on the manufacturing of the cells and solar panels and only the last third of the project cost is spent on the installation and ancillary equipment (Breeze, 2005).

Although PV technology is globally regarded as “expensive” renewable energy, larger deployment attracts the advantages of economy of scale and therefore might be feasible option for this specific study when compared to domestic household installations. With the emphasis increasing on the renewable energy resources PV technology will become increasingly common, raising demand and raising the need for advances in the technology and science. This will in turn drive a lowering of cost (Breeze, 2005).

Solar PV technology is still regarded as new technology, as the technology and science is still developing at a rapid pace. Silicon technology, though, has been around for some time and its reliability, long term operation, plant lifetime and operation is well understood and can be predicted. Based on this experience and knowledge, the power generation potential of any site on earth can be determined, if its solar radiation is known (Breeze, 2005).

Environmentally, solar PV is regarded as one of the most benign renewable energies known to man. Solar PV does not emit any atmospheric emissions during operation. It does not create any noise (Breeze, 2005).

Life time analysis studies on the carbon dioxide footprint of a solar PV project have been conducted and have shown that it emits 100 to 170 g of carbon dioxide per kilowatt-hour of

electricity it produces. Impressive compared to typical gas fired power stations which are in the order of 430 g/kWh and typical coal power stations in the order of 960 g/kWh (Breeze, 2005).

Solar plants are easily deployed and can be constructed in a short space of time if all the material and components are readily available (Breeze, 2005).

### **2.5.5 Examples of solar power plants**

The world's largest solar PV power plant, called the Topaz Solar Farm came online in October 2014. It is located in the Carizzo Plain California, USA. It has a nameplate generating capacity of 550 MWp. It consists of nine million Cd-Te (Cadmium-Tellurium) thin film solar panels, on 25 km<sup>2</sup> of land and was constructed by a company known as First Solar. It is soon to be surpassed by Sunpower's Solar Star, which is due for completion late in 2015 and will have a capacity of 579 MW (Dailymail, 2014; PV Magazine, 2014; GreentechMedia, 2014).

The following solar PV projects have been successfully implemented on dormant mine sites:

- The first large scale solar PV farm was constructed on the closed Wheal Jane tin mine in Cornwall, UK (Whitbread-Abrutat et al., 2011).
- The world's previously largest PV power plant at the time of construction (Geosol Solar Park) was constructed on a former lignite mine ash dump, in Espenhain, Leipzig, Germany, which use to be one of the dirtiest regions in Europe (Whitbread-Abrutat et al., 2011).
- Another successful example is the Gottelborn coal mine site in Germany that was converted into a solar plant that today produces 8 MW of electricity from 50 000 PV panels (Whitbread-Abrutat et al., 2011).
- A solar plant was successfully constructed on top of the Questa Mine TSF and commissioned in April 2011 (Gulde et al., 2011).
- In 2009, a study was done by Worley Parsons, to determine the feasibility of developing the world's biggest solar power station in Australia, with an initial output of 250 MW of electricity. The project was estimated to cost A\$1 billion. It is interesting to note that two of the biggest sponsors of this project was BHP Billiton and Rio Tinto, each of them a respected mining house in its own right, proving that there is an increasing urge from the mining fraternity to improve their environmental image (Carter, 2009).
- Another example is Newmont Mining in Australia that carried out a feasibility study in 2008 to assess different solar energy options to provide them with electricity, in order to reduce their carbon footprint (Carter, 2009).

### **2.5.6 Alternative forms of solar power generation**

It is important to note that there are various other methods of converting the sun's energy into a useful resource. This section discusses the most common methods.

Alternative electricity generation options that are based on exploiting the heat generated by the sun's solar radiation include parabolic troughs, solar towers and solar dish collectors (Breeze, 2005). All three these options require for sunlight to be collected and concentrated to provide a high energy resource.

Parabolic troughs use parabolic trough shaped mirrored glass to reflect sunlight onto a tube located at the focus of the parabola. These troughs then track the sun across the sky during the day. The heat absorbing tube usually contains heat absorbing oil. This oil is pumped through the pipe and can reach temperatures of up to 400 °C. The heated oil is then pumped through a heat exchanger to produce steam (water), which drives a steam turbine to generate electricity (Breeze, 2005).

Solar towers, also known as Central Solar Plants (CSP) use a similar principle to parabolic troughs. However, in this case the sun is concentrated on a single central facility using special mirrors called heliostats. The central facility has a solar receiver consisting of tubes containing heat transfer fluid. Again, a heat exchanger is used to drive a steam turbine. In some cases the design includes a heavily insulated heat storage tank where the hot fluid can be stored for up to 24 hours, without significant losses in energy. The heat transfer fluid usually is a molten salt, a mixture of sodium and potassium nitrates which can be heated to 550 °C and beyond (Breeze, 2005). An image of such a plant is shown in Figure 2-11. Eskom recently signed a R1.3billion loan agreement to construct a 100 MW CSP facility near Upington in the Northern Cape. This CSP project is expected to generate 525 GWh of electricity annually (Eskom, 2013a).

Parabolic troughs and solar towers are often paired with gas turbines (fossil fuel), to create hybrid electricity plants. This provides the option to use the free energy provided when the sun shines, but it does not fully rely on sun and can produce electricity regardless (Breeze, 2005).

Solar dish collectors are similar in principle to the above options, by reflecting sunlight to the focus of the parabolic mirror dish, to drive a heat engine. This option is really intended for small scale electricity generation, with outputs of 5 to 50 kW per dish, although larger dishes have been experimented with (Breeze, 2005). If a Stirling heat engine is used to generate the electricity, it is often referred to as a Stirling dish. A 25 kW Stirling Dish was installed at the Development of

Southern Africa (DBSA) in 2002 as part of a demonstration project by Eskom's Research, Development and Demonstration division project.

A fourth novel technique can be added to this list, called a solar chimney. This initiative was explored in Australia. It includes a massive greenhouse and a very long chimney. The updraft of hot air through the chimney drives a turbine, which generates electricity. This system however, is extremely ineffective. A 40 km<sup>2</sup> greenhouse and a 1 km chimney will generate only 200 kW of electricity (Breeze, 2005).

Another effective way of utilising the sun's energy is to heat water for domestic use. An example of this is solar heating of swimming pools or solar geysers. Eskom is currently busy with a study regarding the potential of solar water heating in an attempt reduce electricity consumption. They have installed solar water heating pilot systems on a commercial building, a school for the disabled and an industrial site to assess the potential benefits (Eskom, 2013f).

The benefits of solar energy utilisation are compelling. It includes being environmentally conscious, sustaining economic growth and job creation, diversifying the country's fuel supply, rapid deployment and potential across the globe to develop new technology and innovation. The most important advantage of solar energy is that the fuel is abundant, free and inexhaustible. The total amount of energy irradiated from the sun to the earth's surface is enough to provide for the globe's annual energy consumption 10 000 times over.



Figure 2-11: An example of a 10 MW CSP in USA (Image courtesy of NREL)

## 2.6 PUMP STORAGE SCHEME POWER GENERATION

A pump storage scheme is a form of hydropower. Hydro power is oldest form of renewable electricity generation and today accounts for almost 20% of global power generation. Construction of hydropower plants is strongly opposed in many countries all over the world due to environmental concerns and the disturbance which it creates when damming up water for power generation. However, it is still one of the largest and easiest exploitable renewable energy resources on earth (Breeze, 2005).

The success of a hydropower scheme is a function of the volume of water and the available hydraulic height (also called the head of water). These schemes are usually built in rivers, therefore using the natural elevation drop of the river bed and the volume of water supplied by the upstream river catchment.

### 2.6.1 Brief principle of operation

There are three ways in which to exploit hydro energy, namely:

- The first is a run-of-river system. This system causes the least environmental disturbance as only some of the water running in the natural river is diverted to generate electricity using a hydro turbine generator. No dam is constructed to accumulate water. Therefore, this scheme is entirely dependent on the run of the river (hence the name) and rainfall patterns on the rivers upstream catchment area. This could result in zero electricity generation during drought periods (Breeze, 2005).
- The second scheme is called a storage/reservoir scheme, where a dam is constructed to accumulate water from the upstream catchment. This water can then be released at will, through a hydro turbine plant to generate electricity. This cause significantly more environmental disturbance as a dam now has to be constructed in an environmentally sensitive area and the downstream environment, which is dependent on the run of the river, now receives less water (although it does limit possible flood damage). Water is accumulated during high rainfall period and used up during dry periods. Therefore, this scheme is able to supply electricity all year round. In order to ensure that there is enough water in the reservoir (dam) to generate electricity during the dry periods a significant amount of water has to be accumulated and therefore the dams have to be rather large (dependent on how much electricity is to be generated). After the water has been used to generate electricity it is released down the river to continue its natural course (Breeze, 2005).

- The third scheme is called a pump storage scheme. This scheme is similar to the above reservoir scheme as water is accumulated in an upper reservoir and then released in a controlled manner to drive a hydro turbine (usually connected to the national electricity grid) to generate electricity when the demand is high. The difference however is that the released water is then accumulated in a second lower reservoir located at a lower elevation. This water is then pumped back into the upper reservoir during so-called off-peak periods, when there is surplus electricity available in the national electricity grid. Such a scheme requires electricity to make electricity. Apart from rainfall, evaporation and the occasional release of water (when the upper reservoir is filled to capacity) this is a closed system and can therefore always supply electricity when demanded. This type of scheme is used when there is a “base and peak load electricity” system, as is the case with Eskom in South Africa. When demand increases to the extent that the peak electricity resources are to be used, the water can be released back down to the lower reservoir (Breeze, 2005).

A pump storage scheme is a method of energy storage where the potential energy of water stored in the upper reservoir can be released and converted into electricity when needed (Eskom, 2014e). Due to the capability of supplying electricity during peak periods, the need for additional non-renewable energy generation is reduced. Even though the pump storage scheme consumes more electricity than it generates, the electricity it does consume is surplus electricity that would have been wasted.

In some cases a pump storage scheme might be a profitable method of electricity generation. This is the case if the cost of electricity used to pump water from the lower to the upper reservoir is significantly cheaper than what the generated electricity can be sold for. However, this is the case if a suitable tariff structure exists, such as that used by Eskom (2014f). More detail of the applicable tariff structure is provided in Section 3.3.3.

South Africa’s climate varies from arid to sub-tropical. However, the majority of the country is classified as sub-arid, including most of the historical mining areas, where the mean annual evaporation (MAE) exceeds the mean annual precipitation (MAP). Due to the limited water resources available and South Africa’s erratic rainfall there are limited opportunities for the implementation of run-of-river hydro-electricity schemes. The majority of suitable sites are being exploited already. There are four pump storage schemes currently operational in South Africa. The Steenbras Power Station, the first pump storage scheme in South Africa, is currently owned and operated by the City of Cape Town. The Drakensberg and Palmiet pump storage

schemes, owned by Eskom, have generation capacities of 1000 MW and 400 MW respectively. Eskom will be adding the Ingula pump storage scheme (located 23 km north east of Van Reenen) to their compilation soon, with a generating capacity of 1 332 MW expected to be fully operational by the end of 2014 (Eskom, 2013c).

In the case of this specific project, the possibility of using the abandoned TSF to develop a pump storage scheme was assessed. There are a number of factors which make a dormant TSF a suitable site for the development of a pump storage scheme:

- A TSF has a concave basin with a relatively large catchment area
- A TSF is constructed of fine silty material, with a low permeability, which limits seepage losses of water.
- In some instances the dormant TSF might still have an operational penstock. If stable with sufficient capacity this penstock might be used as a conduit to transport the water for the pump storage scheme.
- In some cases, a TSF has an existing return water dam(s) at a lower elevation in which process and storm water was stored during operation before the water was reused in the tailings process. Therefore, the Return Water Dam (RWD) can be used as lower reservoir if it has sufficient capacity.
- These dormant TSFs often have good support infrastructure such as access roads, electrical and water reticulation and storm water management systems, which was used during its operation.
- In the case of Johannesburg, these facilities are located close to where electricity is being consumed, hence limited transmission is required.

### **2.6.2 Determining the available water resource**

In order to estimate the electricity generation potential of a pump storage scheme it is important to determine the volume of water available for electricity generation.

This can be estimated with reasonable accuracy by setting up a water balance of the TSF site, based on the historical weather data available for the site. The water balance simulates a reoccurrence of the available rainfall record.

A water balance is a tool often used in the mining industry to quantify water flow volumes on a mine. It is based on the universal principle of conservation of mass, meaning matter cannot be created or destroyed. The same principle applies to a water balance: water cannot be created

within the system, neither can it disappear without being removed from the system. Water added and removed from the system are simply accounted for using the following formula:

$$\textit{Inflow} - \textit{Outflow} = \textit{Attenuation}$$

A historical water balance is often used to size water management infrastructure, such as pumping systems or attenuation facilities. Such a water balance is based on historical weather records of the applicable site and it is assumed that the record is representative of conditions that can be expected during the future life of the project. In such a case, information such as recorded dam volume, recorded pumping rates and recorded weather data is valuable information with which the system can be calibrated for accuracy. The simulation of the reoccurrence of the historical weather data for the site is then used to make predictions and determine the probability of certain events occurring.

A water balance can also be set up to act as an operational water balance, to be used as a tool to manage and calculate water volumes in a mine system, by continuously updating the system with real-time data.

A historical water balance can be applied to determine the water resource available for a pump storage scheme on a TSF. It can be used as a tool to estimate the volume of water available for electricity generation, as well as to determine the reliability of the water source.

The inflows and outflows from the system are quantified as accurately as possible on a daily basis. The difference between the inflows and outflows amounts to the volume that has to be contained in either the TSF pond (upper reservoir) or the lower reservoir. The inflows into the system usually consist of rainfall on the catchments of the TSF and lower reservoir respectively. The outflows consist of evaporation from the open water surfaces of the TSF pond and the lower reservoir respectively, as well as seepage from the TSF.

The allocation of quantities to each of the above mentioned flows for the chosen study site applicable to this project is discussed in detail in Section 3.6.1.

Once the volume of water available for electricity generation on any given day has been determined, the release and pumping volumes between the two reservoirs can be varied.

The following two sections discuss how the amount of electricity generated or consumed is determined from the release and pumping rates respectively.

### 2.6.3 Determining the generating capacity and associated electricity production of a pump storage scheme

The power  $P_T$  (in watts) that can be generated by releasing water through a turbine, from the upper to the lower reservoir, can be calculated with the following formula (Chadwick et al., 2004):

$$P_T = \rho g Q_T H_T \eta_T$$

Where  $\rho$  is the density of the fluid ( $\text{kg/m}^3$ ).

$g$  is the gravitational acceleration, assumed to be  $9.81 \text{m/s}^2$ .

$Q_T$  is the flow rate of water through the turbine ( $\text{m}^3/\text{s}$ ) and can be calculated by dividing the volume of water to be released by the time during which water will be released ( $Q_T = V_T/t_T$ ).

$H_T$  is the net head of the water upstream of the turbine (m), discussed below.

$\eta_T$  is the efficiency of the turbine system (dimensionless), including the turbine and generator efficiencies, typically in the order of 85 to 95%.

The graph in Figure 2-12 shows efficiency (combined efficiency of the turbine and the generator) curves for three different turbine types from two different European turbine manufacturers. The green and blue curves show the combined performance of four 15  $\text{m}^3/\text{s}$  and three 20  $\text{m}^3/\text{s}$  Francis turbine sets (total flow rate of 60  $\text{m}^3/\text{s}$ ) respectively manufactured by Global-Hydro Energy (2014). The red curve shows the combined performance of twelve 5  $\text{m}^3/\text{s}$  Francis turbines manufactured by Wasserkraft (2014). Wasserkraft only manufactures turbines up to 7 MW in capacity. However, it is interesting to note that their official document (Wasserkraft, 2014) states that the provided efficiencies include a safety margin and the efficiencies can be higher during operation.

The electricity  $E_T$  (in watt-hours) that can be generated by the turbine is a function of its power  $P_T$  and the duration  $t_T$  of electricity generation. Hence:

$$E_T = P_T t_T = \rho g H_T V_T \eta_T$$

The net head of water ( $H_T$ ) upstream of the turbine (unit m) can be calculated with the following formula:

$$H_T = H_S - h_f - h_L$$

Where  $H_S$  is the total static head available (height difference between the upper reservoir level and the turbine).  $h_f$  and  $h_L$  are the friction and secondary losses in the outlet pipe. The friction ( $h_f$ ) and local head losses ( $h_L$ ), opposes the flow of water, where the static head ( $H_S$ ) aids the flow of water (as when releasing water, the water flows with gravitation, as opposed to what happens when pumping takes place against gravitation, as discussed below). Therefore, the friction ( $h_f$ ) and local head losses ( $h_L$ ) are subtracted from the static head ( $H_S$ ). Normally with the design of hydro plants allowance is made for a reduction in head during turbine operation. However, when applied to a TSF (which has a shallow pond with a large surface area) this reduction is deemed to be negligible. The friction ( $h_f$ ) and local head losses ( $h_L$ ) are functions of the flow velocity, outlet pipe lengths and outlet pipe diameters. The friction losses ( $h_f$ ) can be calculated with the following formulae in units of meters (Chadwick et al., 2004):

$$h_f = \frac{\lambda L v_T^2}{2gD}$$

Where  $L$  is the outlet pipe length (m).

$v_T$  is the flow velocity in the outlet pipe pipe during release (m/s).

$D$  is the outlet pipe diameter (m).

$\lambda$  is the dimensionless outlet pipe friction factor and can be calculated with the following formula (Barr, 1975):

$$\frac{1}{\sqrt{\lambda}} = -2 \log \left( \frac{k_s}{3.7D} + \frac{5.1286}{Re^{0.89}} \right)$$

Where  $k_s$  is the internal roughness of the outlet pipe (m).

The Reynolds' number ( $Re$ ) is a dimensionless parameter calculated with the formula (Chadwick et al., 2004):

$$Re = \frac{\rho D v_T}{\mu}$$

Where  $\mu$  is the dynamic viscosity of the fluid in (kg/ms) released through the turbine.

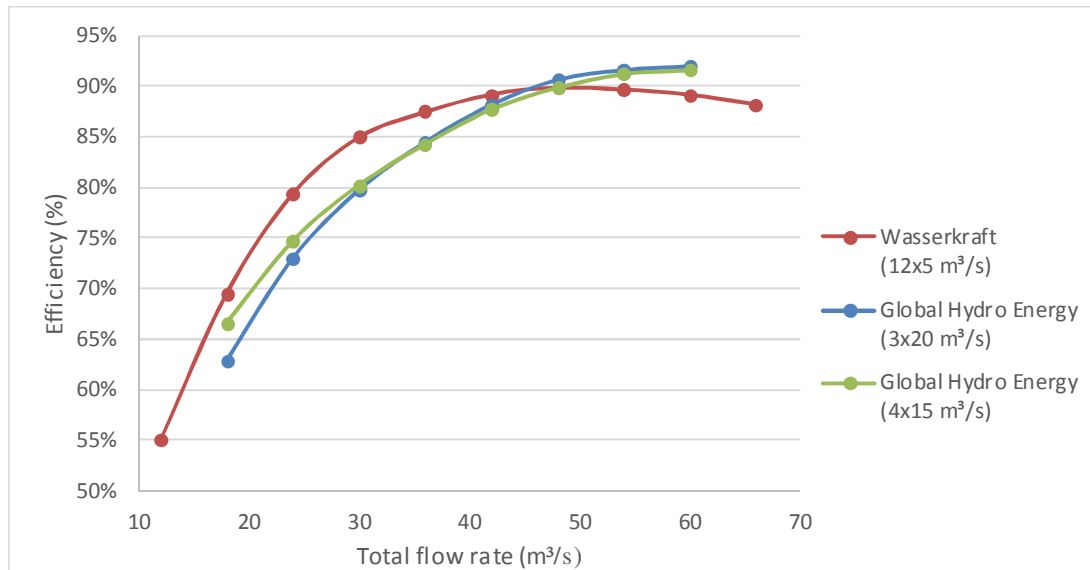


Figure 2-12: Graph plotting efficiency of three different types of turbines against flow rates

#### 2.6.4 Determining the pump capacity required and associated electricity consumption

The power  $P_p$  (in watts) that is required by a pump, when pumping water from a lower to an upper reservoir, can be calculated with the following formula (Chadwick et al., 2004):

$$P_p = \frac{\rho g Q_p H_p}{\eta_p}$$

Where:  $Q_p$  is the flow rate of at which water is pumped (unit m³/s) and can be calculated by dividing the volume of water to be pumped in a day by the time during which pumping will take place ( $Q_p = V_p/t_p$ ).

$H_p$  is the net head that has to be overcome to pump the water to the upper reservoir. In the case of pumping the friction ( $h_f$ ) and local head losses ( $h_L$ ), opposes the flow of water, but so does the static head (as pumping occurs against gravitation) and therefore the static head, friction and local losses are all *added*.

$$H_p = H_s + h_f + h_L$$

$\eta_p$  is the efficiency of the pumping system (dimensionless). Conservative design efficiencies of 70 to 80% are normal practice. Figure 2-13 shows typical efficiencies for pumps. It can be seen that the efficiencies typically increase with

an increase in flow rate. With flow rates above 700 l/s if the system is properly engineered, the pump is sized correctly and it is operated close to its ideal specific speed a pump can reach an efficiency of above 90% (Jones et al., 2008). The main reason for this being that pumps of this capacity is not mass produced and is often built to the client's specifications and hence high efficiencies are possible.

The electricity  $E_P$  (in watt-hours) consumed by pumping is a function of the power  $P_P$  and the duration  $t_P$  of electricity consumption. Hence:

$$E_P = P_P t_P = \frac{\rho g H_P V_P}{\eta_P}$$

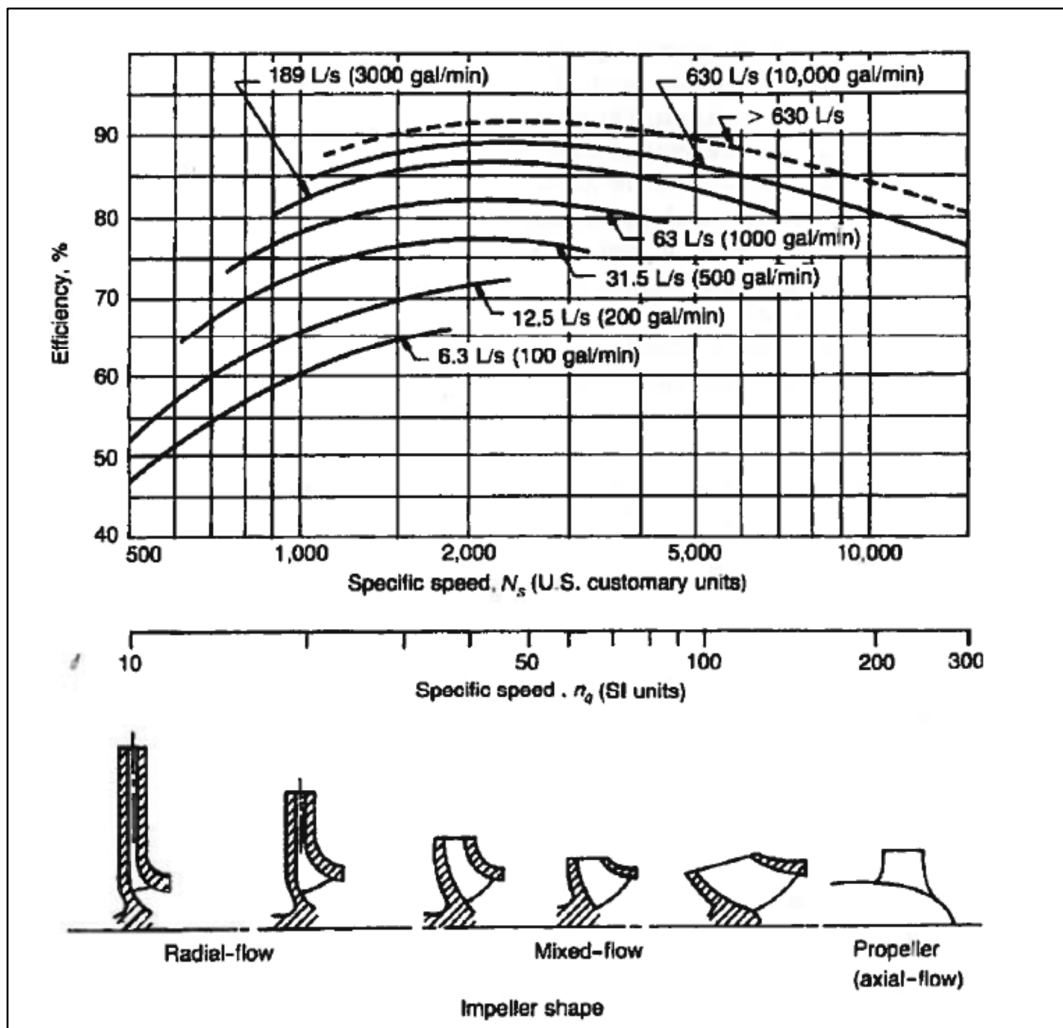


Figure 2-13: Graph plotting efficiency of pumps against specific speed for various flow rates (Jones et.al, 2008).

## 2.7 SUMMARY OF FINDINGS FROM LITERATURE REVIEW

The following summarises the key aspects from the literature review:

- South Africa has a legacy of derelict mine infrastructure, including dormant TSFs, which requires proper closure/rehabilitation. It is the current generation's responsibility to mitigate, or at least minimise, the environmental effects as far as possible.
- Eskom generates 95% of electricity of which 93% is generated by coal fired power stations. South Africa's abundant and relatively cheap low-grade coal makes coal-fired power stations an attractive base load option, but the associated emissions have a detrimental effect on the environment. However, a global shift towards renewable energy, as well as South Africa's energy shortage, has forced the NERSA to encourage greener alternatives. This feasibility study is one of many seeking for opportunities to generate more electricity, which is sustainable and with reduced carbon emissions.
- Dormant TSFs are often more favourable locations for the generation of renewable energy resources than green field sites.
- The operating principles of both solar PV and pump storage schemes are discussed in Sections 2.5.1 and 2.6.1 respectively.
- Solar and water resources available for electricity generation can be predicted with a reasonable degree of accuracy using guidelines in Sections 2.5.2 and 2.6.2 respectively.
- Factors influencing the efficiencies of a solar PV plant and a pump storage scheme are listed in Sections 2.5.3, 2.6.3 and 2.6.4 respectively.

From the literature, it seems that there might be potential to use TSFs for solar PV and pump storage electricity production (or a combination thereof) which will be investigated by means of hypothetical feasibility analysis of an existing TSF in the remainder of this dissertation.

### **3 FEASIBILITY ANALYSIS OF ELECTRICITY GENERATION OPTIONS ON DORMANT TSFS**

#### **3.1 INTRODUCTION**

This chapter discusses the methodology followed to determine the financial feasibility of developing a solar PV plant, a pump storage scheme, or a combination thereof on the ERGO TSF, once it is decommissioned. The main aim is to find the optimal installed electricity generation capacity which generates the highest possible return on investment for each of the options. The following topics are discussed in this chapter:

- Identification of a site to base the study on
- The factors that are common to all the options considered
- Assessing the financial feasibility of the Solar PV option
- Assessing the financial feasibility of the Pump Storage option
- Assessing the financial feasibility of combining the Solar PV and Pump Storage options at ERGO.

#### **3.2 SITE IDENTIFICATION**

As mentioned in Section 2.2, many towns and cities have developed around mining hubs over the last century, the most significant of these being the city of Johannesburg. There are more than a hundred TSFs across Johannesburg, varying in area, shape and height.

Due to the economy of scale, there are advantages to developing some of the larger sites. For example, the cost per unit of electricity produced decreases as the scale of the project increases, because the fixed cost of the project is shared between more output units. Therefore, it was decided to base the study on the largest TSF in Johannesburg, namely the ERGO TSF, near Brakpan on the East Rand of Johannesburg, which can be seen in Figure 3-1. ERGO is the largest *gold* TSF in the world (Kleynhans, 2014). Not only does it currently occupy the largest footprint area of all gold TSFs in the world, it is due for expansion soon, which will almost double the footprint in size, increasing the footprint from approximately 800 ha (shown in Figure 3-2) to 1 500 ha (illustrated in Figure 3-3). The facility currently has a maximum height of approximately 85 m. The facility will be raised to a final height of approximately 140 m above natural ground level before it will eventually be closed in 2050.

Seeing that this study is probably the first high level feasibility study of many to follow to assess the possibility of generating energy from Johannesburg's dormant TSFs, it was decided to assess

the largest facility. If any of the concepts proves to be feasible, future studies can refine the concept and apply it to smaller facilities. However, if it proves *not* to be feasible for the largest facility, it is unlikely to be feasible for smaller facilities.

The ERGO site is owned by Durban Roodepoort Deep Gold Limited (DRD), specialising in the remining of abandoned TSFs. Due to advancements in the processing of gold from ore over the last century it is now feasible to extract a large portion of the remainder of gold from the tailings, which was discarded when the TSFs were first constructed. The majority of the TSFs across Johannesburg still have a sufficiently high grade of gold contained in it to make it viable for DRD to reprocess them and consolidate those to large facilities such as ERGO. This does not apply to all the TSFs across Johannesburg, as those that have been constructed in recent times do not bear a high enough grade of gold to make remining a feasible option.

According to Kleynhans (2014), the abandoned TSFs that DRD remines were given to them at no cost, as they take over the liability from the City of Johannesburg. Once all the gold bearing tailings have been remined from the facility, the footprint is revegetated and the concentration of contaminants are monitored for a period of time. Once the contaminants reach a low enough concentration, the land is given back to the city council to be reused for other purposes.

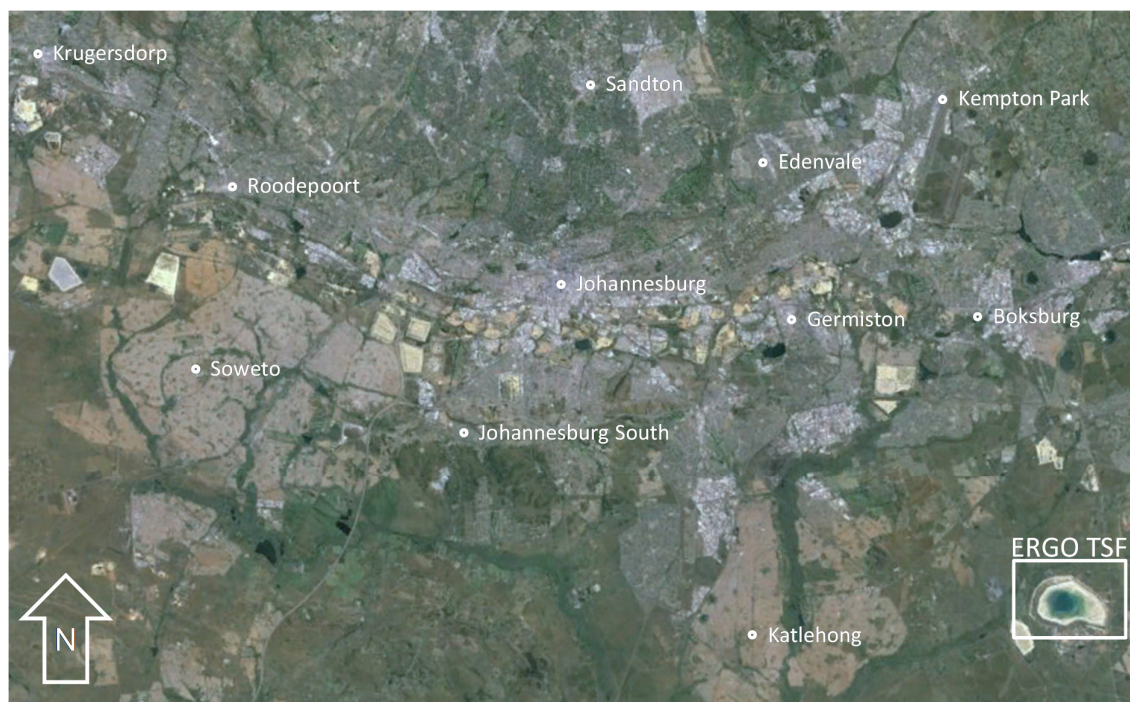


Figure 3-1 Location of ERGO relative to some of the large suburbs in Johannesburg

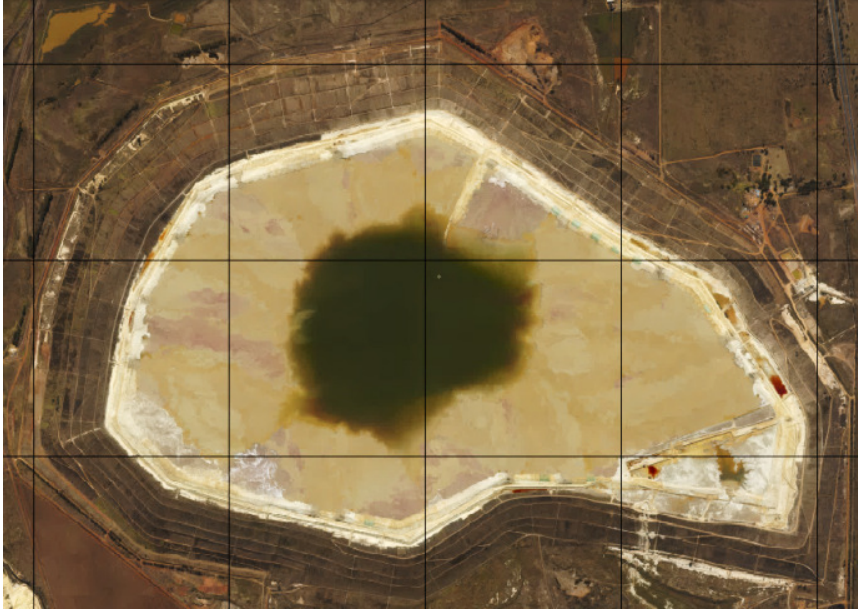


Figure 3-2: Lidar photograph of the current 800 ha ERGO footprint



Figure 3-3: AutoCAD drawing of the planned extension to 1 500 ha footprint

### **3.3 COMMON FACTORS**

The remainder of this report is focussed on determining the feasibility of developing either a solar PV plant, a pump storage scheme, or a combination thereof on the ERGO TSF, once it is decommissioned. In order to adjudicate between the three options mentioned above, it is important to compare them based on common parameters. Hence, the following section discusses all the factors that are common to all three options.

#### **3.3.1 Life of the facility**

As mentioned in Section 3.2, according to Kleynhans (2014), the ERGO TSF is only due for decommissioning and closure in 2050. Hence the following hypothetical scenario was created:

- The ERGO TSF is decommissioned with immediate effect (at the start of 2015) and a closure design is implemented (i.e. assuming that the ERGO TSF will not be re-commissioned).
- The construction of any one of the options is instantaneous, meaning the capital investment is spent immediately. Hence, all construction costs considered are in 2014/2015 Rand value (no spread of capital or inflation has been allowed for).
- The plant is commissioned immediately and electricity production can start as from 1 January 2015, i.e. the 2015 electricity tariffs (as discussed in Section 3.3.3 below) apply. All current financial conditions (for example the current inflation rate, the current prime interest rate) and electricity tariff structures applicable today will be used to assess the financial feasibility.
- All electricity tariff increases currently approved are expected to continue, until the end of the life of the electricity plant.
- Where historical weather data was used, it was assumed that the last 50 years of weather data will reoccur in the same order and magnitude.
- All options are assessed over a 50 years project life cycle.

#### **3.3.2 Assessment of financial return**

The various options were assessed based on their Internal Rate of Return (IRR) over the project lifetime and their respective reliability. Both the IRR and reliability of each option are dependent on the availability of the resource to be exploited (i.e. in the case of the Solar PV it is sunlight and in the case of the pump storage scheme it is water available to release). In the case of Solar PV electricity generation, the resource to be exploited is sunlight energy and in the case of pump

storage it is a volume of water at a high relative elevation. This is explained in greater detail in the subsequent sections.

The IRR is defined as the discount rate at which the net present value of the projected cash flow (sum of all expenses and incomes) is zero. The project cash flow consists of the initial capital investment and the operational income generated thereafter. There are two factors that determine the IRR, namely the period over which the IRR is calculated and the relative size of the operational income when compared to the initial expenditure. A positive IRR indicates that the net present value of the operational income generated over the calculation period exceeds the initial capital investment, and hence profit can be made. If the IRR is negative, it indicates a net loss, which should be avoided at all cost.

The resource available determines the income that can be generated from the development, which is to be maximised. However, it also determines the size of the infrastructure to be constructed (generating capacity), which in turn determines the initial capital investment required, of which the cost is to be minimised. Finding the optimal installed electricity generation capacity which generates the highest possible return on investment is the main aim of this study.

The initial capital expense associated with each of the options is discussed in subsequent sections. However, because the trade commodity for all the options assessed in this report is electricity, the same rates were used throughout to determine the potential income.

In order to determine whether one of the options is feasible or not, the IRR was compared to two fixed values:

- The first is inflation (approximate mean rate of change of the Consumer Price Index for 2014), currently in the order of 6.3%, it has an average of 5.9% since 1994, varying between 10.0% and -0.7% (Statistics South Africa, 2014; Trading Economics, 2014). If the IRR exceeds the current inflation percentage of 6.3% it was deemed to be an “inflation exceeding” investment, which indicates a positive change in monetary value.
- The second is the current prime interest rate (also referred to as the prime lending rate) in South Africa, which is currently 9.25% (South African Reserve Bank, 2014). If the IRR exceeds the prime interest rate it was deemed to be *feasible*.

When the Net Present Value of income over the life of the facility had to be calculated the inflation rate of 6.3% was used for this purpose.

### 3.3.3 Determining the income with Megaflex tariffs

It is assumed that all generated electricity can be fed into the electricity grid. Eskom, who regulates the national electricity grid, then sells the electricity at various tariffs. The Eskom tariffs for 2014/2015 are available on their website (Eskom, 2014f).

The ERGO TSF is located within the Ekurhuleni Metropolitan Municipality (EMM). Normally EMM buys electricity from Eskom at so-called “Megaflex tariffs” (Eskom, 2014f) and then redistributes it to the end user at various rates (Ekurhuleni Metropolitan Municipality, 2014). It is therefore difficult to allocate an average rate per kilowatt-hour for electricity fed into the grid. However, EMM can benefit from a joint venture with DRD (with whom the closure liability of the ERGO TSF lies), as any electricity fed into the grid will result in a saving for EMM on their Eskom Utility Bill.

The Megaflex tariffs at which Eskom provides electricity to EMM for re-distribution are shown in Figure 3-4 (Eskom, 2014f). It is important to note that there are seasonal and time-of-use differential tariffs. Seasonally, Eskom differentiates between a low and a high demand season, the latter being when it is winter in South Africa. Each day of the week is divided into a peak, standard and off-peak brackets for which different tariffs apply. The diagram in Figure 3-4 illustrates the different brackets based on demand in South Africa. It represents 25 peak hours, 62 standard hours and 81 off-peak hours in every week.

It is expected that these tariffs will increase with time due to inflation and other factors. The National Energy Regulator of South Africa (NERSA) announced in February 2013 that they will allow Eskom to raise their tariffs by a maximum of 7.4% per annum for the following 5 years, i.e. the period 2013/14 to 2017/18. It was assumed that Eskom’s tariffs increase will be remain constant at 7.4% per annum beyond 2018, for the 50 year life cycle, which is deemed to be a conservative assumption.

It is important to note that the tariffs that are applied to generated electricity (to determine the income of the project) are time dependent, as the time of day, the season and inflation beyond 2015 are to be taken into account. These tariffs were applied throughout the study to determine the potential income. Hence it is implied that the differential tariff structure and inflation will remain the same over the 50 year life of the facility.

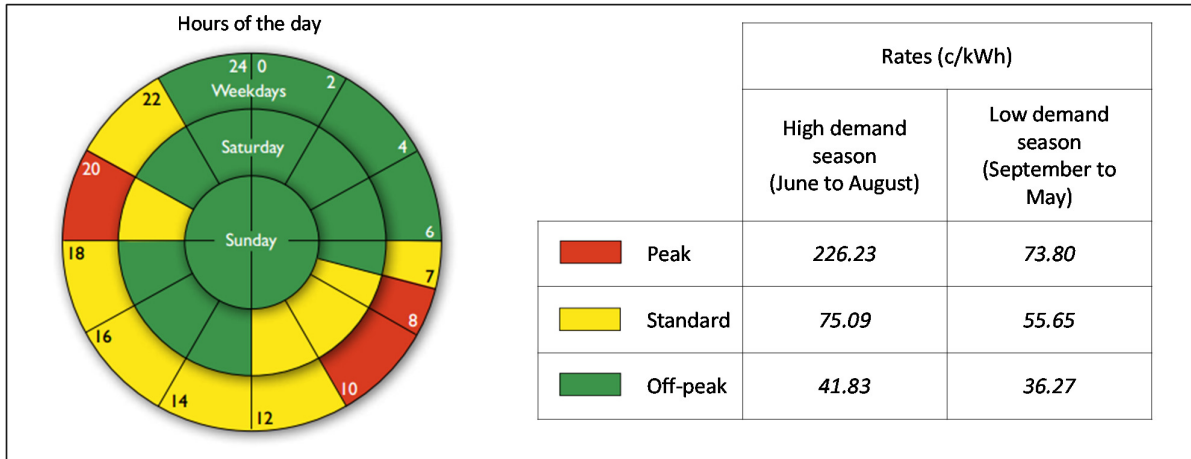


Figure 3-4: Megaflex tariffs (Eskom, 2014f)

### 3.3.4 Default option

As mentioned in the introduction in Section 1.2 one of the main objectives of the study is to find a post closure land use option that can generate sufficient income to offset the closure cost. In order to compare other options, it is important to keep the default option in mind. The default option includes the measures to be implemented as a minimum if none of the other options are chosen (discussed below). This can also be referred to as the “do nothing” option.

According to Kleynhans (2014) the current approved closure plan consists of wind erosion protection of the top and side slopes (by means of netting), whilst vegetation is established. Vegetating the facility includes seeding and fertilisation of the soil and the installation of an irrigation system. This closure plan will have the following implications:

- Reduce wind erosion.
- Result in cleaner catchment runoff. However, the runoff contamination will probably remain outside potable water standards.
- It will not prevent rainwater from seeping into the TSF.
- It will not prevent ground water contamination.
- The source of contamination will diminish with time as the contaminants will dilute and disperse. However, the polluting life of the facility will extend to many years.

It may be noted that environmental legislation may in future become more stringent, probably to include compulsory capping of these facilities. Until such time, the default option remains as described above. Should legislation become more stringent, the cost of the default option will increase considerably, which will make the other post closure land use options described in this report more attractive.

DRD is currently implementing similar closure measures (to the default option) on three of their Crown Mines TSFs near Soweto (these facilities can be seen located close to the Soccer City Stadium shown in Figure 2-4). According to Kleynhans (2014) the cost of this project is in the order of R80 000 per hectare for the rehabilitation of the top surface and R190 000 per hectare for the vegetation of the side slopes.

The on-going maintenance has to be sustained for at least 18 to 24 months, and costs for these three TSFs (combined area of approximately 450ha) add up to R1 million per month, mostly spent on fertiliser and irrigation. Hence, the final rehabilitation of the ERGO TSF, considering its final 1 500 ha footprint, will cost in the order of R260 to 280 million. It is important to note that this closure option generates no income, resulting in sunken capital to the investor.

### **3.4 OTHER BENEFICIAL POST CLOSURE LAND USE OPTIONS CONSIDERED**

Two other beneficial post closure land use options were considered for the ERGO site, namely:

- wind power generation and
- rain water harvesting

Both these options were assessed on the same principles as the post closure land use options that are to follow in this report, except that, with the rain water harvesting option, the tradable commodity is not electricity but raw water supply.

#### **3.4.1 Wind power generation at the ERGO site**

The wind power generation option was abandoned at an early stage of the study. Firstly due to the fact that a continuous wind record could not be found for the Johannesburg region. Secondly, due to the available data showing that the wind resource in Johannesburg is marginal to viably generate wind power.

Wind speed and direction data was obtained from the South African Weather Service (SAWS) for three weather stations surrounding the ERGO site. The data was only recorded once a day either at 8:00, 14:00 or 20:00. This limited data provides no indication of wind duration. Hence, it cannot be used to reliably assess the feasibility of wind power. Wind patterns are similarly unpredictable as rain and hence cannot be modelled as accurately as solar radiation, for example. A continuous monitoring record is recommended in order to assess the daily and seasonal variability of the wind at the ERGO site. Breeze (2005) recommends at least one year of long and short term wind data is required to confirm the wind regime.

With the data recorded by the SAWS (2014), a reading of 0 m/s indicates calm conditions. This occurs 17%, 39% and 21% of the time at the three respective weather stations for which data was obtained. This has a significant effect on the average wind speed at all these locations, which are 3.3 m/s, 1.6 m/s and 2.5 m/s respectively.

Studies by Blight (2007) have shown that amplification of wind speeds occur over the crest of a TSF, due to the TSF causing an obstruction in the wind's flow path. According to models/graphs by Blight (2007) the amplification factor applicable at the crest of the final 140 m high ERGO TSF would be in the order of about three times the wind typically recorded with an anemometer at a weather station (typically installed at 10 m above ground level). Hence, the average wind speeds recorded at the three stations might increase to 8.7 m/s, 4.2 m/s and 6.6 m/s respectively, if applied to the ERGO site. From the limited data that was obtained from SAWS (2014) the wind power resource at ERGO is marginal, therefore it might be viable to explore further, seeing that modern wind turbine technology can exploit wind speeds of as low as 5 m/s (Breeze, 2005). However, a continuous wind record is required to access the duration of these wind speeds.

Therefore, before any further studies are done on the possibility of constructing a wind farm on top of the ERGO TSF, it is recommended that a continuously monitoring anemometer be installed on top of the ERGO TSF. In addition, the elevation of the anemometer has to be monitored occasionally (because the TSF is still being constructed and gaining height) as wind speed is strongly related to height about ground level (or surrounding topography). Such a study is essential in order to obtain more accurate wind speed data, specifically for the ERGO site.

#### **3.4.2 Rain water harvesting from the ERGO site**

The rain water harvesting option was also abandoned at an early stage of the study, as feasibility calculations indicated that it is not financially feasible.

The communities that are most likely to benefit from such a rain water harvesting scheme are those located in close proximity to the ERGO TSF. According to the national census done by Statistics South Africa in 2011, there are at least 205 193 people living in 62 375 households in the three informal settlements directly to the East of the ERGO TSF, which include Geluksdal, Tsakane and Langaville. The closest of these is Geluksdal, which is located less than a kilometer from the toe of the ERGO TSF.

The basic water supply policy approved by Cabinet entails providing 6 000 litres of potable water per household per month *free of charge* (DWAF, 2007). This monthly water allowance is in line

with the 25 litres per capita per day defined in the DWAF's white paper of 1994, assuming an average household of eight people (DWAF, 2007; CSIR, 2005).

The projected consumption amounts to a total of approximately 375 000 m<sup>3</sup> of water per month which will have to be supplied from the rain water harvesting scheme, *for which no income will be received* as this water is supplied free of charge. The ERGO TSF catchment will be able to deliver this volume of water 98% of the time, which matches the 98% reliability specified by DWAF's white paper of 1994 (CSIR, 2005). This 375 000 m<sup>3</sup> of water, that will have to be supplied on a monthly basis, requires purification with associated operating costs (to adhere to the South African National Drinking Water Standard (SANS 241: 2005). This does not include the cost of infrastructure that will be required, including lining of the TSF basin and construction of a pipeline. Hence, it was concluded that a rain water harvesting scheme cannot be implemented unless it is subsidised. Although the subsidy route was deemed to defeat the purpose of obtaining a self-sustaining post closure land use option for the ERGO TSF, it was explored further.

Currently all water resources in the Gauteng region are being utilised and hence the water supply from the Upper Vaal River System is augmented with raw water imported from the Lesotho Highlands Water Project (LHWP) at R2.32 per cubic meter (DWA, 2014). This is the rate at which a subsidy scheme would have to pay for the water for the development of any informal settlement to provide the water free of charge. An IRR was calculated over a 50 year life cycle, using R2.32 per cubic meter rate to determine the potential income (benefit gained as this water will now come from the ERGO TSF catchment and will not have to be bought in from the LHWP) and only considering the lining cost of the ERGO TSF basin (not including any other infrastructure such as the pipeline). The calculated IRR was 2.4%. It was therefore concluded rain water harvesting from the ERGO TSF will not provide a feasible post closure land use option, even if subsidised as the current inflation rate of 6.3% exceeds the IRR of 2.4%.

### **3.5 EVALUATION OF SOLAR PHOTO VOLTAIC POWER GENERATION POTENTIAL**

The following section explains the analysis done to determine the financial feasibility of a Solar PV plant on top of the ERGO TSF. The following procedure was followed:

- Determining the available solar resource at ERGO
- Verifying the resource calculations with measured data
- Sizing the solar plant
- Calculating the output from the plant
- Allocating costs for construction

- Determining the potential income and IRR
- Optimising the solar plant to generate maximum return on investment
- Determining the reliability of energy output and associated income
- Analysing the sensitivity of assumed parameters.

### 3.5.1 Determination of the solar resource at ERGO

The generic formulae discussed in Section 2.5.2 was used to determine the theoretical solar resource available at the ERGO site.

The altitude and azimuth angles of the sun were determined at five minute intervals between sunrise and sunset for every day of the calendar year. The combination of these two angles was used to determine the position of the sun relative to the ERGO TSF and to plot a sun path diagram similar to the example in Figure 2-9. The input parameters into these equations are time of day, day of the year and the latitude of ERGO.

The ERGO TSF is so large that its latitude and longitude coordinates vary with a few minutes each. Hence an approximation was made from Google Earth to find coordinates of the centre of the facility, although it is not deemed to have a significant effect on the outcome. The following coordinates were used:

- Latitude: 26.3<sup>0</sup>S (varying between 26<sup>0</sup>20'S and 26<sup>0</sup>23'S)
- Longitude: 28.3<sup>0</sup>E (varying between 28<sup>0</sup>18'E and 28<sup>0</sup>20'E)

Once the altitude and azimuth angles of the sun were known at five minute intervals the clear sky direct beam radiation and clear sky diffuse radiation (per square meter) of area were determined, as explained in Sections 2.5.2.3 and 2.5.2.4 respectively, again at five minute intervals. The radiation caused by light reflected onto the panels from the ground and other surfaces (as illustrated in Figure 2-10) was deemed to be negligibly small and therefore ignored, which is conservative.

All formulas were calculated as a function of the collector's properties, i.e. its tilt and azimuth angles. It was assumed that the tilt and azimuth angles of the solar panels are fixed, i.e. the system will not entail a tracking system (as described in Section 2.5.1). According to SolarEff (2014) the increase in absorbed light (if the sun is tracked) and resultant increase in electricity output, does not justify the additional capital expenditure and maintenance cost.

By adding the clear sky direct beam and diffuse radiation components the solar resource was determined at the ERGO plant. This is the maximum power (in a unit of watts) that can be expected at ERGO under ideal clear sky conditions. As mentioned in the literature review in

Section 2.5.1, at around twelve noon on a cloudless day the result is expected to be between 1.0 kW and 1.4 kW of power on every exposed square meter (Zweibel, 1990, Breeze, 2005). By multiplying the maximum power with 5 minute time intervals (one twelfth of an hour) the maximum energy (in a unit of kilowatt-hour) provided by the sun was determined. The maximum energy of each 5 minute interval was then added to determine the cumulative daily energy total. It is expected to be between 5 to 9 kWh of energy for every square meter of exposed area (Zweibel, 1990, Breeze, 2005).

The skies are not always clear, therefore conditions are not always ideal and therefore the numbers mentioned above are not necessarily realistic. Hence, some adjustment has to be made for cloud cover.

### **3.5.2 Verification of resource calculations with NASA data**

In order to know whether the data calculated in Section 3.5.1 is of the correct order of magnitude it was necessary to compare it with known values. NASA has calculated solar energy data using the Pinker/Laszlo shortwave algorithm and added cloud cover data from the International Satellite Cloud Climatology Project to produce a realistic solar energy data base. The data is available free of charge on the internet (NASA, 2014). It provides 22 years of radiation data from 1 July 1983 to 30 June 2005. NASA divided the globe into one degree longitude and one degree latitude regions. The red block in Figure 3-5 shows the region between the latitudinal coordinates 26° and 27° South and the longitudinal coordinates 28° and 29° East within which the ERGO site is located. This region covers an area of approximately 11 100 km<sup>2</sup>, but it is believed that the solar resource conditions will have limited variation within this region.

The NASA data lists total clear sky radiation, diffused radiation and actual radiation, all on a horizontal surface (hence no reflected radiation). The NASA data has a unit of kilowatt-hour per square meter of area per day (kWh/m<sup>2</sup>/day). The 22 years of data was converted to one calendar year by calculating the average for every calendar day in order to compare it with the data calculated in Section 3.5.1.

The first objective was to verify the calculations discussed in the previous section with recorded data, by assuming the tilt angle of the collector is zero degrees (to simulate a horizontal surface).

The second objective was to calculate a cloud cover factor for every calendar day of the year. This was done by dividing the actual radiation with the total clear sky radiation and then calculating the average for each calendar day over the 22 year record. This cloud cover factor is then multiplied with the calculated data to determine a *realistic* solar resource estimate.

The reasons why the NASA data was not used directly as the basis for this study are:

- It only provides daily radiation data. Due to the fact that the tariff structure used for this study applies different rates at different times of day, it was necessary to calculate the data in finer increments.
- The calculations in Section 3.5.1 are essential in order to optimise the plant.

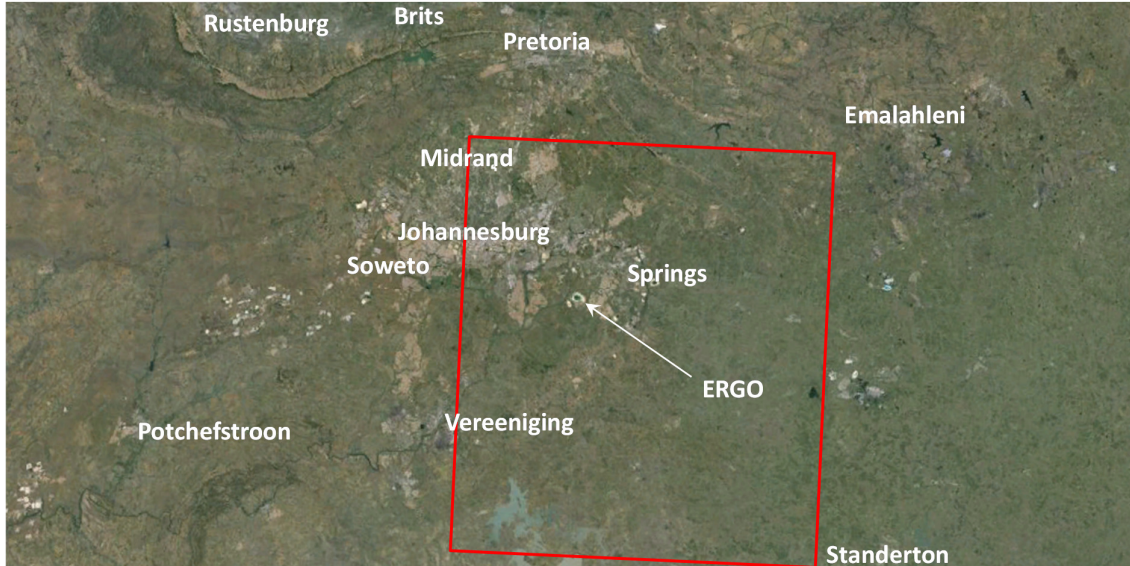


Figure 3-5: Region for which the NASA solar data is applicable

### 3.5.3 Determining the size of the solar plant

Once it is known that the calculations provide accurate results and the daily cloud cover factors are known, the plant can be sized. It was decided to base the sizing of the plant on SolarEff's recommendations (SolarEff, 2014). SolarEff is a solar supplier located in Roodepoort Johannesburg. They specialise in roof top installations in the Johannesburg region. SolarEff recommended to use Yingli Solar's YGE 60Cell 40mm Series of solar panels (Yingli Solar, 2012). These panels have dimensions of 1 650 mm in length, 990 mm in width and are 40 mm thick. It was decided to place them in arrays of 4 wide and 60 in length, i.e. a total of 240 panels per array, as illustrated in Figure 3-6. Each array has dimensions of 99 m in length and approximately 4 m wide. The array can then be tilted to face to sun and to optimise production. Once tilted the 4 m dimension will then be the diagonal dimension.

The spacing of the arrays is dictated by the shadow angle (as explained in Section 4.1.1) and tilt angle of the array respectively and can be calculated as shown in Figure 3-7.

It was decided to put 15 arrays in a block and allow 10% of the block dimensions for service corridors to determine the dimensions of a single block, as per Figure 3-8. It was assumed that only the top of the TSF will be covered with solar panels and not the side slopes as well. It was assumed that close to the end of the life of the facility an “aggressive step in” method of tailings deposition will be adopted, to fill the basin of the TSF and create a flat top surface on top of the TSF. The area of the top surface of the TSF at the final 140 m height (at closure) will be approximately 726 ha. This total area was divided by the dimensions of a single block to determine how many of these blocks can be constructed on top of the TSF. The number of blocks was then multiplied with 15 arrays per block and 240 panels per array to calculate the total number of panels that can be fitted on the top flat surface of the TSF.

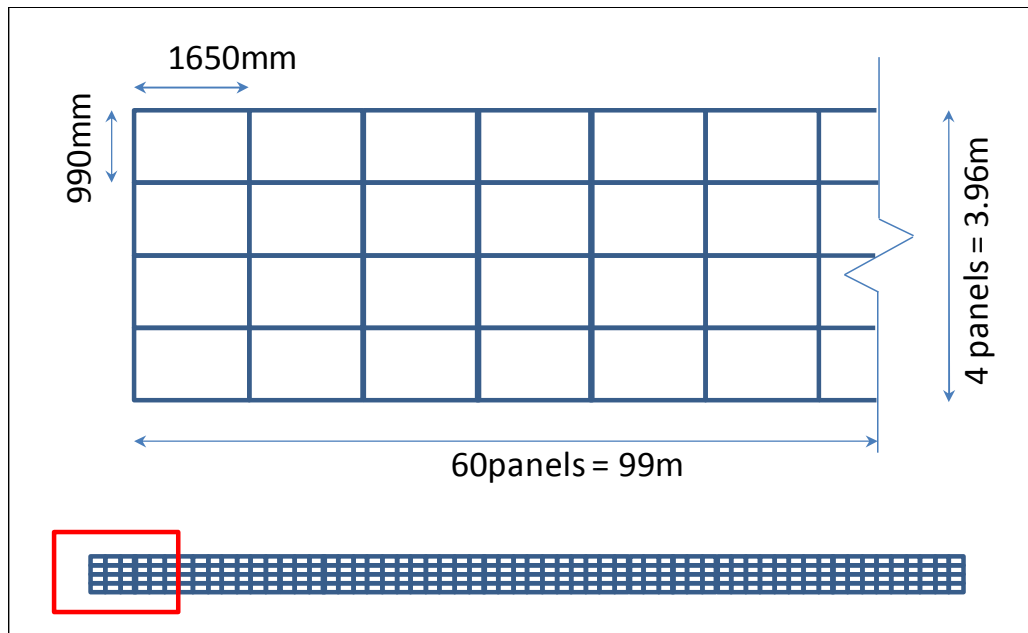


Figure 3-6: Placement of panels in arrays

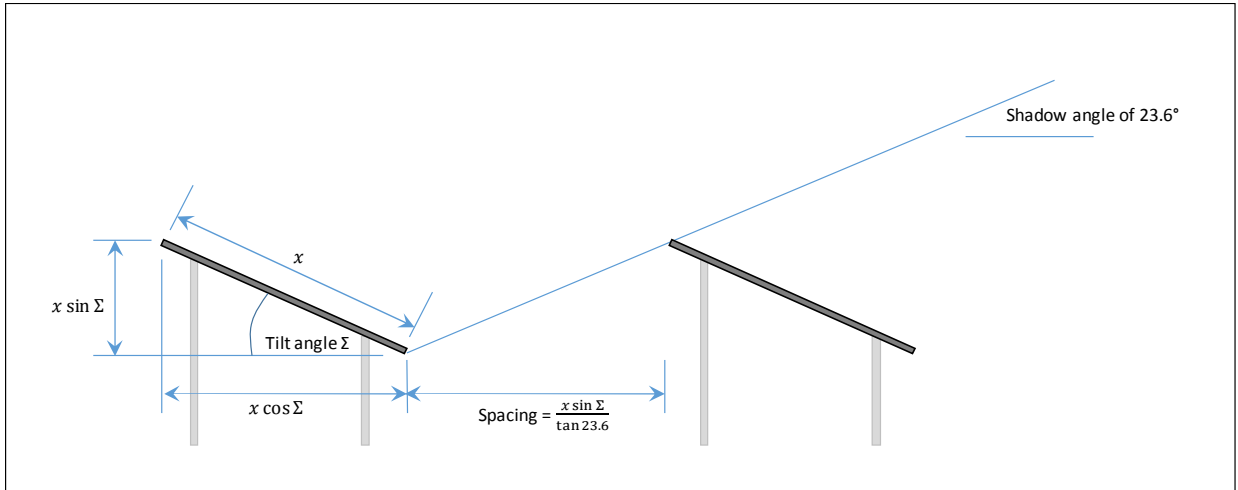


Figure 3-7: Determination of the spacing of arrays

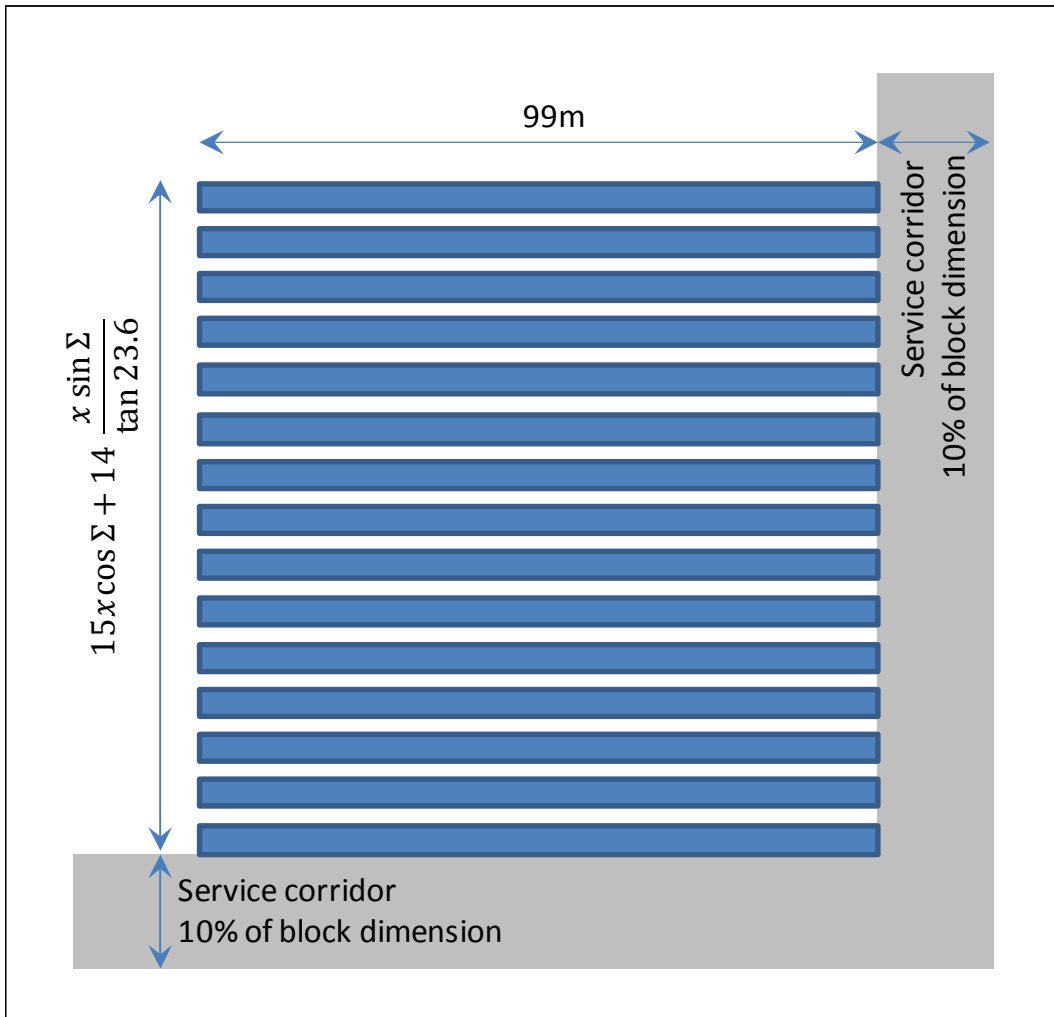


Figure 3-8: Layout of a block of arrays

### 3.5.4 Determination of the plant output

Once the number of panels was known, the total panel area was calculated. The total panel area was then multiplied with the total clear sky radiation on an inclined surface and multiplied with the cloud cover factor as determined in Section 3.5.2. The outcome is the sun's potential ( $SP$ ) on any given day during the calendar year if the ERGO TSF was covered in blocks of solar panels as explained above.

Solar panels are not 100% effective in converting the sun's potential into solar power. Hence the efficiency of the solar panels are to be taken into consideration, as well as the degradation in plant performance with time.

The efficiencies ( $\eta_{SP}$ ) of the Yingli Solar's YGE 60Cell 40mm Series (Yingli Solar, 2012) vary between 14.1% and 15.9% under standard test conditions. It was decided to assume an average value of 15.0% for the basic calculations and then assess the sensitivity of the outcome to a change in efficiency in the sensitivity analysis section of this report.

Mention is made of the standard test conditions, because the efficiency is measured at a temperature of 25 °C. It is known that temperature of a solar cell is indirectly proportional to the cell's efficiency, i.e. if the temperature rises, the efficiency decreases. However, due to the elevation of the TSF site, the fact that only the top of the TSF is to be covered with solar panels and the open mounting structure, a continuous draft of wind should keep the panels at a reasonably moderate temperature. Hence no additional reduction in efficiency due to temperature change has been allowed for.

Solar plants have finite life spans. It is known that the power output diminishes with time. However, the supplier warrants that:

- After ten years the plant will still operate at 91.2% of the minimal rated power output (average degradation of 0.88% per annum).
- After 25 years it will still operate at 80.7% of the minimal rated power output (average degradation of 0.70% per annum).

These degradation values were assumed in the analysis. There are no warranties of performance beyond 25 years. It was assumed that the same rate of degradation from 10 to 25 years will apply beyond 25 years (average of 0.70% per annum). A sensitivity analysis was conducted in Section 3.5.9 and the results discussed in Section 4.1.9, to assess the influence of a potential change in the assumed degradation rate.

The sun's potential was multiplied with the panel efficiency and degradation to determine the daily production of a solar plant on the ERGO TSF site over a 50 year life cycle.

### 3.5.5 Allocation of construction costs

SolarEff (2014) provided indicative cost estimates for this project. Their prices were as follows:

- Supply of the solar panels (only) will cost R9 to R10 per watt-peak (defined below).
- Supply of the whole system, including panels, mounting structures, direct current cables and inverters (to invert DC current to AC current to connect to the grid) will cost about R17 per watt peak
- Supply and installation of the whole system will cost in the order of between R20 and R22 per watt peak.

These prices are applicable to large scale projects and can therefore not be used to obtain a cost estimate for small scale projects. The rate of R22 per watt peak was used as a conservative estimate for construction cost of the plant. The sensitivity of this assumption is assessed in the sensitivity analysis in Section 3.5.9.

Watt-peak is a term used in the solar power industry to rate solar panels and is the output of a solar panel when subjected to standard test conditions (STC). A 250 watt-peak solar panel will provide between 250 and 255 W (0 to 5W power output tolerance) of power when exposed to 1000 W/m<sup>2</sup> of irradiance, directly from above (zero degree incidence angle) at a constant 25 °C cell temperature. These are the standard test conditions as stipulated by EN 60904-3. The cost of panels are based on this watt-peak rating. The STC outputs of the Yingli Solar's YGE 60Cell 40mm Series vary between 230 and 260 watt peak (Yingli Solar, 2012), as shown in Table 3-1. It was decided to use the 245 watt peak panel as the basis for this study (as it is the panel with a 15% efficiency assumed earlier). The efficiencies can be verified, with the following formula:

$$\eta_{SP} = \frac{\text{panel performance under STC}}{\text{STC irradiance} \times \text{panel dimensions}} = \frac{245Wp}{1000W/m^2(1.65 * 0.99)} = 15\%$$

Hence, for the purpose of this study the installation of a single panel will cost R5 390.00. The total cost of construction will be the total number of panels calculated in Section 3.5.3 multiplied with the unit cost. The final cost will be in the order of several billion Rands (see results in Table 4-1) and therefore small cost items such as connection to the national electricity grid has been ignored (assuming that the local grid can evacuate the generated power).

The power output capacity of plant is also rated in terms of watt-peak, calculated by multiplying the number of panels with the power output of a single panel. This output capacity is often also referred to in industry as the "nameplate" capacity. This nameplate capacity is what the plant would produce if it is exposed to 1 000 W/m<sup>2</sup> of irradiance. However, this is not the maximum

plant output (as the sun's irradiance occasionally exceeds 1 000 W/m<sup>2</sup>), as illustrated by the results in Section 4.1.5.

Table 3-1: Performance and corresponding efficiencies for various panels (Yingli Solar, 2012)

Panel performance under STC (Watt-peak)	230	235	240	245	250	255	260
Corresponding panel efficiency (%)	14.1	14.4	14.7	15.0	15.3	15.6	15.9

### 3.5.6 Determination of potential income and IRR

The Megaflex tariff structure as discussed in Section 3.3.3 allows for different tariffs per kilowatt-hour for electricity generated during different times of day (hereafter referred to as Megaflex time brackets).

In order to calculate the income that can be generated the amount of electricity generated in every time bracket was multiplied with the tariff applicable to every Megaflex time bracket.

In order to calculate the amount of electricity generated (in kWh) the following expression was used:

$$\text{Electricity generated} = SP \times CCF \times \text{Solar Panel Area} \times \eta_{SP} \times \text{degradation factor}$$

Where  $SP$  is the sun's potential, i.e. the maximum energy provided by the sun in 5 minute time intervals (the outcome of Section 3.5.1) are added for each Megaflex time bracket to determine the clear sky solar potential for that time bracket (in kWh/m<sup>2</sup>).

$CCF$  is the cloud cover factor, the outcome from Section 3.5.2 (dimensionless).

Area of solar panels, outcome from Section 3.5.3 (m<sup>2</sup>)

$\eta_{SP}$  is the efficiency of solar panels, assumed to be 15% as motivated in Section 3.5.4.

Degradation factor which is time dependent, motivated in Section 3.5.4.

Once the amount of electricity generated in each time bracket was determined, the applicable Megaflex tariff identified as per Section 3.3.3 and the inflation of Eskom tariffs was determined.

With this the potential income for each time bracket over the 50 year operational life was calculated.

By adding the income from each of the time brackets the annual income was calculated. By sorting the annual income for each year and using the construction cost calculated in Section 3.5.5 the IRR was calculated with an Excel function.

Seeing that this site will not have battery storage (usually the item that requires the most maintenance), once installed this solar plant will require minimal operation and maintenance. In fact it can be controlled via a remote computer and therefore no one is required on site (Breeze, 2005). Occasional cleaning and servicing of panels might be required, but these costs are deemed to be negligible compared to the overall cost of installation.

### **3.5.7 Optimisation of the plant to generate maximum return on investment**

As mentioned in Section 3.5.1, all formulas were calculated as a function of the collector's properties, i.e. its tilt and azimuth angles. The aim of this optimisation exercise was to determine the optimal orientation of the panels to generate the maximum IRR over its 50 year life cycle. The solver function of Microsoft Excel was used to determine the optimal combination of tilt and azimuth angles of the arrays. It uses an iterative approach to search through various combinations, in order to find the optimal combination which maximises the IRR of the plant.

### **3.5.8 Reliability of daily plant production and associated income**

Once the daily electricity production and its associated income were calculated, some statistical analysis of the data was conducted to determine the reliability of the plant (to produce a certain amount of electricity and income in a day). This was done by determining the percentage of time that the calculated production was above a certain value  $x$ . This was then assumed to be the reliability of the plant to produce at least  $x$  kilowatt hours or Rands in a single day of operation. The spread of daily production values was also determined and plotted on discrete distribution histograms. An attempt was made to find a representative continuous normal distribution which matches the discrete histogram, which can be used as an estimating tool of the probability that the plant will produce daily electricity or income within a certain range. The results of this reliability analyses are shown in Section 4.1.8.

### 3.5.9 Sensitivity analysis

Various assumptions were made through the previous sections and this section was aimed at assessing the sensitivity of the IRR to a change of the assumed parameters. This was done by calculating the IRR for a range of values that the assumed parameter can possibly be (whilst keeping all other variables constant). The following assumed parameters were assessed and results discussed in Section 4.1.9.

- Panel performance, which include panel efficiency and watt-peak value, which is interdependent (assumed in 15% and 245 Wp in Section 3.5.4 and 3.5.5 respectively).
- Degradation of the plant performance beyond 25 years (assumed to be 0.70% per annum in Section 3.5.4).
- Unit capital cost (assumed to be R22/Wp in Section 3.5.5).
- Total area available for construction of the plant (assumed to be 276 ha in Section 3.5.3), in order to obtain a first order estimate for smaller TSFs.

## 3.6 EVALUATION OF PUMP STORAGE SCHEME DEVELOPMENT POTENTIAL

The following section explains the assessment of the financial feasibility of developing a pump storage scheme on top of the ERGO TSF. The following procedure was followed:

- Determining the volume of water available for power generation at ERGO
- Determining the daily release and pumping volumes
- Calculating the power generation and pumping capacities
- Determining the potential income that can be generated and consumption cost
- Allocating costs for construction
- Determining the optimum release rate to generate maximum return on investment
- Analysing the sensitivity of assumed parameters.

### 3.6.1 Determination of the water resource available for power generation

The commodity being sold is hydroelectricity, and hence the required resource is a volume of water at a high elevation. The master plan for this option is to use the rainwater from the TSF catchment to generate electricity, as illustrated in Figure 3-9. As explained in Section 2.6.1, the basic operating principle of a pump storage scheme is to release water from one reservoir (at a high elevation) to another (at a lower elevation) where it is contained until it is pumped back to the top reservoir.

For the purpose of this study it was assumed that only the water from the TSF and lower reservoir catchments will be used and it will not be supplemented from an external source.

Releasing the water entails opening a valve/slucice in the outlet pipe (a conduit pipe between the upper and lower reservoirs) to allow water to flow through a turbine connected to a generator which produces electricity. This is typically done during the peak consumption period, when the demand and applicable electricity tariffs are high. The water is accumulated in a lower reservoir and then pumped back to the pond on top of the TSF (upper reservoir), when the demand and applicable electricity tariffs are low and when there is surplus electricity in the national electricity grid.

In order to determine the generation potential of the pump storage scheme the volume of water available (the resource) was determined by means of a water balance calculation. The discussion of the assumptions made in the water balance modelling is the aim of this section.

The resource available can be estimated with reasonable accuracy by carrying out a water balance of the ERGO TSF site. The water balance simulates a reoccurrence of the rainfall record and then determines theoretical values for the daily flow and attenuation of water within the pump storage system.

Weather data was obtained from the South African Weather Service (SAWS, 2014) for four of their weather stations surrounding the ERGO TSF, namely:

- Johannesburg international airport (SAWS station number 04763989/04763990 with a 55 year record)
- Nigel (SAWS station number 04768350 with a 25 year record)
- Springs (SAWS station number 0476762A3 with a 21 year record)
- Vereeniging (SAWS station number 04387843 with a 23 year record)

The data was recorded daily and consist of various parameters. These parameters include minimum and maximum temperatures, daily rainfall, wind speed, wind direction and relative humidity. Three of the four stations have records for all the parameters. The Vereeniging station only has rainfall data available. A summary of the weather data is provided in Appendix A. The data from the Airport station was predominately used throughout the study, first because it has the longest record. It is the only record which is longer than the 50 year projected life cycle of this project. Secondly, because it was the most complete data set, the average of the other data sets was only used where gaps were found in the Airport data set.

The water balance (as explained in Section 2.6.2) is based on the principle of conservation of mass in a closed system. The difference between the inflows and outflows from the system,

should match the change in volume which is contained in the system. The water balance modelling was done in daily time steps, because the weather data was recorded in daily time steps and therefore provides the most accurate results with the data available.

Figure 3-10 shows the water balance diagram used for the pump storage scheme (hereafter referred to as the system) at the ERGO TSF. It was assumed that the only inflow into the system (adding water to the system) is rainfall on the TSF and the lower reservoir catchments. The outflows (loss of water from the system) consist of evaporation from the TSF pond and lower reservoir area, as well as seepage of water into the tailings of the TSF (which is either locked up in interstitial pores and is collected by the drainage system or seeps into the groundwater regime). The volume of water contained within the system is either contained in the TSF pond (upper reservoir) or the lower reservoir, or is circulated between them.

Allocation of values to the inflows, outflows and containment volumes are discussed below.

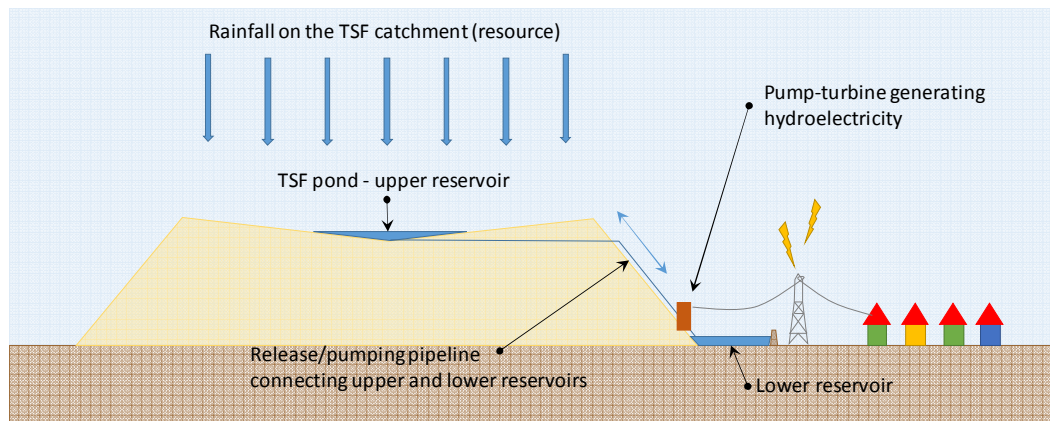


Figure 3-9: Illustration of pump storage scheme configuration on a TSF

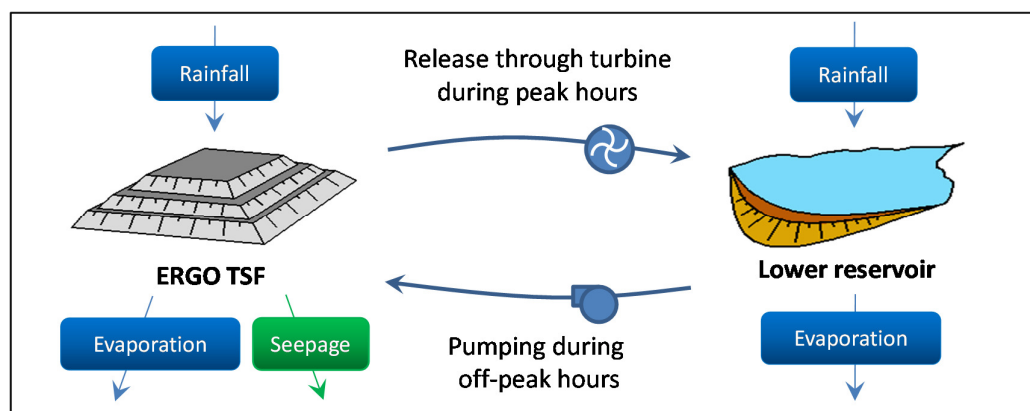


Figure 3-10: Water balance diagram for a pump storage scheme at the ERGO TSF

### 3.6.1.1 *Inflow due to rainfall runoff*

The inflows into the system consist of rainfall on the catchments of the TSF and attenuation dam respectively.

Rainfall runoff (m<sup>3</sup>/day) for each of the respective catchments is calculated with the following formula:

$$\text{Rainfall runoff} = \text{Daily rainfall} \times \text{catchment area} \times \text{runoff factor}$$

Where *Daily rainfall* (mm) from the rainfall record is converted to rainfall depth (m).

The areas of the respective catchment (m<sup>2</sup>) used for the modelling are indicated in Table 3-2.

The runoff factors (dimensionless) allocated to each of the respective catchments are shown in Table 3-2. These are general default factors that are used in practice if there are no measured data with which to calibrate the system.

As mentioned above, the rainfall depth was taken from the rainfall record. The mean annual precipitation (MAP) for the site was calculated from the record to be in the order of 693 mm. It is similar to the 684 mm MAP proposed for the quaternary sub-catchment C22c (within which the ERGO TSF is located) by Midgley et al. (1995).

The final landform of the 140 m high ERGO TSF was modelled in AutoCAD Civil 3D, of which an illustration is shown in Figure 3-11. This was done by extrapolating the current 1:3.5 side slopes of the TSF to an elevation of 1 695 mamsl (its final elevation envisaged for closure in 2050).

For water balance modelling purposes the TSF was divided into four distinct catchments, each with its own area and runoff factor, namely, the pond area (blue area in Figure 3-11), the “wet” and “dry” beach areas (combined green area in Figure 3-11) and the side slopes (grey graded area in Figure 3-11).

The area of the top of the TSF (blue and green areas combined) was measured from the AutoCAD model at approximately 850 ha at closure. The side slopes of the TSF measures to be approximately 650 ha. Hence the total catchment area contributing water for power generation is approximately 1 500 ha.

The area of the TSF pond was calculated on a daily basis as a function of the volume of water in the pond, discussed in Section 3.6.1.4. All rain that falls directly onto the water surface of the pond will contribute to the volume of the pond and hence a runoff factor of 100% is applicable.

The remainder of the top area of the TSF (top area minus the pond area, i.e. the green area in Figure 3-11) is then divided into two distinct catchment areas namely the saturated “wet” beach and the unsaturated “dry” beach (with a 20% and 80% split of the remainder of the top catchment respectively). The split has been calibrated with measured pond volume data during previous water balance studies done for other TSFs in South Africa (FWA, 2013; PBA International SA, 2011).

Deposition of tailings on a TSF (during its operational years) takes place on the perimeter of the TSF. The coarsest particles settle out first. As the slurry flows down the beach towards the pond, the beach slope flattens which decreases the flow velocity of the slurry and causes the finer particles to settle out. Hence, the water flowing into the TSF pond carries the finest particles, which then settle out beneath the pond. The resultant cross-section of the TSF looks approximately as illustrated in Figure 3-12 (applied to the ERGO TSF from a guideline document published by the Chamber of Mines of South Africa, 1996).

As the particles sizes decrease from the wall, down the beach towards the pond, the pore spaces between particles decrease, which causes the permeability of the tailings to decrease with orders of magnitude difference between the tailings in the wall and that beneath the pond. An example of this is shown for a *diamond* TSF with the graph in Figure 3-13. The result is that the lower the permeability of the tailings (closer to the pond), the slower the seepage rate of the interstitial water (water contained in the pores) and the higher the runoff factor to be applied to rainfall. Hence, the runoff factors for the “wet” beach are higher than for the “dry” beach as can be seen in Table 3-2.

Although the runoff from the side slopes (grey area in Figure 3-11) cannot gravitate towards the TSF pond, the rainfall runoff from the side slopes was also taken into account, because this water can be diverted to the lower reservoir via runoff canals. It therefore contributes to the water in the system.

The runoff factors for the side slopes, wet and dry beaches were initially based on guidelines given for the rational deterministic method in the SANRAL Drainage Manual (SANRAL, 2007) and was refined with calibration data of previous TSF water balance studies.

It has also been found with previous water balance studies that the runoff factors does not remain constant, but increases as the top layer of tailings is saturated following a few days of constant rain. To account for this the effect, the rainfall patterns over the previous five days in the rainfall record were taken into account. The minimum runoff factors were applied if no rainfall occurred over the previous five days. It was increased by 20% of the differential for every day that rainfall

did occur and reached a maximum value if it rained all of the last five days. Only the number of rain days was taken into account, not the volume of rainfall that occurred.

The lower reservoir does not exist yet and it was assumed that it will be constructed as part of the pump storage scheme development. The rainfall runoff water will be contaminated by the contaminated tailings catchment area and hence Section 19 of the National Water Act, Act 36 of 1998, as amended, will apply. Environmental legislation will most likely require for the lower reservoir (which will be newly constructed under current legislation) to be lined with a suitable lining system such as those suggested in the Minimum Requirements for Waste Disposal by Landfill (DWAF, 1998). Hence, a runoff factor of 100% was applied to the lower reservoir area. Its area and capacity was determined as a function of the volume that has to be contained, which is a function of the optimal release rate between the top and bottom reservoir.

Table 3-2: Catchment areas and allocated runoff factors (PBA International SA, 2011)

Catchment	Sub catchment	Catchment area	Runoff factors	
			Ranging from	Ranging to
TSF	Pond	Varies as a function of pond volume	100%	100%
	Wet beach	20% of remainder of top catchment	40%	90%
	Dry beach	80% of remainder of top catchment	5%	50%
	Side slopes	Constant 650ha (6 500 000m <sup>2</sup> )	5%	50%
Lower reservoir	Lined	Constant (function of maximum simulated volume)	100%	100%



Figure 3-11: Illustration of envisaged TSF catchment area at closure

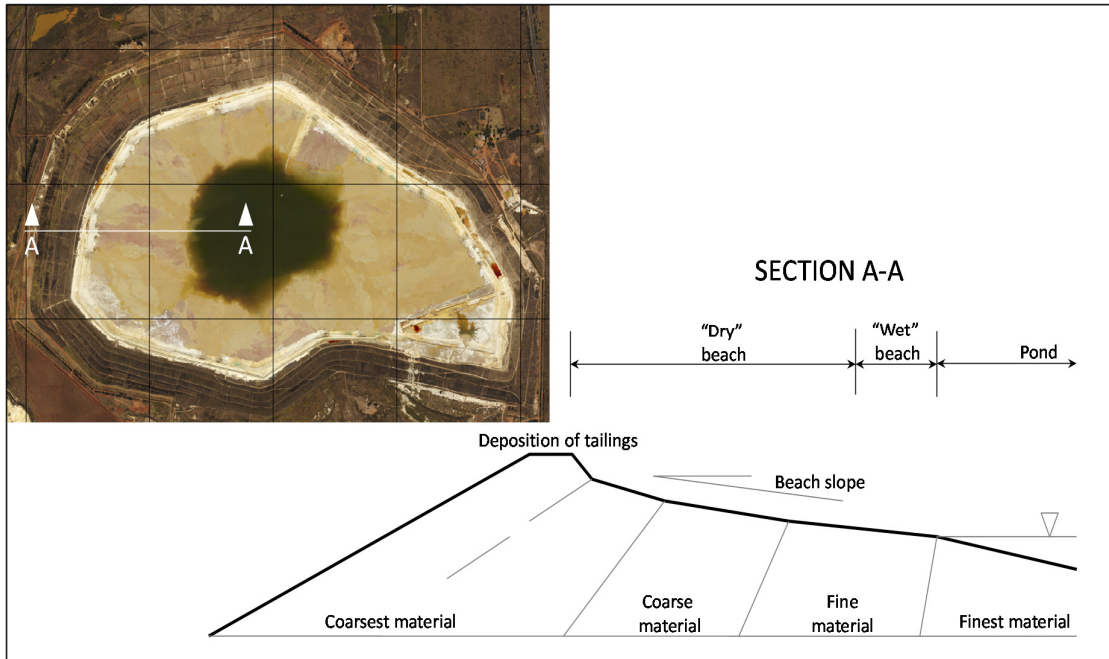


Figure 3-12: Typical distorted cross-section of a TSF (Chamber of Mines of South Africa, 1996)

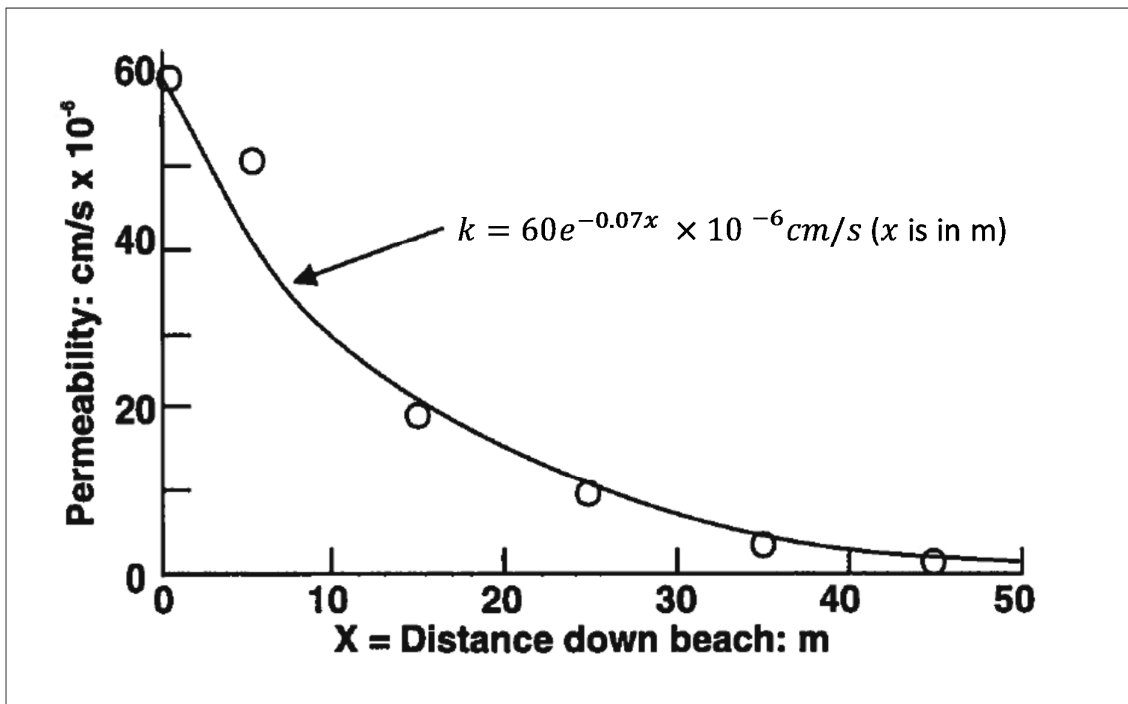


Figure 3-13: Example of the variation of permeability with distance down the beach of a diamond TSF (Chamber of Mines of South Africa, 1996)

### 3.6.1.2 *Losses due to evaporation*

The weather data record obtained from the South African Weather Service does not explicitly provide daily evaporation depth ( $ET_0$  in mm per day). Hence, it had to be estimated using the other available weather parameters. It was estimated using the following simplified version of the FAO-56 Penman-Monteith equation (Valiantzas, 2013):

$$ET_0 \approx 0.0393R_S\sqrt{T+9.5} - \left(22.46 \left( \frac{R_S\phi^{0.15}}{[4\sin(2\pi J/365 - 1.39)\phi + 12]^2} + 0.92 \right)^2 \right. \\ \left. - 0.024(T+20) \left(1 + \frac{RH}{100}\right) - 0.0165R_S u^{0.7} \right. \\ \left. + 0.0585(T+17)u^{0.75} [(1.03 + 0.00055TR^2) - RH/100] + 0.0001Z \right)$$

Where:  $R_S$  is the solar radiation (MJ/m<sup>2</sup>/day)

$T$  is the average daily temperature (in °C), i.e. average between the minimum ( $T_{min}$ ) and maximum ( $T_{max}$ ) temperatures

$\phi$  is the latitude angle of the ERGO site (radians)

$J$  is the Julian calendar day number for the day for which the evaporation is required

$RH$  is the relative humidity (%)

$u$  is the wind speed (in m/s)

$TR$  is the difference in daily temperature (in °C) between the minimum ( $T_{min}$ ) and maximum ( $T_{max}$ ) temperatures

$Z$  is the elevation of the ERGO site (in meters above mean sea level)

It can be seen that the Valiantzas (2013) equation above is rather complex, taking numerous weather parameters into account. It was calculated for each day of the rainfall record, using the weather data supplied by the South African Weather Service.

The mean annual evaporation (MAE) calculated for the site is in the order of 1 403 mm. The calculation of MAE is of the same order of magnitude as the 1 625 mm proposed for the quaternary sub-catchment C22c, Evaporation zone 11A (within which the ERGO TSF is located) by Midgley et al. (1995). This is approximately double the depth of the MAP, which was stated earlier as 693 mm. This indicates a net negative water balance, meaning that the volume of water lost due to evaporation from an exposed water surface of  $X$  m<sup>2</sup> would be roughly double the volume of water gained from rainfall on the same area (assuming a runoff of 100%). However,

with the ERGO TSF, the rainfall catchment is approximately six times larger (although the runoff factor is not 100%) than the average exposed pond surface from which evaporation occur.

Once the daily evaporation depth (m) was determined, it was multiplied with the TSF pond surface area (m<sup>2</sup>) to determine the evaporation volume (m<sup>3</sup>) from the TSF pond. The TSF pond surface varies daily (the same are the area to which the 100% rainfall runoff factor applies in Table 3-2). The evaporation depth is also multiplied with the lower reservoir water surface to determine the evaporation volume lost from the lower reservoir on a daily basis.

### 3.6.1.3 *Losses due to seepage*

Seepage of rain water into the unsaturated pores of the beach material has been accounted for with the allocation of suitable runoff factors in the Section 3.6.1.1. However, continuous seepage of water takes place from the pond. This accounts for a significant component of water losses from the system. Seepage losses are a difficult component to estimate accurately due to the wide range of permeability values of the tailings (varying by orders of magnitude). The seepage flow rate was based on Darcy's empirical law:

$$q = k i A$$

Where:  $q$  is the flow rate (m<sup>3</sup>/day)

$k$  is the coefficient of permeability (m/day)

$i$  is the hydraulic gradient, assumed to be 1.

$A$  is the cross-section area (m<sup>2</sup>) of tailings through which flow occurs, i.e. the area of the pond (variable).

The coefficient of permeability was derived from excess pore water pressure dissipation tests conducted during a Cone Penetration Test (CPTu) investigation conducted at the ERGO site in May 2014 (FAT, 2014). A conservative estimate of  $1.5 \times 10^{-8}$  m/s was used based all the available results and converted to meters per day. The seepage (m<sup>3</sup>) was then estimated on a daily basis based on the size of the TSF pond on a given day.

### 3.6.1.4 *Modelling of water stored in the TSF pond and lower reservoir*

The inflows and outflows to and from the TSF pond, illustrated in Figure 3-10, were quantified as accurately as possible on a daily basis. The difference between the inflows and outflows amounted to the volume of water stored in the TSF pond. For the purpose of modelling, the shape

of the TSF pond was assumed to resemble an inverted cone. It was assumed that the beach slope (measured from a recent Lidar survey of the ERGO TSF) will remain the same until it reaches its final height of 140 m. With an average measured beach slope of 1:300 (V:H), it was possible to estimate the depth and area of the pond based on the daily storage volume, with the following formulae:

$$TSF \text{ pond depth} = \sqrt[3]{\frac{Volume \text{ in TSF pond}}{30\,000\pi}}$$

$$TSF \text{ pond surface area} = \sqrt[3]{810\,000\pi(Volume \text{ in TSF pond})^2}$$

The volume in the lower reservoir was determined by adding the daily rainfall on its catchment, and water released from the upper reservoir. The evaporation from its water surface and the pumping that takes place from the lower reservoir were deducted.

The above sections discussed all the assumptions made to determine the volume of water in the system (the resource) available for power generation. The following sections are aimed at determining the flow within the system (release and pumped between the upper and lower reservoirs), which either generates or consumes electricity. Cost implications of the development are discussed in the following sections.

### 3.6.2 Determining the flow between the upper and lower reservoirs

Certain operational rules were simulated within the water balance model to determine the allowable flow between the two reservoirs. In order for  $X$  m<sup>3</sup> of water to be released from the top to the lower reservoir, three conditions had to be satisfied:

- There has to be a sufficient volume (more than  $X$  m<sup>3</sup>) of water (above the dead water volume) in the upper reservoir to be released.
- There has to be sufficient retention capacity in the lower reservoir to receive the released water.
- To minimise the volume of water that has to be contained in the lower reservoir (which is still to be constructed), the volume of water released to the lower reservoir on any given day has to be returned to the top reservoir on the same day during the off-peak hours.
- The maximum release/pumping volumes are limited by the outlet pipe size (which governs the turbine and pump capacities respectively).

The same rules apply for the pumping of water from the lower to the top reservoir.

Based on the water balance simulation model, the amount of water available for release on any given day during the rainfall record was estimated. For the purposes of the financial model it was assumed that the rainfall record will reoccur.

The release rate and the timing of release of water are the only controllable variables in the setup and operation of the pump storage system. The release rate dictates the outlet pipe size and electricity generating capacities respectively.

All other parameters are either dictated by the TSF's final geometry (such as the height of the facility and the length of the outlet pipe), the properties of the water or the properties of the pump-turbine system (which is to be engineered to be as efficient as possible). All of these parameters have limited controllability and are therefore assumed to be fixed.

The timing of the releases are dictated to a large extent by the electricity tariffs. In order to generate the highest possible daily income, electricity is to be generated and consumed when the tariffs are at its highest and lowest respectively. It is therefore assumed that water will be released through the turbine to generate electricity during the peak consumption period, when the demand is high. This is the case for 5 hours per day on weekdays only (between 7:00 and 10:00 in the morning and again between 18:00 and 20:00 at night, indicated in red in Figure 3-4).

Pumping is assumed to take place during the 8 off-peak hours at night on weekdays between 10pm and 6am, indicated by the green period in Figure 3-4. Any additional water in the lower reservoir (due to accumulation of rainfall from the side slopes or the lower reservoir catchment) is pumped back to the top reservoir during the off peak hours on weekends. Hence, the daily release and pumping volumes ( $m^3$ ) and associated pumping rate ( $m^3/h$ ) were calculated by writing them as a function of the release rate ( $m^3/h$ ):

$$\text{Daily release volume} = \text{Release rate} \times 5 \text{ peak hours per day}$$

$$\text{Daily release volume} = \text{Daily pumping volume}$$

$$\text{Daily pumping volume} = \text{Pumping rate} \times 8 \text{ off - peak hours per day}$$

Hence, the only remaining controllable variable is the rate at which water can be released from the upper reservoir to the turbine (in  $m^3/h$  or  $m^3/s$ ).

### 3.6.3 Determining the electricity generation potential and production

The formulas provided in Sections 2.6.3 of the literature review were used for determining the power generation and associated production by the turbine. The assumptions made and values adopted are explained below.

Where the symbols have the meaning as described in Section 2.6.3:

$\rho$  was taken as 1000 kg/m<sup>3</sup>.

$Q_T$  was the only controllable variable, that was optimised in Section 3.6.7.

$\eta_T$  was assumed to be in the order of 90%, based on the literature in Section 2.6.3. The influence of this assumption was assessed in the sensitivity analysis in Sections 3.6.9 and 4.2.4.

$H_S$  was assumed to be 140 m as this will be the final height of the ERGO TSF at closure.

$L$  was measured from a Lidar survey to be in the order of 1500 m.

$v_T$  was limited to 3m/s, for the purposes of this first order estimate, upon recommendation by Van Dijk (2014). The friction ( $h_f$ ) and secondary losses ( $h_L$ ) in the outlet pipeline (which are subtracted from  $H_S$  to determine  $H_T$ ) are both directly proportional to the square of  $v_T$ . Therefore it is recommended to keep  $v_T$  as low as possible in order to maximise  $H_T$ . The outlet pipe had to be sized accordingly to keep the velocity in the pipe to 3 m/s. The influence of this assumption was assessed in the sensitivity analysis in Sections 3.6.9 and 4.2.4. According to Van Dijk (2014) if the system is properly engineered and operated at low velocities the secondary loss component ( $h_L$ ) is negligible.

$D$  was calculated as a function of the flow rate and assumed velocity of 3 m/s, with the following formula:

$$D = 2 \sqrt{\frac{Q_T}{\pi v_T}}$$

It was assumed that the outlet pipe will be a steel pipeline with a  $k_s$  value of approximately 0.03 mm.

$\mu$  was taken as that of water at 25°C of  $0.891 \times 10^{-3}$  kg/ms.

By substituting all the assumptions above into the formulas in Section 2.6.3, the formulas were forms, with the only remaining variable being the flow rate  $Q_T$ :

$$D = 2 \sqrt{\frac{Q_T}{\pi v_T}} = 2 \sqrt{\frac{Q_T}{\pi(3)}} = 0.65147\sqrt{Q_T}$$

It is to be noted that for large  $Q_T$  values, the required outlet pipe diameter might become impractically large as far as implementation is concerned. Hence, this formula can only be used to obtain the size of a single “representative” outlet pipe. Refinement is required when the detail design is conducted. It is recommended for the flow to be split into a number of suitably sized outlet pipes, preferably diameters should not exceed 2.5 m.

The calculation sequence adopted is summarised below:

$$Re = \frac{\rho D v_T}{\mu} = \frac{1000(0.65147\sqrt{Q_T})(3)}{0.891 \times 10^{-3}} = 2\,193\,502\sqrt{Q_T}$$

$$\frac{1}{\sqrt{\lambda}} = -2 \log \left( \frac{k_s}{3.7D} + \frac{5.1286}{Re^{0.89}} \right) = -2 \log \left( \frac{1.244 \times 10^{-5}}{Q_T^{0.5}} + \frac{1.165 \times 10^{-5}}{Q_T^{0.445}} \right)$$

*Solve  $\lambda$  for each  $Q_T$  value*

$$h_f = \frac{\lambda L v_T^2}{2gD} = \frac{\lambda(1500)(3^2)}{2(9.81)(0.65147\sqrt{Q_T})} = 1056.2 \frac{\lambda}{\sqrt{Q_T}}$$

$$H_T = H_S - h_f - h_L = 140 - 1056.2 \frac{\lambda}{\sqrt{Q_T}} - 0$$

$$P_T = 1000(9.81) \left( 140 - 1056.2 \frac{\lambda}{\sqrt{Q_T}} \right) (0.9) Q_T = 1\,236\,060 Q_T - 9\,325\,190 \lambda \sqrt{Q_T}$$

$$E_T = P_T t_T = (1\,236\,060 Q_T - 9\,325\,190 \lambda \sqrt{Q_T})(5) = 6\,180\,300 Q_T - 46\,625\,949 \lambda \sqrt{Q_T}$$

*Solve  $P_T$  and  $E_T$  for each  $Q_T$  value*

For example, with a flow rate of 10 m<sup>3</sup>/s, a single outlet pipe of 2.06 m diameter is required ( $\lambda$  equates to 0.00965) to drive a turbine with a capacity of 12.1MW (at an efficiency of 90%) in order to generate 60.4 MWh of electricity in the 5 peak hours on a weekday.

### 3.6.4 Determining the pump capacity required and associated electricity consumption

A similar exercise was carried out for the required pumping capacity.

The formulas provided in Section 2.6.4 of the literature review were used for determining the pumping capacity required and consumption of electricity during pumping. The assumptions made and values adopted are explained below.

$\eta_P$  was assumed to be in the order of 90%, based on the literature in Section 2.6.4. The influence of this assumption was assessed in the sensitivity analysis in Sections 3.6.9 and 4.2.4.

It was assumed that the same pipeline will be used for pumping and releasing of water. Hence, the diameter of the outlet pipe is dictated by the release capacity, i.e. the same for the pumping pipeline. However, because the diameter of the pipeline is fixed, the velocity of flow in the pipeline had to be calculated.

From Section 3.6.2 the following was derived:

$$\text{Daily release volume} = \text{Daily pumping volume}$$

$$\therefore \text{Pumping rate} = \text{Release rate} \times \frac{\text{5 peak hours per day}}{\text{8 off peak hours per day}}$$

$$Q_P = 0.625Q_T$$

Similar as for the turbine, all of the equations in Section 2.6.4 can be reduced to simpler forms by substituting the assumed values and writing them in terms of either the flow rate  $Q_P$  or  $Q_T$ :

$$v_P = \frac{Q_P}{\text{Cross sectional area of pipe}} = \frac{Q_P}{\frac{Q_T}{3}} = 1.875m/s$$

$$Re = \frac{\rho D v}{\mu} = \frac{1000(0.65147\sqrt{Q_T})(1.875)}{0.891 \times 10^{-3}} = 1\,370\,939\sqrt{Q_T}$$

$$\frac{1}{\sqrt{\lambda}} = -2 \log \left( \frac{k_s}{3.7D} + \frac{5.1286}{Re^{0.89}} \right) = -2 \log \left( \frac{1.244 \times 10^{-5}}{Q_T^{0.5}} + \frac{3.741 \times 10^{-6}}{Q_T^{0.445}} \right)$$

Solve  $\lambda$  for each  $Q_T$  value

$$h_f = \frac{\lambda L v^2}{2gD} = \frac{\lambda(1500)(1.875^2)}{2(9.81)(0.65147\sqrt{Q_T})} = 412.6 \frac{\lambda}{\sqrt{Q_T}}$$

$$H_T = H_S + h_f + h_L = 140 + 412.6 \frac{\lambda}{\sqrt{Q_T}}$$

$$P_p = \frac{1000(9.81) \left(140 + 412.6 \frac{\lambda}{\sqrt{Q_T}}\right) (0.625) Q_T}{0.9} = 953\,750 Q_T - 2\,810\,838 \lambda \sqrt{Q_T}$$

$$E_p = P_p t_p = (953\,750 Q_T - 2\,810\,838 \lambda \sqrt{Q_T})(8) = 7\,630\,000 Q_T - 22\,486\,700 \lambda \sqrt{Q_T}$$

*Solve  $P_p$  and  $E_p$  for each  $Q_T$  value*

Continuing the example from Section 3.6.3, if water is released at 10 m<sup>3</sup>/s for the 5 peak hours in a weekday, through a 2.06 m diameter outlet pipe and pumped back during the 8 off-peak hours ( $\lambda$  for the pumping equates to 0.00896) a pump with a capacity of 9.5 MW is required (at an efficiency of 90%) and it will consume 75.7 MWh of electricity in the 8 off-peak hours in a weekday.

From this example it is to be noted that the system consumes 75.7 MWh to generate 60.4 MWh of electricity. Hence, the electricity net output of the system is *negative*. This is the case, regardless of the magnitude of the release rate  $Q_T$ .

### 3.6.5 Allocation of construction costs

A first order estimate of the initial capital investment was calculated by adding the costs of the largest components of project development. The following has been allowed for:

- Cost of electromechanical equipment
- Cost of civil works
- Cost of operation and maintenance
- Cost of construction of the lower reservoir.

Van Vuuren et al. (2011) assessed various methods to obtain a first order cost estimate of developing a hydropower scheme. Hence, the cost of the electromechanical equipment, civil works, operation and maintenance for this project were determined from Van Vuuren's (2011) recommendations. The formulae have been converted to South African Rand using 2009 exchange rates.

To determine the cost of the *electromechanical equipment* ( $C_{EM}$ ) two sets of equations were considered, originally proposed by Anvarado-Ancieta (2009) and Saini and Singal (2008) respectively. The higher cost of the two was conservatively adopted, which was that proposed by Saini and Singal (2008). Inflation of the formulas, as mentioned by Van Vuuren et al. (2011), was done to reflect the current (2015) value of money. Table 3-3 shows the formulas used for the calculation of the various components making up the electromechanical costs.

Table 3-3: Formulas used to calculate cost of electrocmechanical equipment as a function of generating capacity and head (Saini and Singal, 2008, adapted by Van Vuuren et al., 2011):

Item	Capital cost (Rand 2015 value)
Turbine with governing system ( $C_a$ )	$C_a = 10\,509(10^{-3}P_T)^{-0.1902}H^{-0.2167}P_T$
Generator with excitation system ( $C_b$ )	$C_b = 12\,927(10^{-3}P_T)^{-0.1807}H^{-0.209}P_T$
Mechanical and electrical auxiliaries ( $C_c$ )	$C_c = 8\,440(10^{-3}P_T)^{-0.19}H^{-0.2122}P_T$
Main transformer and switchyard equipment ( $C_d$ )	$C_d = 3\,743(10^{-3}P_T)^{-0.1817}H^{-0.2082}P_T$
Total cost	$C_{EM} = 1.13(C_a + C_b + C_c + C_d)$

Where  $P_T$  is the installed capacity of the turbine in the system (in kW), which can be written as a function of the release rate  $Q_T$ .

$H_T$  is the effective head, assumed to be the total 140 m static head  $H_S$  (as assumed in Section 3.6.3, conservatively ignoring any losses).

The cost of civil works ( $C_{CW}$ ) was also based the formulae provided by Saini and Singal (2008) and adapted by Van Vuuren et.al (2011). Table 3-4 shows the formulas used for the calculation of the various components making up the civil works costs. Note that the cost of civil works does not include lining of the TSF basin (an option that is discussed later on).

Table 3-4: Formulas used to calculate cost of civil works as a function of generating capacity and head (Saini and Singal, 2008, adapted by Van Vuuren et al. (2011):

Item	Capital cost (Rand 2015 value)
Intake structure ( $C_e$ )	$C_e = 3\,828(10^{-3}P)^{-0.2368}H^{-0.0598}P$
Penstock (Outlet pipe) ( $C_f$ )	$C_f = 1\,305(10^{-3}P)^{-0.3722}H^{0.3866}P$
Powerhouse building ( $C_g$ )	$C_g = 16\,567(10^{-3}P)^{-0.2354}H^{-0.0587}P$
Tail race channel ( $C_h$ )	$C_h = 7\,497(10^{-3}P)^{-0.376}H^{-0.624}P$

Total cost	$C_{CW} = 1.13(C_e + C_f + C_g + C_h)$
------------	--

The cost of the lower reservoir ( $C_{LR}$ ) was based on a recent water storage dam design project involving a capacity of 850 000 m<sup>3</sup>, with a double composite lining system. An indicative cost of R400 per cubic meter of storage volume was assumed for the construction of a suitably lined lower reservoir facility. This includes construction and consultation fees.

$$C_{LR} = 400 \times \text{Required lower reservoir storage volume}$$

Although the maintenance and operational costs ( $C_{MO}$ ) associated with the turbine and pumping units are not part of the capital cost, but rather a running expense, Van Vuuren et al. (2011) provided the formulae in Table 3-5 to estimate these costs as a function of the capital cost of works.

Table 3-5: Percentages making up the operation and maintenance costs as a function the cost of works (Van Vuuren et al. 2011):

Item	Capital cost (Rand 2015 value)
Civil works	0.25% of $C_{CW}$
Mechanical works	2% of $C_{EM}$
Electrical works	4% of $C_{EM}$
Total cost	$C_{MO} = 0.0025C_{CW} + 0.06C_{EM}$

As far as environmental authorisation is concerned, costs of environmental impact studies have not been allowed. However, these costs are negligible compared to the total initial capital investment required. It was assumed that the facility would have had a Water Use Licence (required by South African law) to use water as part of the tailings deposition process. In future this water will be used to generate electricity. No water course will be affected detrimentally more so than it had been during the construction and operation of the TSF. Hence, it is assumed that only an amendment to the water use license conditions will be required, which can be done based on an Environmental Impact Assessment.

All of the above mentioned costs were added to calculate the total initial capital investment required:

$$\text{Cost of initial capital investment required} = C_{EM} + C_{CW} + C_{LR}$$

$$\text{Cost of operation and maintenance (excluding pumping costs)} = C_{MO}$$

### 3.6.6 Determination of potential income and IRR

As mentioned earlier, water is released to generate electricity during the peak red periods on weekdays shown in Figure 3-4. Any electricity generated ( $E_T$  in kWh) during these periods is sold at the peak period rates (R/kWh) to generate an income. The surplus electricity available in the national electricity grid during the off-peak green periods is used for pumping. Any electricity consumed ( $E_P$  in kWh) during these periods is bought at the off-peak period rates (R/kWh).

The daily operational profit is determined by subtracting the expense of electricity consumed from the income of electricity sold. Due to the fact that the consumption of a pump storage scheme exceeding the generation, the differential of tariffs needs to be sufficiently large in order for the scheme to generate profit.

By adding the daily operational profit over a year the annual income was calculated. By sorting the annual income for each year and using the initial capital investment required (calculated above) the IRR was calculated with an Excel function.

### 3.6.7 Optimisation of the pump storage scheme system

As mentioned at the end of Section 3.6.2, the only controllable variable is the rate at which water can be released from the upper reservoir to the turbine ( $\text{m}^3/\text{h}$  or  $\text{m}^3/\text{s}$ ). It is to be noted that all equations, including the turbine and pump power capacity (W), as well as the electricity generation/consumption (kWh) formulae were written as functions of the release rate  $Q_T$  ( $\text{m}^3/\text{s}$ ). Seeing that the key objective for this development would be to generate the highest possible IRR, the optimal release rate that will achieve this is to be determined. Determining the optimal release rate is about finding a balance between the initial capital investment required and daily operational profit that can be generated, hence optimising the flow capacity to generate the highest possible IRR over the 50 year life of the facility. This was done by varying the flow capacity until the largest possible IRR was found.

Once the optimal release rate was determined, it was substituted into the formulae in Sections 3.6.3 and 3.6.4, to determine the outlet pipe diameter, the turbine and pump capacities, as well as the daily electricity generation and consumption. The financial implications were also determined by calculating the daily income (for electricity generated) and expenditure (for electricity consumed), of which the difference is the daily operational profit. By substituting the turbine capacity in Section 3.6.5 the initial capital investment required was calculated.

### 3.6.8 Reliability of daily plant production and associated income

Due to limited water available in the system for electricity generation, there were year in the rainfall record (simulated with the water balance) that the plant could not operate at full capacity during the dry season. Hence, it was necessary to quantify the reliability of the plant. The reliability is defined as the percentage certainty that the plant will generate the amount of electricity that it was designed for on any given day. This is governed by the availability of a sufficient volume of water, as simulated with the water balance calculations.

There is also a financial implication to the shortage of water. Once the initial capital has been invested, the plant has to generate electricity to produce income. Hence, the financial reliability calculations entailed determining the percentage certainty that the plant will generate a certain amount of income on any given day.

Statistical analysis was conducted on the daily production and daily operational profit data to quantify the reliability of the pump storage scheme to produce a certain amount of *peak* period electricity and operational profit (peak periods are only applicable on weekdays). The statistical analysis included determining the percentage of days during the rainfall record that the pump storage scheme was generating a certain amount of electricity and daily operational profit. This was then assumed to be the future reliability of the pump storage scheme to produce a certain amount of kilowatt hours of electricity or Rands of operational profit in a single weekday of operation. The spread of daily production and operational profit was also determined by plotting it on discrete distribution histograms.

### 3.6.9 Sensitivity analysis

Various assumptions were made throughout this pump storage scheme section and therefore this section was aimed at assessing the sensitivity of the IRR and the overall efficiency of the system to a variation in the assumed parameters. This was done by calculating the IRR and overall efficiencies for a range of values that the assumed parameter can possibly be (whilst keeping all other variables constant). The overall efficiency (%), provides an indication of how much electricity is generated from every unit of electricity consumed and was calculated with the following formula:

$$\text{Overall system efficiency} = \frac{\text{total electricity generated}}{\text{total electricity consumed}} = \frac{E_T}{E_P}$$

The following assumed parameters were assessed and results discussed in Section 4.2.4.

- Total TSF catchment area contributing rainfall runoff to the system (assumed to be 1 500 ha in Section 3.6.1.1) to obtain a first order estimate of the feasibility of implementing a similar system on TSFs with a smaller footprint area.
- Flow velocity in outlet pipe during the release of water (assumed to be 3 m/s in Section 3.6.3).
- Total static head, i.e. total height of the facility (assumed to be 140 m in Section 3.6.3), to obtain a first order estimate of the feasibility of implementing a similar system on TSFs with a lower final height.
- Turbine efficiency (assumed to be 90% in Section 3.6.3).
- Pump efficiency (assumed to be 90% in Section 3.6.4).

Two additional sensitivity analyses were conducted, to determine its effect on the financial feasibility of the study.

- The Eskom Megaflex tariff structure (Eskom, 2014f) was used throughout this study, as per Figure 3-4. The financial feasibility of any pump storage scheme is highly reliant on the tariff structure, in particular, the differential between peak and off-peak tariffs and the durations over which they apply. Hence, this sensitivity analysis investigated the effect that a change in differential tariff structure would have on the feasibility of the pump storage scheme. This was done by keeping the off-peak rates constant and adding a percentage of the differential to determine the peak rates. For example, in the high demand season the peak rate is 203.29 c/kWh and the off-peak rate is 33.44 c/kWh, hence the differential is 169.85 c/kWh. If the Eskom differential percentage is 100%, the peak rate can be calculated as follows:

$$\text{Peak rate} = \text{offpeak rate} + (\% \times \text{differential})$$

$$\text{Peak rate}_{100\%} = 33.44 + (100\% \times 169.85) = 203.29 \text{ c/kWh}$$

If the Eskom differential percentage is 50%:

$$\text{Peak rate}_{50\%} = 33.44 + (50\% \times 169.85) = 118.37 \text{ c/kWh}$$

The same applies for the calculation of the low demand season rates.

- Due to the significant difference between the high and low demand season rates (provided in Figure 3-4), an assessment was done to determine whether the IRR would increase if the release rate ( $Q_T$ ) is increased during the high demand season. Hence an additional sensitivity analysis was added by increasing  $Q_T$  with 50% ( $1.5 \times Q_T$ ) and 100% ( $2 \times Q_T$ ) for the high demand season, repeating the optimisation exercise and calculating the IRR for a range of  $Q_T$  values.

All sensitivity analyses were *only* done for the “no lining” option, as opposed to the lined TSF option which follows.

### **3.6.10 Determining the effect of lining the TSF basin**

As mentioned before, only the water from the system’s own catchment was relied on (in order for the system to be completely self-sustainable in a water-scarce region), and was not supplemented from an external source. Hence it was identified that if the runoff from the catchment can be improved and the seepage can be limited, more water will be available for electricity generation. The proposal is to line the TSF basin with an impermeable barrier system, such as high density polyethylene (HDPE).

This option was assessed by repeating the water balance exercise with the following minor changes:

- The runoff factors of the TSF catchment (assumed in Table 3-2 Section 3.6.1.1) was increased to 100%.
- And the seepage in Section 3.6.1.3 was deemed to be negligible.

Hence the result was an increased volume of water in the TSF pond available for utilisation.

The financial feasibility exercise was repeated, but adding the cost of the lining system to the initial capital investment required. The cost of the lining system was calculated with a conservative rate of R165 for every square meter of lining. This unit rate was based on a recent cost estimate done for the under lining of a large ash-facility (with a total area of 176 ha) (Confidential report, 2014). Hence the total cost of the lining system was calculated to be in the order of R2.475 billion.

The optimisation exercise was repeated and the results are discussed in Section 4.2.5.

## **3.7 COMBINATION OF SOLAR PV AND PUMP STORAGE SCHEME OPTIONS**

There are distinct advantages and disadvantages to each of the previous two post closure land use options discussed, which include:

- The Solar PV system provides clean renewable electricity between sunrise and sunset. Its most significant disadvantage is that the time of electricity generation does not coincide with the time of peak demand. In fact, the majority of electricity generated with

solar PV will be sold at the Standard tariffs (as per Figure 3-4) during weekdays, with only a short peak consumption period in the morning.

- In contrast, the pump storage scheme provides electricity whenever it is switched on (provided there is water in the upper reservoir available for release). Its disadvantage is that it consumes more electricity than it produces, as alluded to at the end of Section 3.6.4. As mentioned in the literature in Section 2.6.1, a pump storage scheme only provides a method of electricity storage and *not* net positive electricity production. The other disadvantage of this option, as presented throughout Section 3.6, is that it relies on the surplus electricity in the national electricity grid to pump water to the upper reservoir during off-peak periods. Hence the system is not completely independent.

From the above it can be seen that there is potential benefit if the above options are combined. The pump storage scheme can be used to store solar PV generated electricity until it is required during peak demand periods. During the sunny hours of a day, the solar PV electricity can be used to pump water to the upper reservoir of the pump storage scheme. Any surplus electricity generated by the solar PV plant (not used for pumping) is fed into the electricity grid. The water is then released from the upper reservoir to generate electricity during the red peak tariff periods in Figure 3-4. Any electricity generated by the solar PV plant during the red peak periods is also fed into the electricity grid. The pump storage scheme can now in principle operate independently as it no longer requires the surplus electricity from the national electricity grid to pump the water to the upper reservoir during the off-peak periods.

Based on the above, combining the solar PV and pump storage scheme options is an ideal solution from a practical perspective as it creates a system independent from external inputs. The following three sections are aimed at assessing whether it is financially beneficial to do so. The following combinations were investigated:

- Combination 1 - Finding the optimal release rate of the pump storage scheme (from a financial feasibility point of view) when used in a combined system if solar PV electricity is used to pump the water from the lower to the top reservoir.
- Combination 2 - The financial feasibility of combining the two options on the same site, while keeping them independent of one another, i.e. selling the PV electricity and not using it to pump water back.
- Combination 3 - The financial feasibility of combining the two options for the system to be completely independent from Eskom, i.e. using the PV electricity to pump water back for later release.

### **3.7.1 Combination 1 - Optimising the release rate of the pump storage scheme in a combined system**

The combination of the two options is simply the sum of the two individual parts. Hence, the same operational principles apply for the combination as for the individual options. Therefore, the same methodologies were followed as described in Sections 3.5 and 3.6 to assess the financial feasibility of combining the two options.

It was assumed that the solar and water resources available for power generation remain constant, as this combined option is assessed for the same ERGO site. The setup of the daily generation potential and associated income equations were done in the same manner as before.

The daily operational profit was calculated with the following formula:

$$\text{Daily operational profit} = \text{Income}_{\text{generated by solar PV}} + \text{Income}_{\text{generated by turbine}}$$

The cumulative annual operational profit was calculated for each of the years over the 50 year life of the facility. The construction costs were allocated in the same manner as described in Sections 3.5.5 and 3.6.5 respectively.

The solar plant was assumed to remain as described in Section 3.5.7, as the orientation of the panels is a function of the solar resource and tariff structure, which remain the same as in Section 3.5.1 and 3.3.3 respectively. The solar plant is constructed as large as possible.

The optimisation of the pump storage scheme release rate as described in Section 3.6.7 does, however, not remain constant as the IRR is influenced by the daily operational profit. The daily operational profit is dependent on the pumping cost. However, when the two options are combined the pumping is powered with the solar PV electricity (as opposed to surplus electricity from the grid). Therefore, the pump storage scheme optimisation exercise was repeated by varying the pump storage scheme release rate to determine the highest possible IRR.

### **3.7.2 Combination 2 - Financial feasibility of a combined solar PV and pump storage scheme option on the same site**

The results of the optimisation of the release rate mentioned in Section 3.7.1 are discussed in Section 4.3.1. However, the results show the highest IRR is achieved if *only* the Solar PV plant is implemented. The reason is that the solar PV generated electricity is worth more per kilowatt-hour if it is independently sold at standard tariffs during generation (see Figure 3-4), instead of buying surplus electricity from the grid during the off-peak periods (an assumption made throughout Section 3.5). If the practical implications mentioned in the introduction of

Section 3.7 are taken into account, it might be worth constructing both the systems regardless of the financial aspect. The reason for doing this is the provision of continuous electricity supply. The result is then expected to be an IRR lower than 10.70%.

The following section discusses the financial implications of operating both the solar PV and pump storage scheme options (as optimised in Sections 4.1 and 4.2) together on the same site, using the surplus electricity in the grid during off-peak periods to pump water to the top reservoir.

If the two systems are implemented independently on the same site, the result is simply the sum of the two independent systems. The detail of each individual system is identical to what was calculated in Sections 3.5 and 3.6. The following formula applies when calculating the daily operational profit:

$$\begin{aligned}
 & \textit{Daily operational profit} \\
 & = \textit{Income}_{generated\ by\ solar\ PV} \\
 & + \textit{Income}_{generated\ by\ turbine} - \textit{Expenditure}_{consumption\ by\ pumping}
 \end{aligned}$$

Combination 2 does not provide an independent solution, as the system is dependent on the surplus electricity from the grid. Hence, the following section assesses the financial feasibility of only using solar electricity to pump water to the upper reservoir, in order to create an uninterrupted electricity supply system, which is independent of Eskom's surplus electricity supply.

### **3.7.3 Combination 3 - Assessing financial feasibility of a combined solar PV and pump storage scheme to be independent of Eskom's surplus electricity supply**

This combination is similar to that discussed in Section 3.7.1 as the solar PV generated electricity is used to pump water to the top reservoir. However, with this combination the optimal pump storage scheme system was adopted (as calculated for the individual pump storage scheme option in Section 3.6.7) and the optimisation exercise was not repeated (as was the case in Section 3.7.1). Hence, the two individual systems' capacities remain constant to that calculated with Sections 3.5.7 and 3.6.7 respectively (results discussed in Sections 4.1.4 and 4.2.2).

The various combinations discussed above are summarised in Table 3-6.

Table 3-6: Summary of combinations investigated

	Combination 1	Combination 2	Combination 3
Solar PV plant	Orientation optimised*	Orientation optimised*	Orientation optimised*
Pump storage scheme	Optimise release rate	Fixed release rate	Fixed release rate
Power supply for pumping	PV power / Eskom surplus	Eskom surplus	PV power

\* Size of the optimum solar system discussed in Section 4.1.3 and 4.1.4.

## 4 RESULTS

This section presents a discussion of the results from the feasibility analysis explained in Chapter 3.

### 4.1 SOLAR PHOTO VOLTAIC POWER GENERATION

The following section presents the results of the calculations done to determine the financial feasibility of a Solar PV plant on top of the ERGO TSF from Section 3.5. The following was discussed:

- The available solar resource at ERGO
- Verification of the resource calculations with measured data
- Optimisation of the orientation and size of the solar plant to generate maximum return on investment
- The resultant plant output and daily electricity production
- Cost of construction, potential income and IRR
- Reliability analysis
- Sensitivity analysis of assumed parameters.

#### 4.1.1 Solar resource at ERGO

The altitude and azimuth angles were determined as explained in Section 3.5.1 and plotted on a sun path diagram in Figure 4-1. The shape of the sun path diagram compares well with the example given by Masters (2004), shown in Figure 2-9. The ERGO TSF is located in the southern hemisphere and hence the sun is at its lowest and highest altitude angles on 21 June and 21 December respectively every year, referred to as the winter and summer solstice respectively. Due to the fact the ERGO TSF (Latitude 26.3°S) is located south of the Tropic of Capricorn (Latitude 23.5°S) the altitude angle at the ERGO site never exceeds 90° as the sun is never directly overhead. By reading from the sun path diagram it is possible to obtain an approximation of the direction and height of the sun on any day of the year at any time between sunrise and sunset. Some interpolation might be required. For example, on 21 March (of any given year) at 9 o'clock in the morning the sun will be at an altitude angle of 40° and an azimuth angle of approximately 68°. The exact values, calculated as explained in Section 3.5.1, are 39.6° and 66.5° respectively.

Early in the morning and late afternoon the altitude angle of the sun is so low that the panels of adjacent arrays cast shadows on one another (illustrated in Figure 4-2). Seeing that the efficiency of solar panels are a direct function of the area of the panel covered in sunlight, shadows cause a significant decrease in panel efficiency. Early morning and late afternoon shadows are unavoidable and hence the designer has to decide how much shadow time will be allowed, as this influences the spacing of the panels. One of the solar suppliers recommended to space the panels far enough apart in order for the panels to be fully radiated by sunlight between 9:00 and 15:00 during the winter, as these are the hours with the best quality sunlight. The shadow line was chosen to be at  $23.6^{\circ}$  as illustrated on Figure 4-1. This results in the panels being fully radiated between approximately 7:00 and 17:00 in summer. For calculation purposes it was conservatively assumed that if the sun is at an altitude angle of lower than  $23.6^{\circ}$  production is zero.

#### 4.1.2 Verification of calculated data

In order to assure that the data calculated with the generic formulas in Section 2.5.2 provides accurate answers, it was compared with known values.

The results of the verification of calculations with NASA data can be seen in Figure 4-3. The *solid* red, blue and purple curves are the diffused, direct beam and total radiation respectively as calculated by NASA (2014). The red, blue and purple *dashed* curves are the calculated values, as per Section 3.5.1 for the diffused, direct beam and total radiation respectively. It can be seen that there is good correlation between the NASA and calculated values. The calculations underestimate the total radiation during the summer months and slightly overestimate it during the winter months. Taking the amount of variables into account, the calculations are deemed to be sufficiently accurate.

The green curve shows the *actual* radiation (taking cloud cover into account) on a horizontal surface as calculated by NASA (2014). The black curve shows the *realistic* solar resource for every calendar day calculated by multiplying the calculated total radiation with the cloud cover factor. It can be seen that the black curve is considerably smoother than the green curve, because a 30 day running average was used. It shows that the calculated daily cloud cover factors provide a representative estimate of the actual recorded data.

It can be seen in Figure 4-3 that the total radiation (both the NASA and calculated data) compares well with the 5 to 9 kWh range of energy for every square meter of exposed area (on an average day), as per the guidelines provided by Zweibel (1990) and Breeze (2005) contained in the literature review in Section 2.5.1.

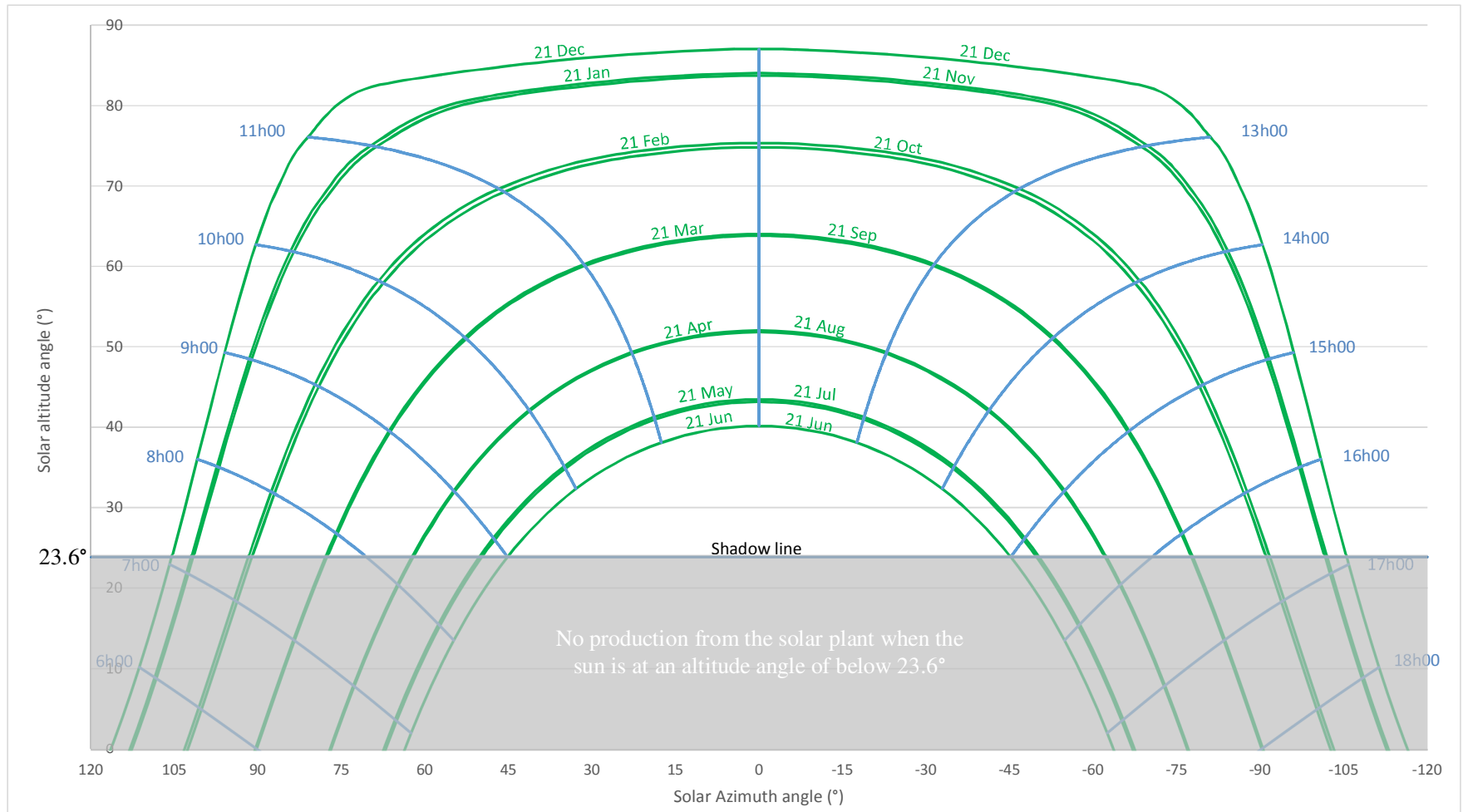


Figure 4-1: Sun path diagram for the ERGO TSF

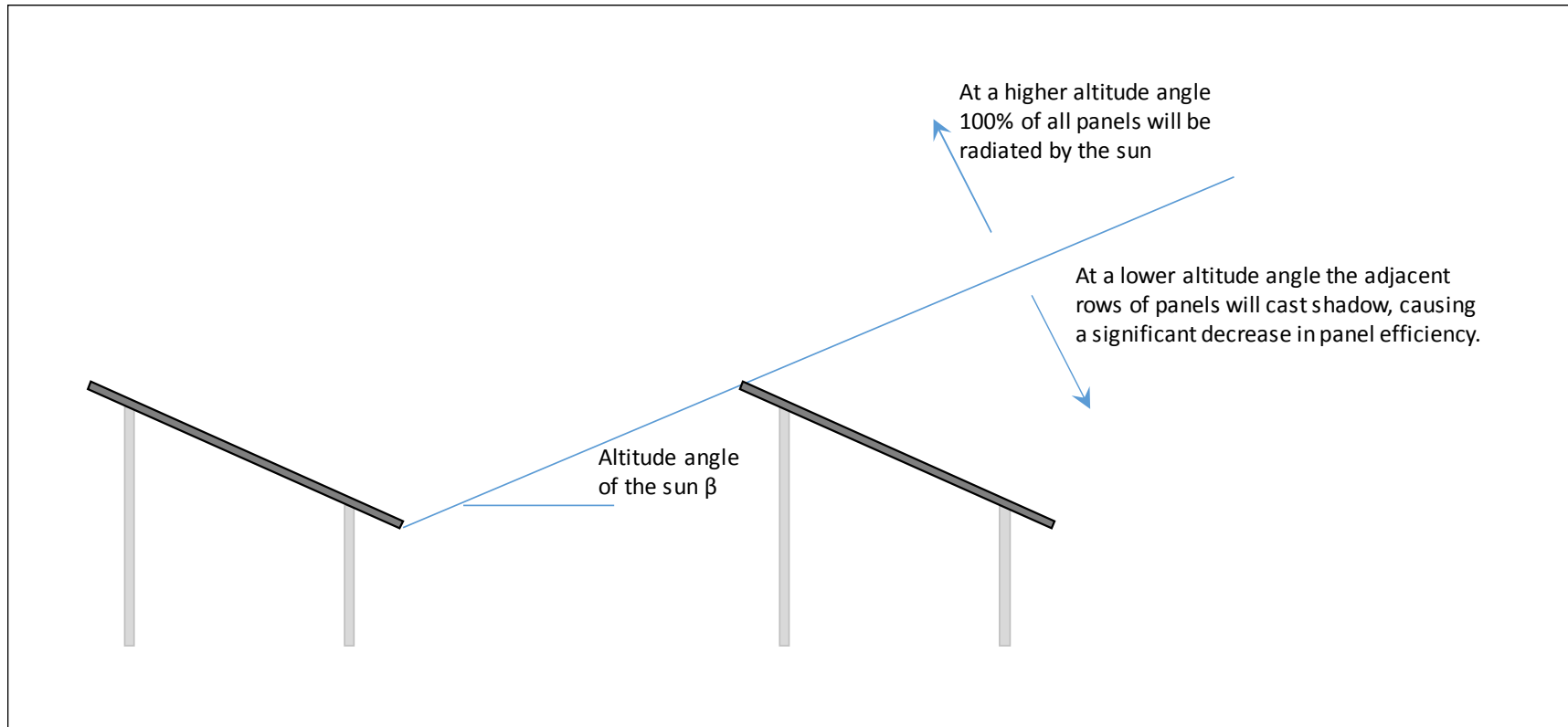


Figure 4-2: Illustration of the shadow line

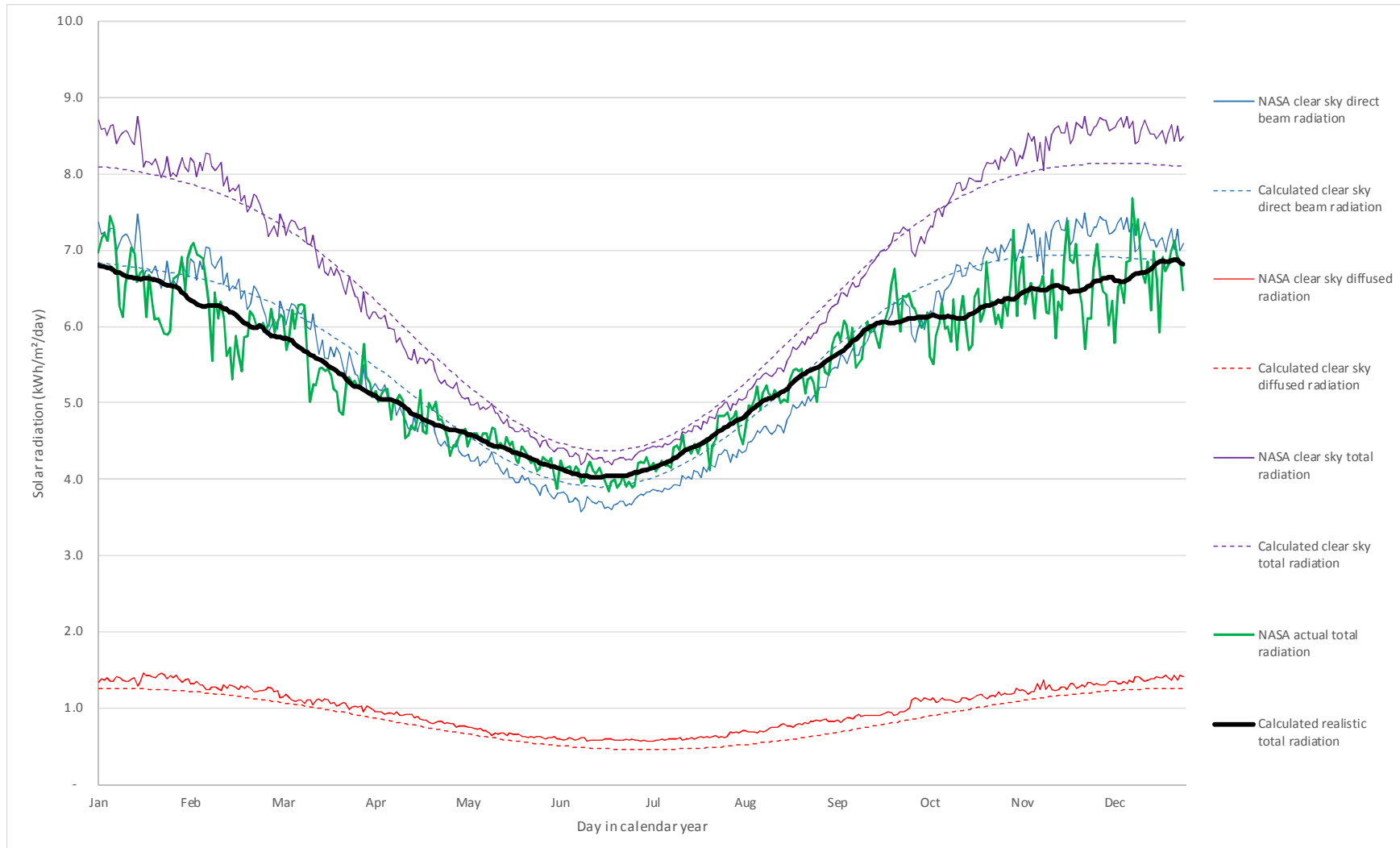


Figure 4-3: Comparison of calculated and recorded average daily solar radiation on a horizontal surface

### 4.1.3 Optimisation of the plant

This section presents the results of the optimisation exercise discussed in Section 3.5.7, as the optimal panel orientation influences all results following thereafter.

As discussed in Section 3.5.1 the solar resource potential was written as a function of the solar panel azimuth and tilt angles respectively. This was specifically done to enable optimisation of these two parameters. As per the methodology discussed in Section 3.5.7 the IRR was determined for various combinations of azimuth and tilt angles. The optimisation results showed that the highest IRR of 10.7% was achieved when values of 16.3° and 27.6° were used for the azimuth and tilt angles respectively.

#### 4.1.3.1 *Variation in azimuth angle*

The graph in Figure 4-4 shows the results of optimising the collector azimuth angle  $\Phi_C$ . The orange curve shows the resultant plant production in units of TWh, with a variation in the collector azimuth angle. It can be seen that the plant produces maximum output if it faces directly towards true north (azimuth angle = 0°).

The blue curve, however, suggests that the arrays should be turned 16.3° towards the East (relative to true North) as this will generate the highest possible IRR over the 50 year lifecycle of the plant. The reason for this being that the sun rises in the East and during week days Eskom applies peak tariffs between 7:00 and 10:00 in the morning. This means that more income can be generated by directing the arrays more towards the sun in the morning to ensure more electricity is generated during the peak tariff hours. Although the benefit of turning the panels 16.3° towards the East (as opposed to directing them directly towards the north) is not significant (only about 0.06% difference in IRR), it is theoretically the best orientation based on the current tariff structure.

#### 4.1.3.2 *Variation in tilt angle*

The optimisation of the tilt angle was based on the performance of a single panel, assuming no other panels in the vicinity, i.e. shadows and spacing of panels don't play a role (addressed in the following section). The graph in Figure 4-5 shows the optimisation of the tilt angle  $\Sigma$  of the panel. The green curve shows the panel performance over a 50 year life with change in tilt angle (whilst keeping the azimuth angle fixed at 16.3°). It can be seen that the panel produces maximum output if it is placed at a tilt angle is 22.5° with the horizontal. This is slightly towards the summer solstice, which takes advantage of the long periods of exposure during the summer months.

The blue curve, however, suggests that the panel will generate the highest IRR when placed at a tilt angle 27.6°, which is slightly towards the winter solstice, as can be seen in Figure 4-6. This orientation takes advantage of the increase in tariffs during the high demand season, which is

enforced during the winter months. Again, it can be seen that the IRR is not that sensitive to a change in tilt angle, as long as the panels more or less tilted towards the equinoxes. Although the benefit of tilting the panels  $27.6^\circ$ , as opposed to tilting them to  $22.5^\circ$  for example is not significant (only about 0.02% difference in IRR), it is theoretically the best orientation based on the current tariff structure.

All calculations from here on were based on a fixed azimuth angle of  $16.3^\circ$  towards the east and a fixed tilt angle of  $27.6^\circ$ . The orientation of the panels was the first topic discussed in Section 3.5, because all other aspects presented in Section 3.5 build on that. Hence the final outcome of Section 3.5 depends on the solar panel azimuth and tilt angles respectively.

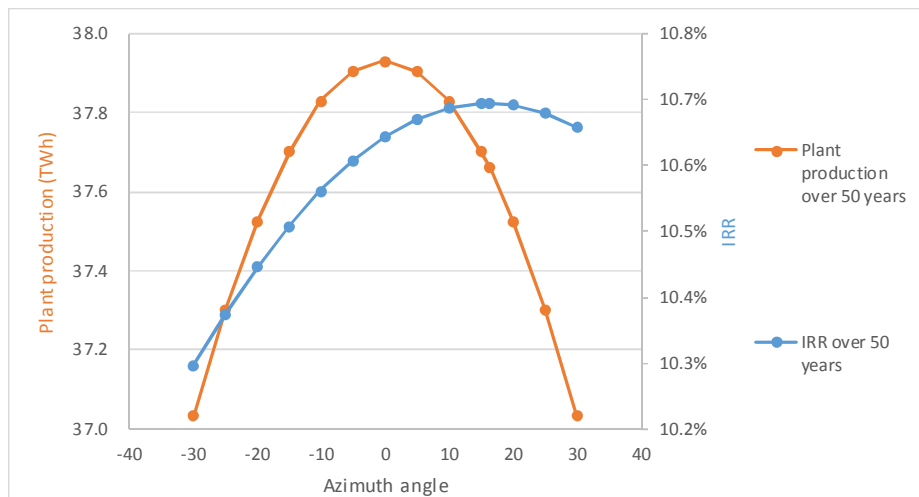


Figure 4-4: Optimisation of the array azimuth angle

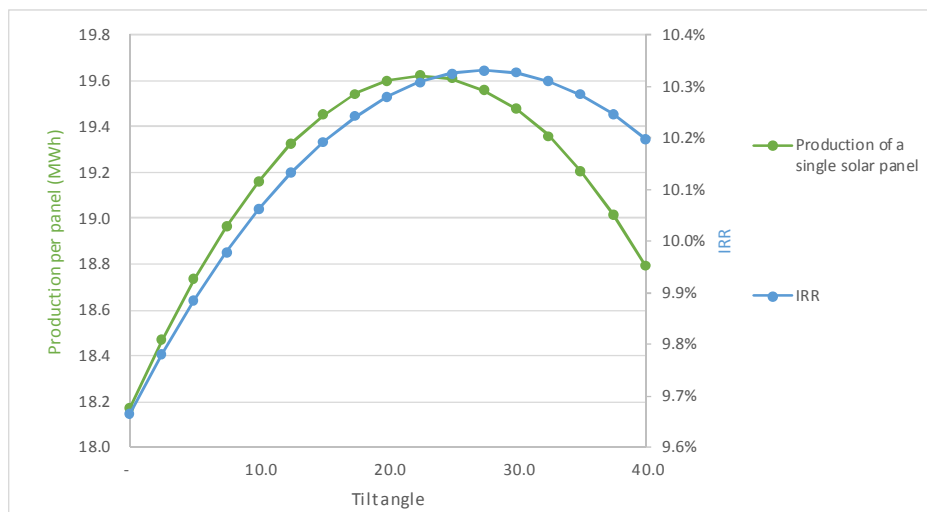


Figure 4-5: Optimisation of the array tilt angle

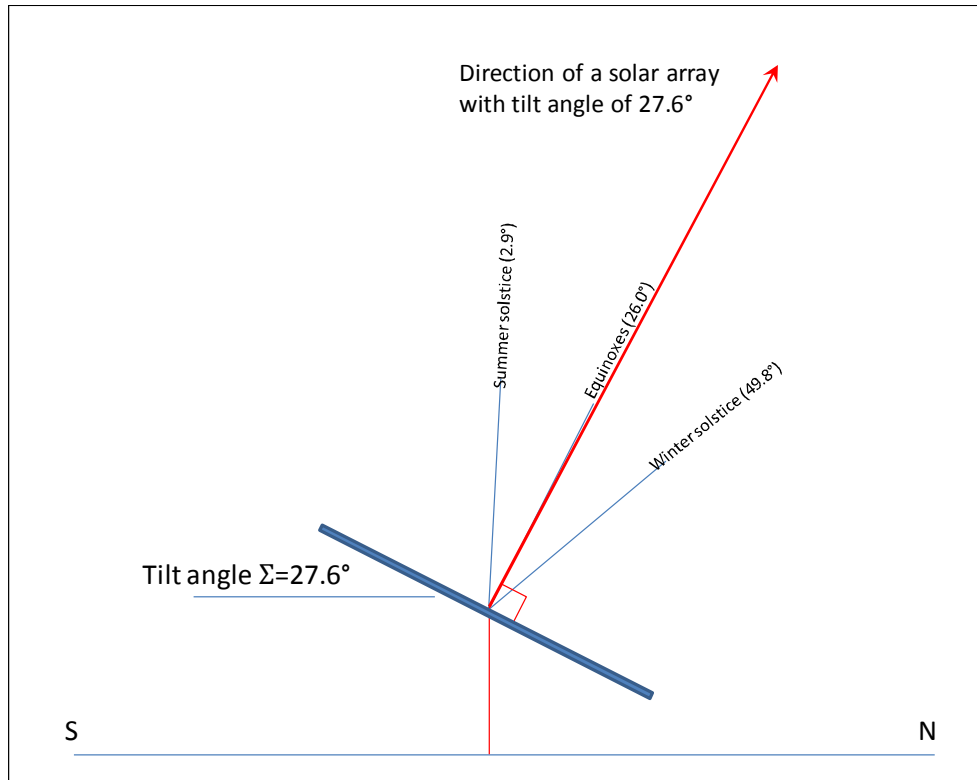


Figure 4-6: Illustration of incidence angles of the sun and direction of the solar array

#### 4.1.4 Determination of the size of the solar plant

As discussed in Section 3.5.3 the spacing between arrays is a function of the tilt angle ( $\Sigma$ ), the shadow angle ( $23.6^\circ$ ) and the array width ( $x$ ) as illustrated in Figure 3-7 and Figure 3-8. Once the tilt angle was fixed at  $27.6^\circ$ , the spacing between adjacent rows was determined. The array width is approximately 4 m wide. Hence, the block layout was finalised to have dimensions of 110 m by 125 m, as calculated in Figure 4-7 and Figure 4-8. This results in approximately 530 of these blocks that can be fitted on the top surface of the ERGO TSF. The optimal system will consist of approximately 1.93 million panels and will have a rated power output of 472 MWp.

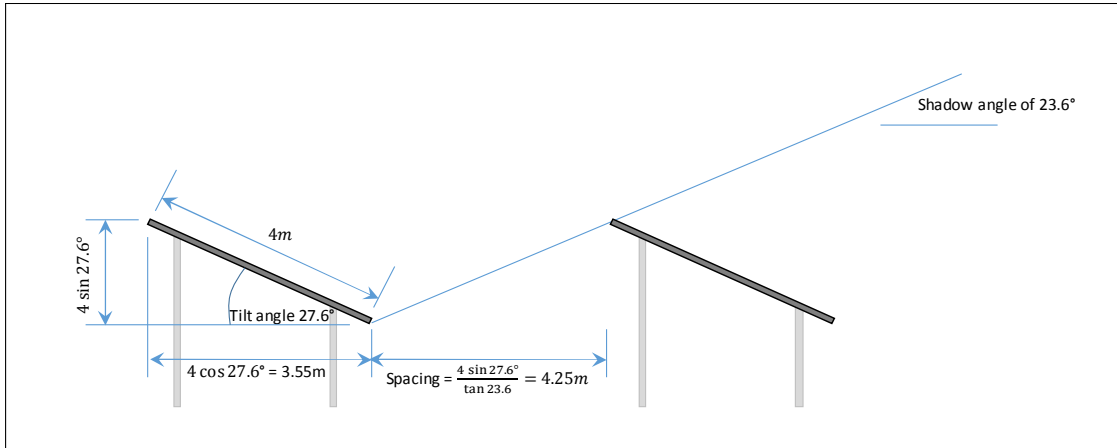


Figure 4-7: Spacing of arrays

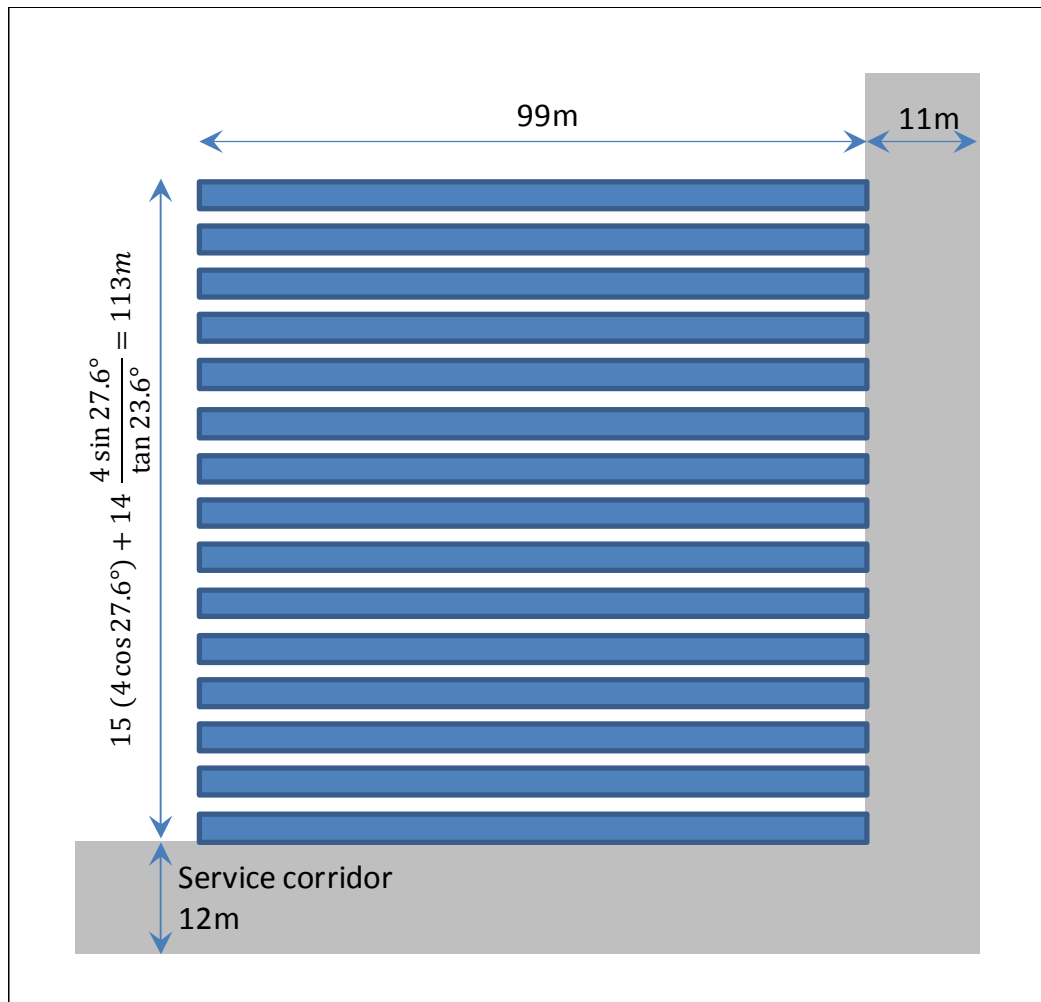


Figure 4-8: Layout of blocks

#### 4.1.5 Daily plant output

The daily plant output differs from day to day depending on the solar declination, the applicable cloud cover factor and the duration of exposure to sunlight.

For the purposes of illustrating the daily plant output results, four specific dates were chosen, 21 December (summer solstice), 21 March (autumnal equinox), 21 June (winter solstice) and 21 September (spring equinox) respectively. The results presented in this section are all applicable to the first year of operation, i.e. no deterioration factor was taken into account. Figure 4-9 shows the paths of the sun on the respective dates mentioned above. This is to illustrate the variation in duration of exposure to sunlight, i.e. production time. It can be noted that the sun paths for March and September coincide.

Figure 4-10 illustrates the sun's daily potential on each square meter of solar panel (i.e. the energy that could be captured with a hypothetical 100% efficiency solar panel). From this graph it can be seen that the yellow curve (21 December) has the longest exposure time, corresponding to the longest day in Figure 4-9, but produces the lowest peak value. That is due to the tilt angle that was optimised to be slightly towards the winter solstice, in order to benefit from the high demand season rates applicable during winter. For the same reason, although the exposure time is shorter during the winter solstice, its production peak is higher than the summer solstice.

It is also interesting to note that during the middle of the day around the times of year of the spring and autumnal equinoxes (if there are clear sky conditions) the sun's potential exceeds that of the standard test conditions ( $1000 \text{ W/m}^2$ ). Hence, the output from a single solar panel should theoretically be higher than the minimal rate power output of 245 Wp assumed in the determination of the construction cost (Section 3.5.5). This is confirmed by the curves in Figure 4-11 which shows the output of a single solar panel at various times of day. The output of the entire plant (under ideal clear sky conditions) is shown in Figure 4-12. It can be seen that the plant's generation capacity can exceed 500 MW under ideal circumstances, although the rated power output is only 472 MWp. This is the same order of magnitude as the Topaz Solar Farm (the largest solar PV plant in the world), which is currently 550 MWp, as mentioned in Section 2.5.5 (Dailymail, 2014, PV Magazine, 2014, GreentechMedia, 2014).

It can be seen in Figure 4-10 that the sun's potential during the equinoxes compares well with the 1.0 kW and 1.4 kW range of power on every exposed square meter, as per the guidelines provided by Zweibel (1990) and Breeze (2005) contained in the literature review in Section 2.5.1.

It is also interesting to note that none of the curves in Figure 4-10, Figure 4-11 or Figure 4-12 are symmetrical around solar noon. The reason being that the azimuth angle of the panels are  $16.3^\circ$  east of north and therefore the production is higher in the morning than in the afternoon.

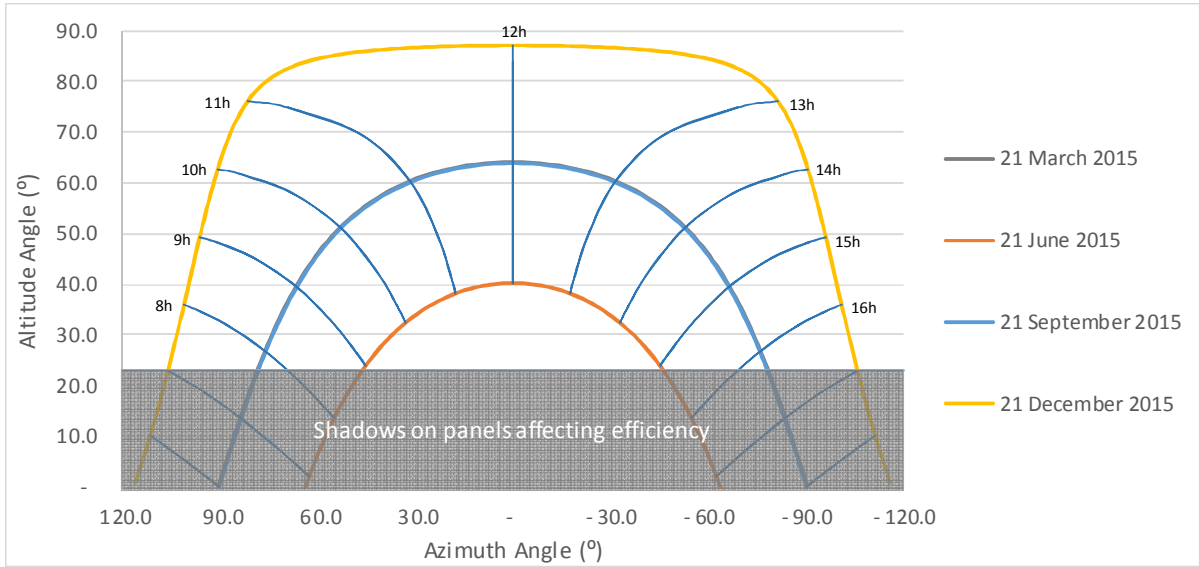


Figure 4-9: Sun path diagram for the ERGO site

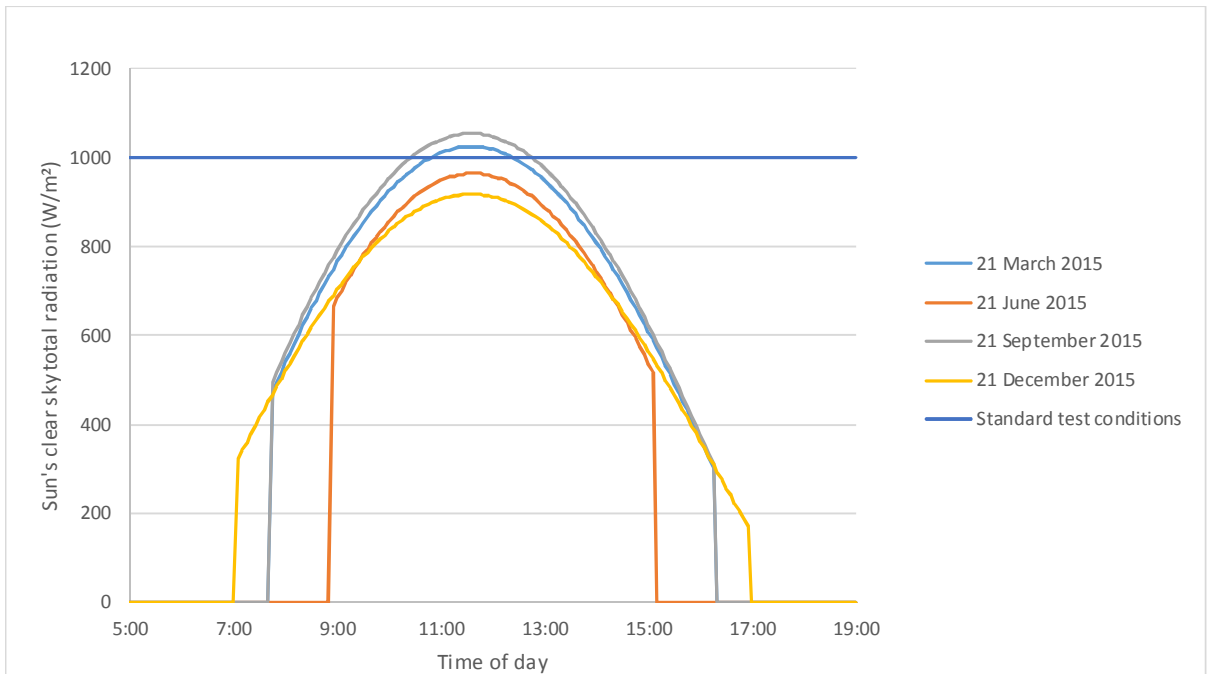


Figure 4-10: The sun's daily clear sky radiation at different times of day

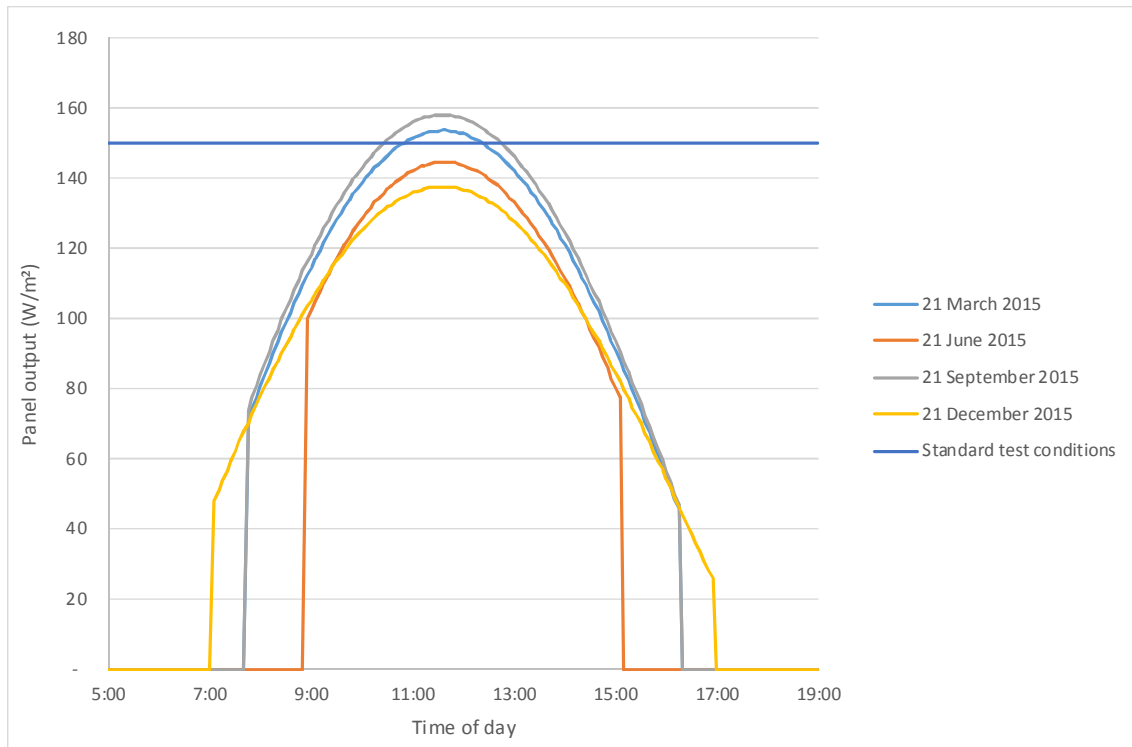


Figure 4-11: Variation of output of a single solar panel during the day (dimensions 990 mm x 1650 mm, 15% efficiency)

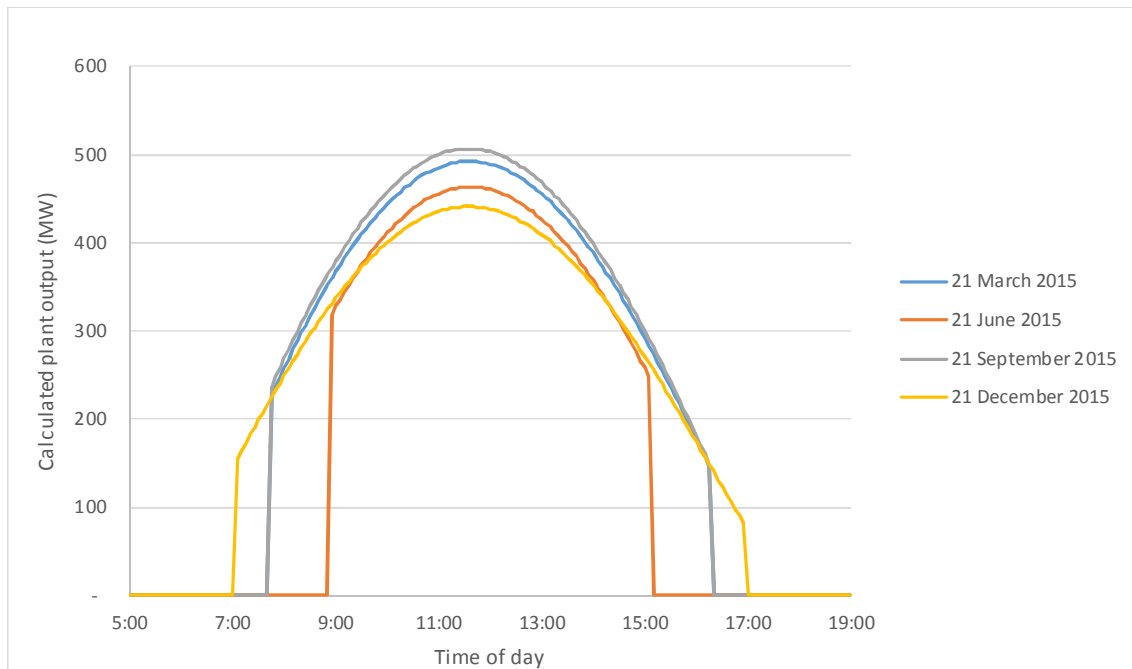


Figure 4-12: Output of the plant at various times of day

#### 4.1.6 Daily electricity production

By integrating the area underneath the “output vs time” curves above and allowing for the cloud cover factor (derived from the NASA data) and plant degradation, the expected daily production of electricity was calculated.

A comparison of the daily solar radiation (kWh) per square meter from the sun on a horizontal surface at the ERGO site and the amount that can be converted to electricity daily by one square meter of tilted solar panel is shown in Figure 4-13 (note the difference in magnitude of the axes). The shapes of the curves are similar, although the converted electricity is significantly lower than the received radiation, due to the solar panels low conversion factor (efficiency of 15%). However, the electricity production curve flattens out over the summer months due to the tilt angle of the panels. Note that the black solar radiation curve (which is the same as that in Figure 4-3) applies to radiation on a horizontal surface and would therefore receive more radiation when the sun is almost directly overhead in the summer months.

By integrating the area underneath the curves in Figure 4-12 and allowing for the cloud cover factor (derived from the NASA data), the daily production from the plant was calculated and presented for every calendar day in Figure 4-14. The variance of daily production over the year can be seen in Figure 4-14. The degradation of the plants performance with time is illustrated and colour coded in Figure 4-14 and Figure 4-15.

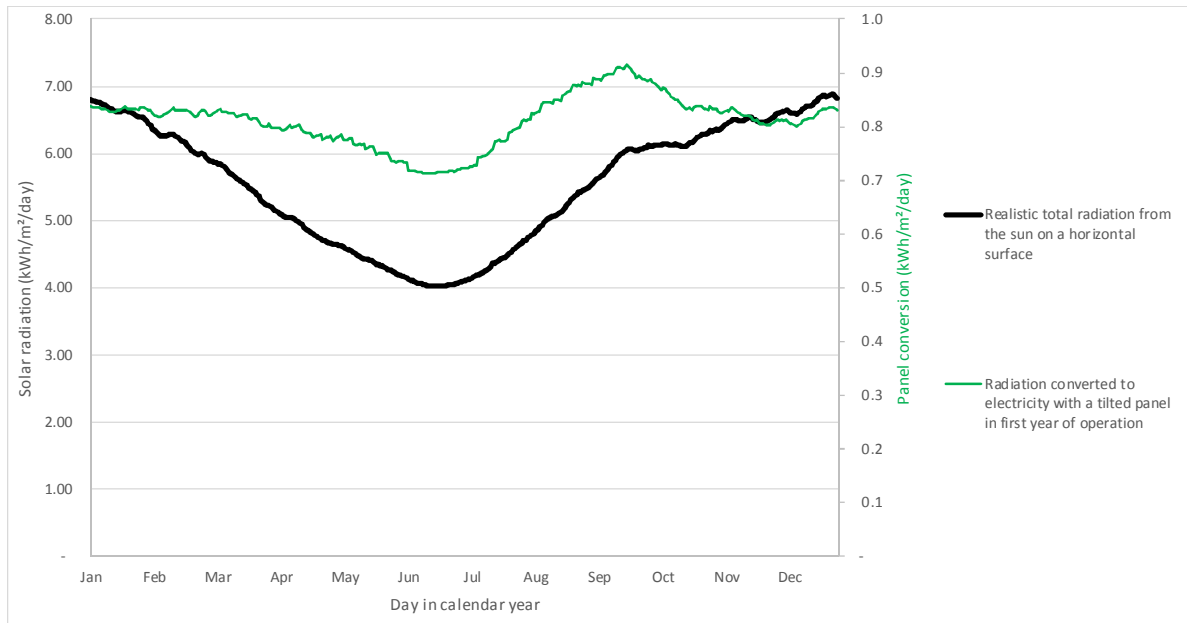


Figure 4-13: Comparison of daily solar radiation on a horizontal surface and the amount converted to electricity by a tilted panel

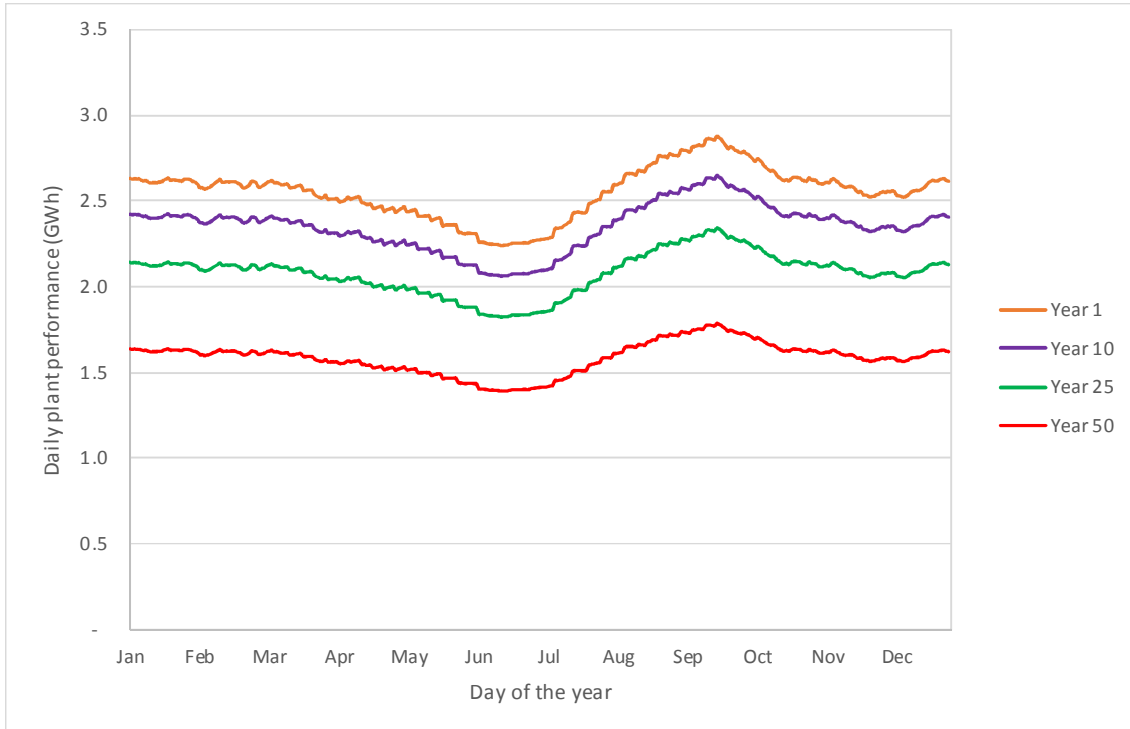


Figure 4-14: Daily electricity production over a calendar year

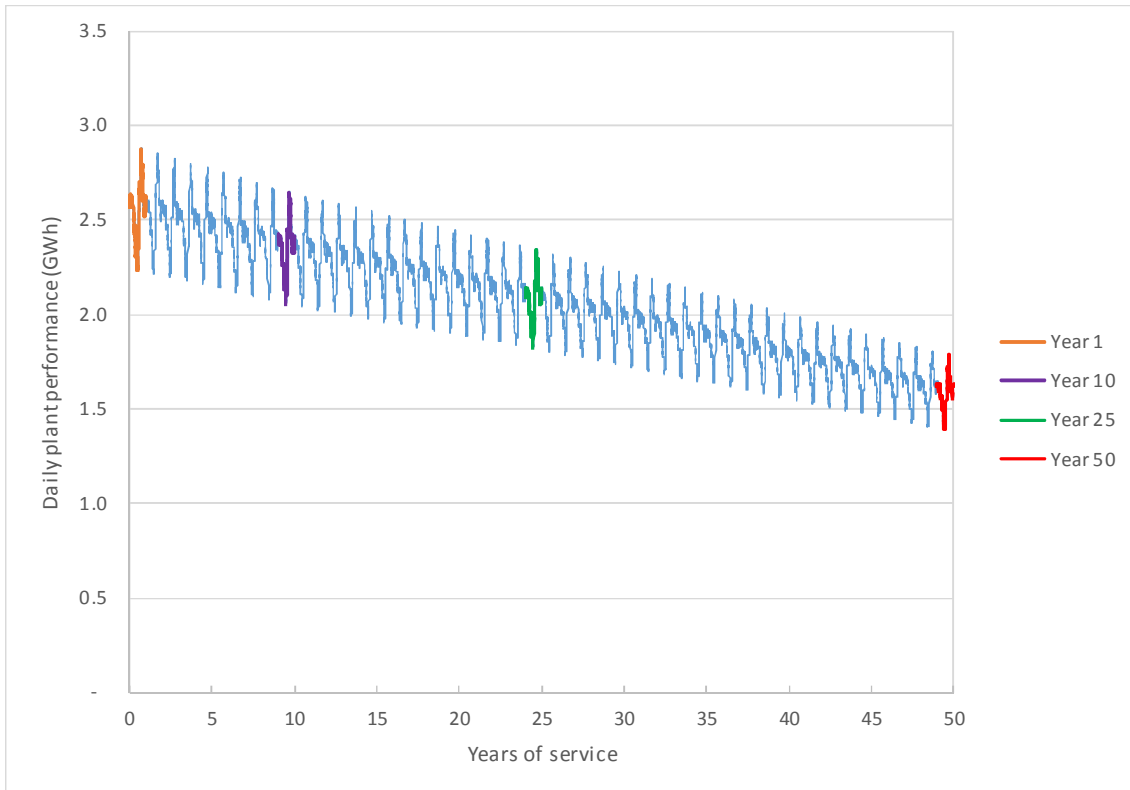


Figure 4-15: Degradation of plant performance over the operational life of the plant

#### 4.1.7 Financial implications

The construction cost of the facility was determined as described in Section 3.5.5 and amounts to approximately R 10.4 billion (2014 prices).

The trade commodity is electricity produced, hence the cumulative electricity production over the life of the plant directly influences the total income generated. The blue curve in Figure 4-16 shows the cumulative production of electricity over the 50 year life of the facility. The solar suppliers use an average production of between 4.50 kWh and 4.75 kWh per kWp of installed capacity per day (applicable to the Johannesburg region) to obtain a first order estimate of plant production (SolarEff, 2014). The green and orange curves in Figure 4-16 show these estimates using these two values respectively. It can be seen that the calculated cumulative production is of the correct order of magnitude.

The potential annual income over the 50 year operational life was subsequently calculated as described in Section 3.5.6 and shown by the blue curve in Figure 4-17. The cumulative income over the 50 year life of the plant is shown Figure 4-17. The drastic increase in income from the plant over its life is due to a projected 7.4% annual increase in Eskom rates over the life of the facility, although the plant production degrades at 0.7% per annum.

By considering the annual income for each year and using the calculated construction cost, the IRR was calculated to be 10.70% at the end of 50 years. The graph in Figure 4-18 shows the progressive increase in IRR over the life of the solar plant. At first the income repays the invested capital, resulting in a negative IRR. It can be seen that a breakeven point is reached during the 14<sup>th</sup> year of operation, beyond which the investment starts generating profit. Table 4-1 summarises the details of the optimal solar plant layout that can be built on the ERGO TSF.

Table 4-1: Summary of optimal solar plant on top of the ERGO TSF

Optimum azimuth angle of solar panels	16.3° East of North
Optimum tilt angle of solar panels	27.6° with the horizontal
Number of panels in plant	1 926 000
Recommended panel	245 Wp (15% efficiency)
Rated plant output	471.9 MWp
Total life production	37.7 TWh
Unit construction cost	R 22 /Wp
Total construction cost	R 10.4 billion
Total income over 50 year life	R 171.0 billion
IRR at 50 years	10.70 %

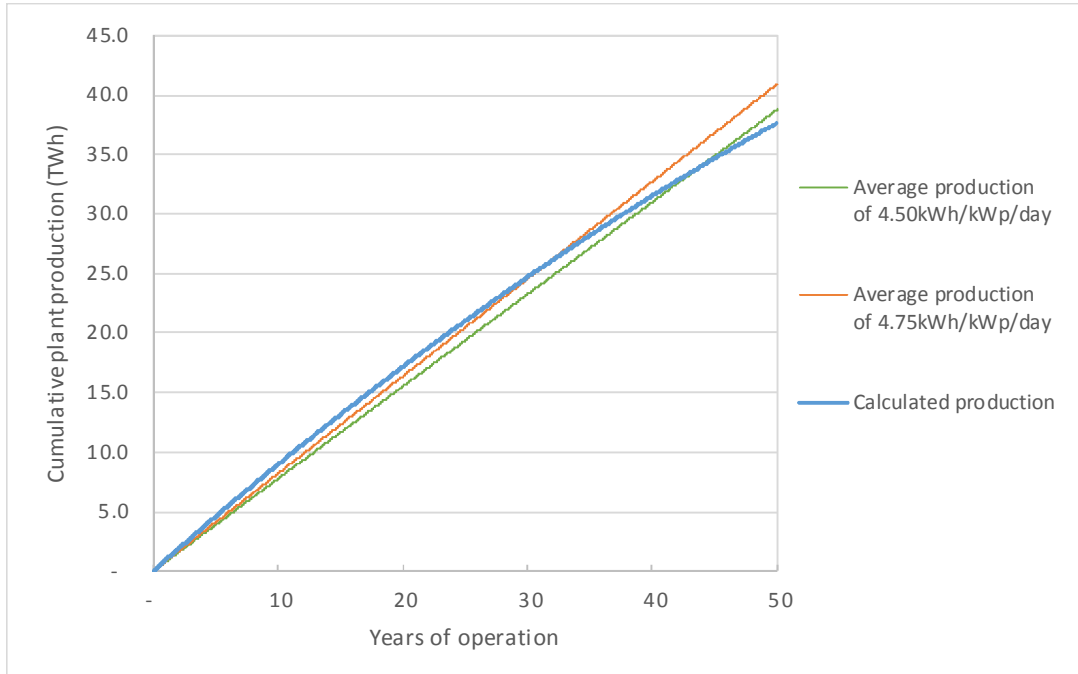


Figure 4-16: Increase of cumulative plant production over the life of plant

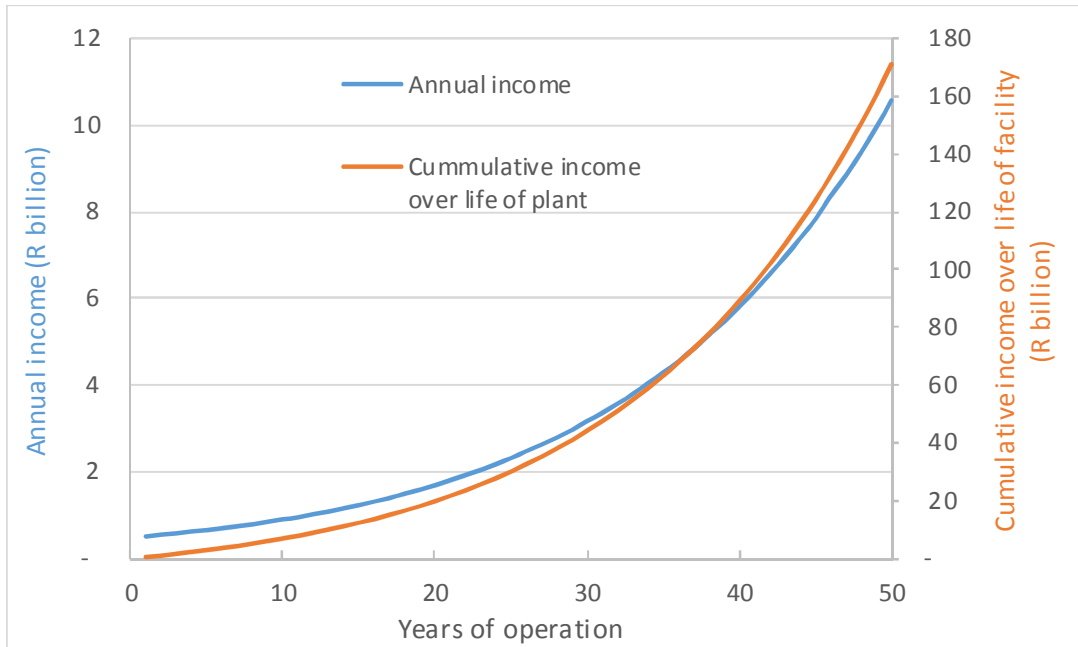


Figure 4-17: Increase in annual and cumulative income over the life of the plant

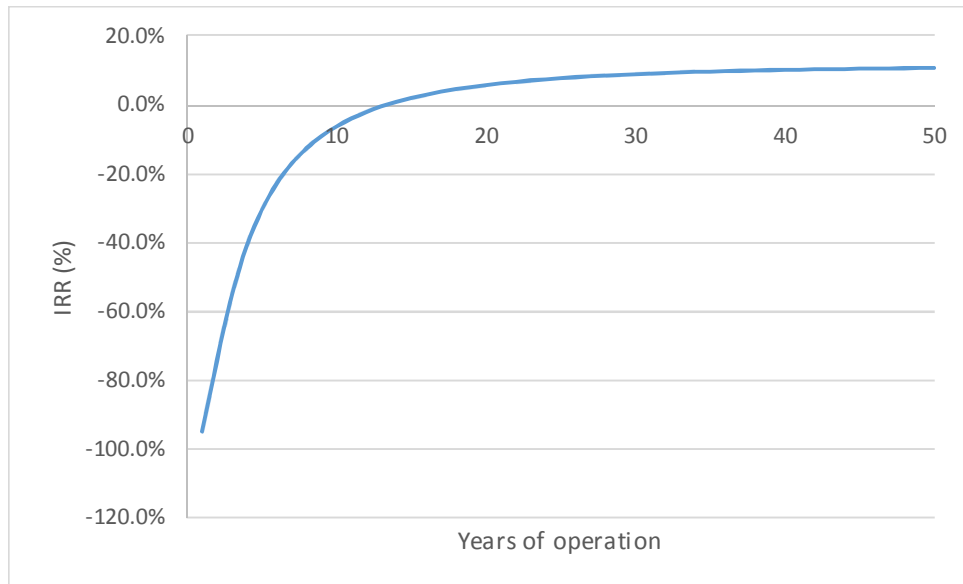


Figure 4-18: Progressive increase in IRR over life of the plant

#### 4.1.8 Reliability analysis

The statistical reliability analysis of the calculated data provides an indication of the certainty that the solar plant will produce a certain amount of electricity (GWh) or income (millions of Rands) on any given day.

The orange curve in Figure 4-19 shows the reliability of the plant in producing a certain amount of electricity in a day (top horizontal axis). The calculations show that 90% of the time (calculated over the 50 year life time) the plant will produce at least 1.25 GWh. In other words, the plant will be 90% reliable to provide 1.25 GWh. The other 10% of the time the conditions (cloud cover) does not allow enough radiation for the plant to produce 1.25 GWh of electricity on that day. Half of the time the plant can reliably produce more than 2.15 GWh. Only 10% of time the plant will be able to produce at least 2.85 GWh.

The orange bar histogram in Figure 4-20 shows the percentage of time that the daily electricity production falls within a certain 0.1 GWh (100 MWh) range. For example, 7.2% of the time the plant will produce between 2.0 and 2.1 GWh per day. Due to the finite number of days in the 50 year life (for which production values were calculated) the histogram represents a discrete distribution.

A normal distribution (continuous orange line curve) was plotted on the same in Figure 4-20, in an attempt to obtain a representative continuous probability density function. A continuous probability function can be used to estimate the probability of the plant producing a daily electricity output within a certain range. For example, if the probability of the plant being able to

produce between 2 and 3 GWh per day is to be determined, the area under the orange line can be calculated within the 2 and 3 GWh interval.

From a visual inspection of the graph in Figure 4-20 it can be seen that the normal distribution does not fit the shape of the histogram that well, but is still deemed to be representative of the spread of calculated values. The reasons why the normal distribution is not ideal, is that a normal distribution relies only on the mean and standard deviation of the data, which are 2.09 GWh and 0.61 GWh respectively. It assumes the data is spread symmetrically around the mean value and therefore does not take the skewness of the data into account, which is visible from the histogram.

Other inaccuracies include that there are no bounds to the normal distribution, i.e. the normal distribution inherently states that there is an infinitesimal probability that the daily production can be infinitely large. This is not possible seeing that there is a maximum daily plant production value that cannot be exceeded (under ideal clear sky circumstances). The same applies towards the negative side. It is unlikely that the plant production will be negative (as the normal distribution suggests), i.e. for the plant to act as a sink, converting power from the grid to heat, is possible but unlikely to be allowed.

Even with the above being mentioned, for the purposes of such a high level feasibility study (containing many assumptions), the normal distribution is deemed to be sufficiently accurate.

The blue curve in Figure 4-19 shows the reliability of the plant being able to generate a certain amount of income in a day (bottom horizontal axis). There is a 90% chance that the plant will produce at least R550 000 (in net present monetary value) in a day. The grey line indicates the average daily income (R1.15 million) required to generate the optimum IRR (10.7%) over the 50 year life of the facility. It is interesting to note that only 42% of the time the daily income will exceed the R1.15 million. It is expected to be 50% of the time. This eccentricity is due to the tariff structure and non-symmetrical distribution of the production data.

The blue bar histogram in Figure 4-21 shows the percentage of time that the daily income falls within a certain R0.1 million (R100 000) range. For example, 10.4% of the time the plant will generate a daily income of between R1.1 million and R1.2 million.

A normal distribution (continuous blue line) was also plotted in Figure 4-21. It can be seen that the normal distribution fits the shape of the daily income histogram well and is deemed to be representative of the spread of calculated values. Based on a visual inspection of Figure 4-20 and Figure 4-21, the normal distribution fits the calculated daily income better than the daily plant production discussed above. The mean and standard deviation of the daily income data are R1.09 million and R0.42 million respectively.

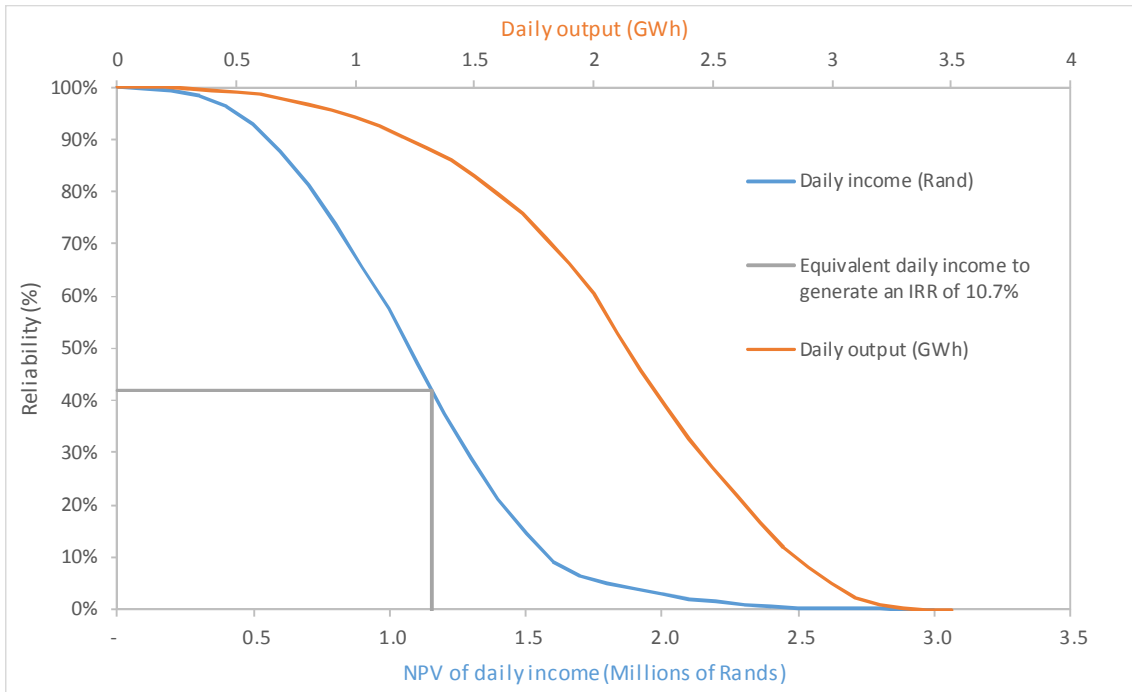


Figure 4-19: Reliability of daily electricity generation and associated income

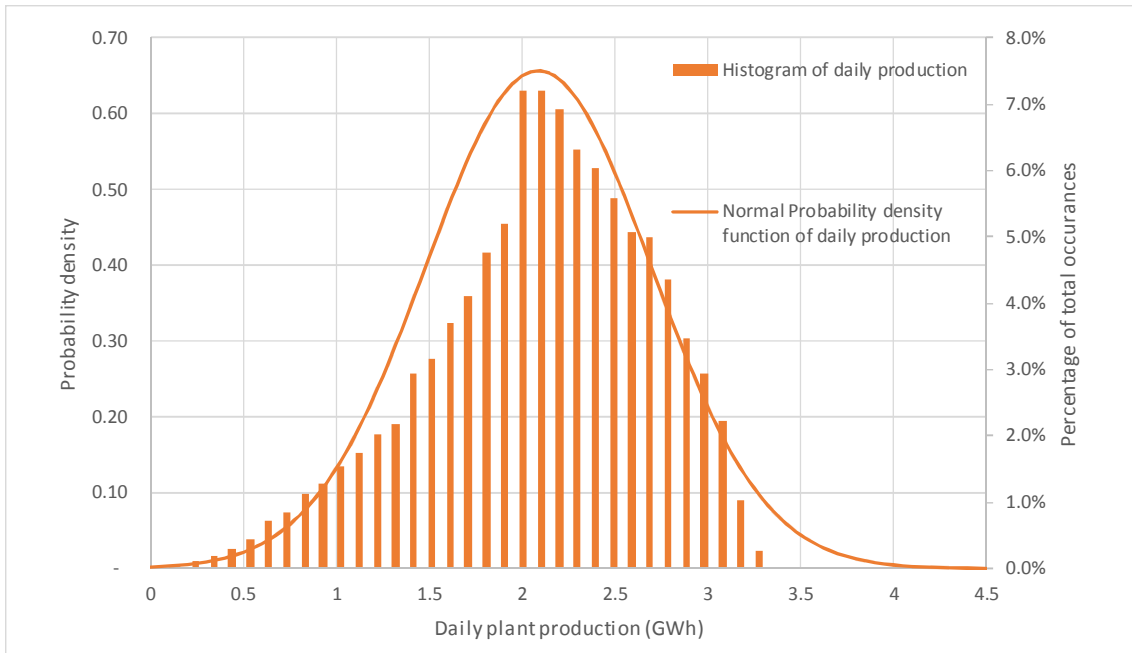


Figure 4-20: Distribution of daily production

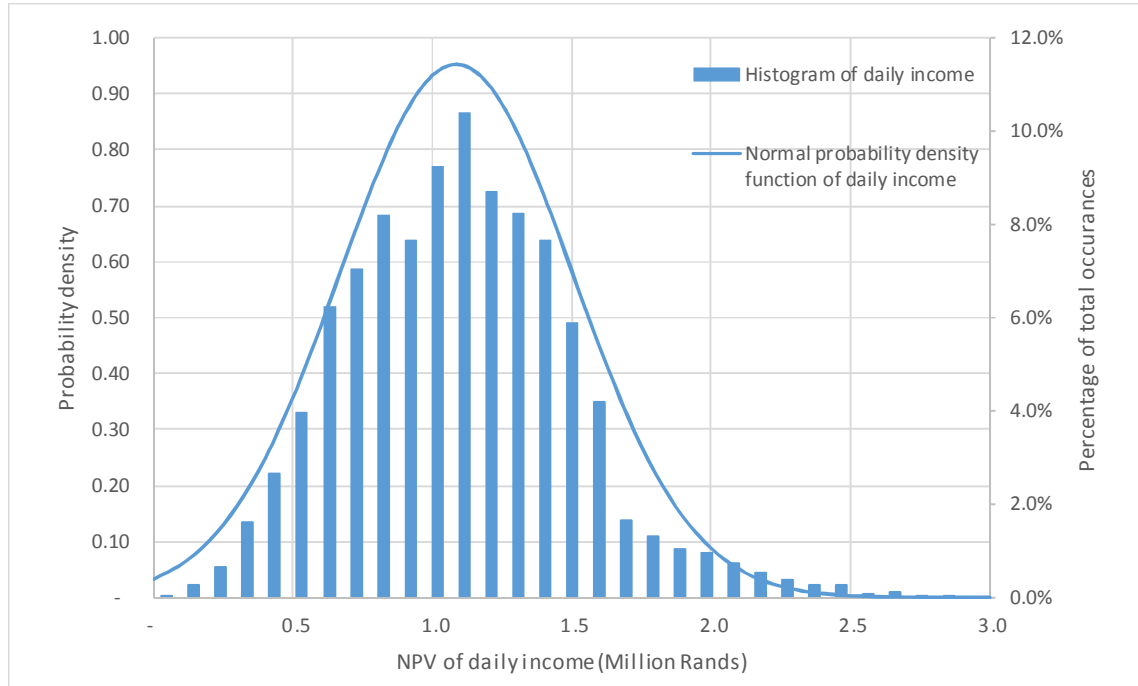


Figure 4-21: Distribution of daily income

#### 4.1.9 Sensitivity analysis results

The sensitivity of a solar PV system to the collector azimuth and tilt angles was assessed in Section 4.1.3. The following section presents the results of sensitivity analyses conducted on some of the other assumed parameters that may influence the performance and feasibility of the solar PV system. The assumed parameters were varied (each within its expected range) to determine the sensitivity of the IRR and total plant production (over a 50 year lifetime) to a change in these assumed parameters (whilst keeping all other variables constant). The following assumed parameters that were assessed:

- Panel performance, including panel efficiency and watt-peak value.
- Degradation of the plant performance beyond 25 years
- Unit capital cost
- Total area available for construction of the plant

##### 4.1.9.1 Panel performance

Panel performance include panel efficiency and watt-peak values, which are interdependent. The efficiency was assumed to be 15%, but within the Yingli Solar's YGE 60Cell 40mm Series can

vary between 14.1% and 15.9%, each with its own corresponding watt-peak output value (Yingli Solar, 2012). For convenience sake Table 3-1 is repeated in Table 4-2 below.

The blue curve in Figure 4-22 shows that the IRR decreases with an increase in efficiency. Note, however, that the watt-peak rating of the panels increase with an increase in efficiency and hence the initial cost of construction also increases if the unit cost of R22/Wp is assumed to remain constant. Hence the IRR decreases with an increase in efficiency. Note that a minimal change in IRR of -0.14% is calculated in spite of a 12% change in efficiency. Hence it can be concluded that the IRR is not sensitive to a change in efficiency within the range available.

The orange curve in Figure 4-22 shows the increase in total plant production due to an increase in efficiency. A 12% increase in cumulative plant production is calculated for the 12% change in efficiency.

It can be concluded that the panel selection does not have a significant effect on the IRR, but have a slight effect on the plant production. Hence, it is suggested that the panels with the highest efficiency be chosen to maximise the plant output.

Table 4-2: Performance and corresponding efficiencies for various panels (Yingli Solar, 2012)

Panel performance under STC (Watt-peak)	230	235	240	245	250	255	260
Corresponding panel efficiency (%)	14.1	14.4	14.7	15.0	15.3	15.6	15.9

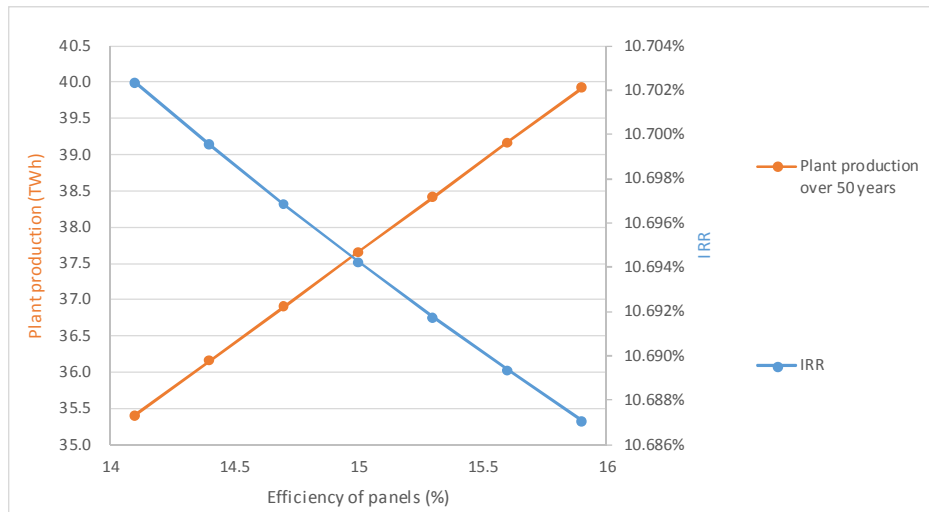


Figure 4-22: Sensitivity of the IRR and total plant production to change in efficiency

#### 4.1.9.2 *Degradation of the plant performance beyond 25 years*

Degradation of the plant performance beyond 25 years was assumed to be on average 0.70% per annum in Section 3.5.4. The blue curve in Figure 4-23 shows that the IRR decreases with an increase in the plant degradation rate. An increase in degradation rate will lead to a decrease in total electricity produced (orange curve in Figure 4-23) which will generate less income, resulting in a lower IRR. Note that a minimal change in IRR of -0.2% is calculated in spite of a 114% change in degradation rate. Hence, it can be concluded that the IRR is not sensitive to a change in degradation rate within the limits expected. This is largely due to the fact that the IRR is already at 7.7% (on the graph in Figure 4-18) after 25 years, by the time the degradation rate warranty expires.

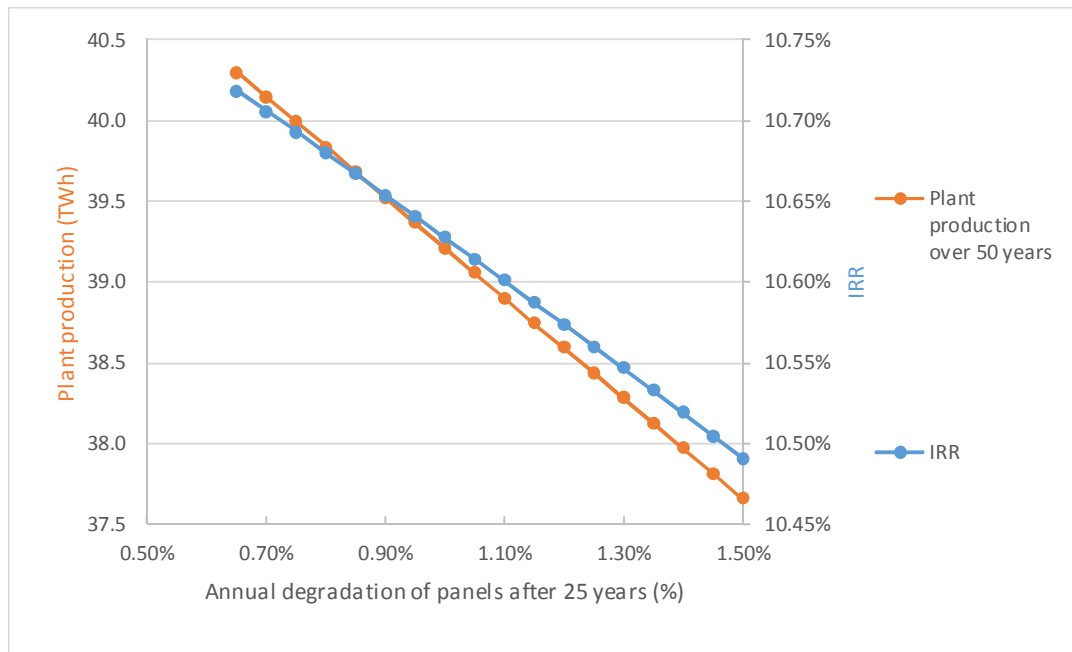


Figure 4-23: Sensitivity of the IRR and total plant production to change in degradation rate

#### 4.1.9.3 *Unit cost*

The unit cost for the construction of the plant was assumed to be R22/Wp per annum in Section 3.5.5.

Trends indicate that advancement in technology in the solar PV field over the last decade has led to a decrease in unit cost. Hence, this analysis shows the benefit a further decrease in unit cost can have on a project of this scale. The curve in Figure 4-24 shows that the IRR increases with a

decrease in unit cost. A decrease in unit cost will reduce the initial capital investment required, but will have no effect on the production of the plant (hence income remains constant), resulting in a higher IRR. It can be concluded that the IRR is sensitive to a change in unit cost, which is positive for the future of solar technology, as technology often becomes cheaper over time.

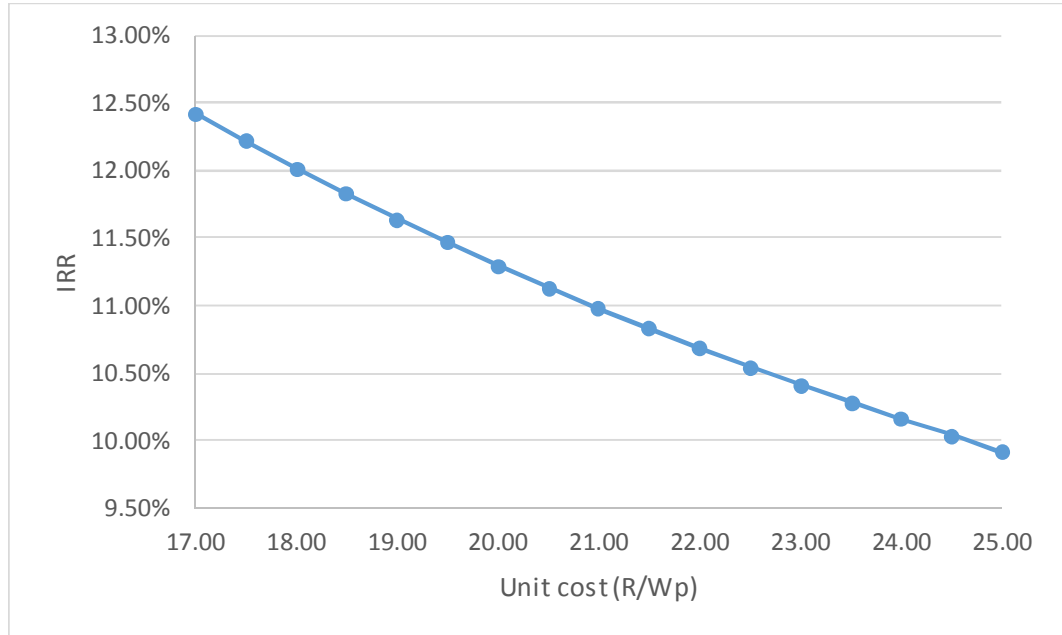


Figure 4-24: Sensitivity of the IRR and total plant production to change in degradation rate

#### 4.1.9.4 *Top area of the TSF*

The area available for the construction of the solar PV plant was assumed to be 276 ha in Section 3.5.3. The blue curve in Figure 4-25 indicates that a change in available area has no effect on the IRR, this is due to the fact that solar resource (the sun) remains the same regardless of the area.

A change in area however does have a significant effect on the total plant production. The larger the available area, the more panels can be fitted onto it, which will increase the plant production and associated income linearly. The construction cost will be similarly affected, resulting in a zero effect on the IRR.

Hence it can be concluded that the IRR is *not* sensitive to a change in area, which means this option can also be developed on smaller dormant TSFs, as long as it is at large enough scale that the economy of scale unit prices apply.

Table 4-3 provides a summary of the sensitivity analyses results.

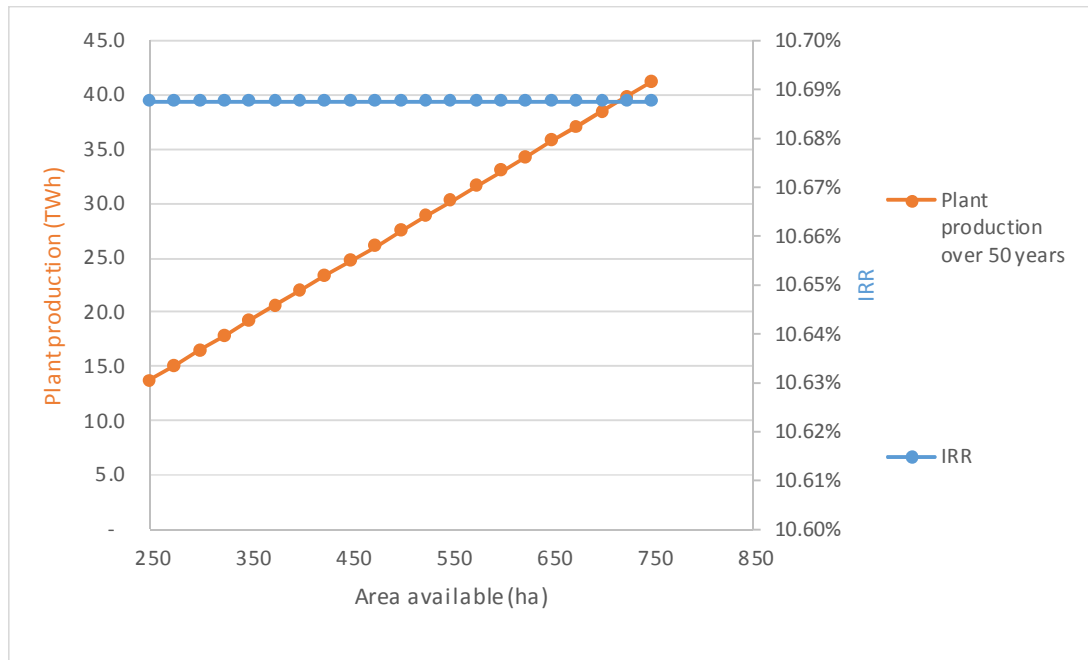


Figure 4-25: Sensitivity of the IRR and total plant production to change in available area

Table 4-3: Summary of sensitivity analysis

Change in parameter	Sensitivity of IRR	Sensitivity of total plant production
Panel performance	Not sensitive	Slightly sensitive
Degradation rate beyond 25 years	Not sensitive	Slightly sensitive
Unit cost	Sensitive	No effect
Available area	No effect	Sensitive

## 4.2 PUMP STORAGE SCHEME DEVELOPMENT

The following section presents the results of the analysis to determine the financial feasibility of a pump storage scheme on the ERGO TSF site. The following results were discussed:

- The available water resource at ERGO TSF
- Optimisation of the release rate to generate maximum return on investment
- Reliability analysis
- Sensitivity analysis of assumed parameters
- The effect of lining the TSF catchment

### 4.2.1 Determination of the water resource available for power generation

A water balance simulation was conducted for the ERGO TSF to determine the volume of water available for power generation at any time.

Figure 4-26 shows the volume of water available in the ERGO TSF pond when the reoccurrence of the rainfall record was simulated with the water balance model when no water is released. It can be seen that each year during the rainy season the volume of water in the TSF pond increases and during the dry season a large portion thereof evaporates. It can be seen that the pond volume varies between about 1 and 6 million cubic meters of water available to generate electricity.

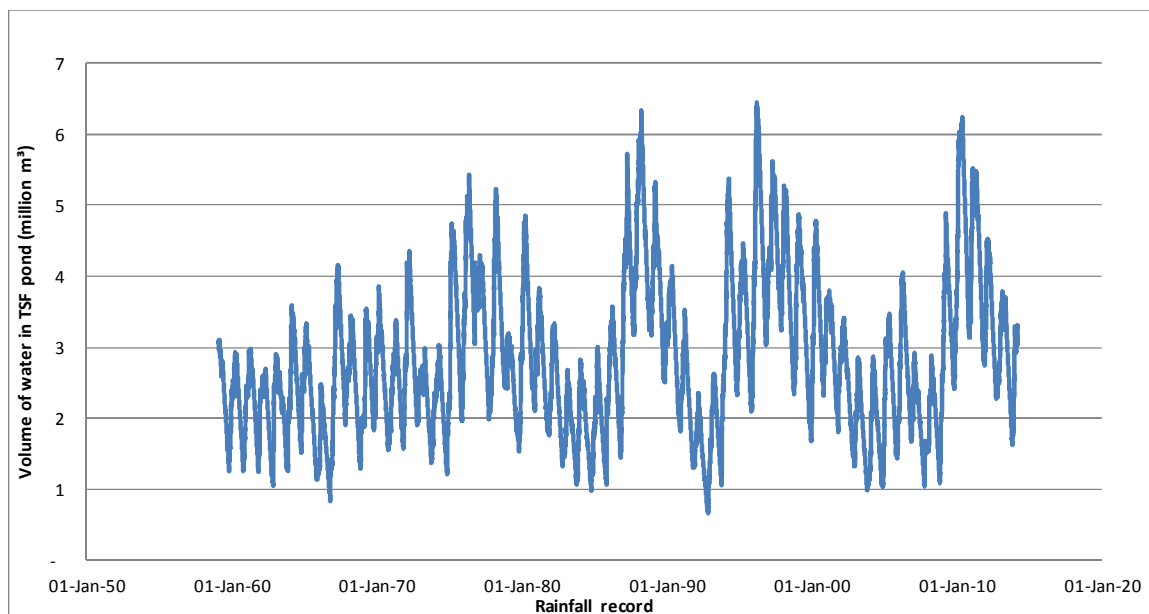


Figure 4-26: Volume of water in the TSF pond available for power generation

#### 4.2.2 Results of the optimisation of the pump storage scheme system

As mentioned in Section 3.6.7 all equations, including the power generation capacity (W), electricity generation/consumption (kWh), cost and profit formulae, were written as functions of the only controllable variable namely the release rate  $Q_T$  ( $\text{m}^3/\text{s}$ ). The IRR was calculated for a range of  $Q_T$  values to determine the optimal IRR which can be generated. The results are presented in Figure 4-27 and Figure 4-28 respectively.

Figure 4-27 shows the results of the analysis against a range of release capacities. The red curve shows the initial capital investment required for various release capacities. The purple curve shows the net present value (NPV) of the cumulative daily operational income over the 50 year project life. The green curve shows the difference between the purple and red curves, which is the NPV of the total profit that can be made over the 50 year project life. The blue curve is that of the IRR (secondary vertical axis on the right) for the various release capacities. It is interesting to note that the blue IRR curve and the green total profit curves do not peak at the same release capacity. The reason for this being that the peak of the green curve takes place when the total net profit is at an absolute maximum (meaning the red and purple curves are the furthest apart at the specific release capacity), where the blue curve peaks where the return made for every Rand invested is at a maximum.

In Figure 4-28 the same results are presented against a range of release capacities, with the horizontal axis plotted on a logarithmic scale. It was found that this better illustrates the peaks of the blue and green curves. It can be seen that the total profit green curve peaks at around 720 000  $\text{m}^3/\text{h}$  (or 200  $\text{m}^3/\text{s}$ ). It can also be seen that the IRR reaches a maximum of 10.27% if the pump storage scheme has a release capacity of 230 000  $\text{m}^3/\text{h}$  (63.8  $\text{m}^3/\text{s}$ ). It can therefore be concluded that the internal rate of return for every one Rand of invested capital is a maximum when the release capacity is 230 000  $\text{m}^3/\text{h}$ , although the total net profit (over a 50 project life) is a maximum when the capacity is 720 000  $\text{m}^3/\text{h}$ . At 720 000  $\text{m}^3/\text{h}$  the scale is larger than for 230 000  $\text{m}^3/\text{h}$ , meaning the initial investment required is larger, the net income is larger and hence the net profit is larger. However, at a scale of 230 000  $\text{m}^3/\text{h}$ , the profit made for every one Rand of capital invested is maximum.

Table 4-4 provides the details of the pump storage scheme system with a capacity of 230 000  $\text{m}^3/\text{h}$  (63.9  $\text{m}^3/\text{s}$ ). Note that a generating capacity of 78.2 MW has been calculated. In order to convey water at such a high flow rate a large inlet structure and outlet pipe are required. In fact, to maintain the recommended 3 m/s flow velocity (Van Dijk, 2014), a single 5.2 m diameter outlet pipe has to be installed. However, due to practical reasons it might be better to split it up into four 2.6 m diameter outlet pipes, each with its own 20 MW turbine.

Indicative prices were obtained from three European turbine manufacturers, Voith, Global Hydro Energy and Wasserkraft respectively. Voith (2014) provided an indicative cost for reversible pump-turbines. Global Hydro Energy (2014) and Wasserkraft (2014) provided cost estimates for turbines only, which would have to be combined with separate pumps. A comparison of the cost estimates can be seen in Table 4-5. Prices for separate pump (with these capacities) could not be obtained. It can be concluded that the formulae by Saini and Singal (2008), adapted by Van Vuuren et al. (2011), provided sufficiently accurate estimates for the turbine and generator units, for the purpose of this study.

The construction cost of the civil works may exceed that predicted values (based on the empirical relations used) as construction on tailings is likely to be more challenging than conventional sites.

Table 4-4: Particulars of a system with a release capacity of 230 000 m<sup>3</sup>/h (63.9 m<sup>3</sup>/s)

Parameter	Result
Release capacity of outlet pipes	230 000 m <sup>3</sup> /h (optimum at 229 632 m <sup>3</sup> /h)
Single “representative” outlet pipe size	5.2 m (at assumed flow rate of 3 m/s)
Generation capacity	78.2 MW
Electricity generation on a weekday	391.2 MWh (during 5 peak hours)
Total production over 50 year life	4.76 TWh
Required pumping power input	60.6 MW
Electricity consumption on a weekday	485.3 MWh (during 8 off-peak hours)
Total consumption over 50 year life	5.93 TWh
Overall system efficiency ( $E_T/E_P$ )	80.3%
Required lower reservoir volume	1 334 000 m <sup>3</sup>
Percentage of peak time operating at capacity*	77%
Initial capital investment required	R 1 601 million
Cost of electromechanical equipment ( $C_{EM}$ )	R 492 million (31% of total cost)
Cost of civil works equipment ( $C_{CW}$ )	R 642 million (40% of total cost)
Cost of lower reservoir construction ( $C_{LR}$ )	R 467 million (29% of total cost)
Annual cost of maintenance and operation ( $C_{MO}$ )	R 31 million
NPV of cumulative operational profit	R 4 028 million
NPV of net profit over 50 year life	R 2 396 million
IRR over 50 year project life	10.27%

\* Percentage of days that the turbine will operate at full capacity (i.e. % of weekdays through the 50 year life for which there is a sufficient volume of water in the TSF pond for the turbine to be running at full capacity for the entire 5 peak hours a day).

Table 4-5: Comparison of indicative prices by European turbine manufacturers

Manufacturer	Offer	Cost in Euro*	Cost in Rands
Voith	3 Reversible pump-turbines	€ 27.6 million	<b>R 378 million</b>
	4 Reversible pump-turbines	€ 33.1 million	<b>R 454 million</b>
Global Hydro Energy	3 Turbines only (no pumps)	€ 7.5 million	R 103 million
	4 Turbines only (no pumps)	€ 8.4 million	R 115 million
Wasserkraft	12 Small turbines only	€ 12.3 million	R 168 million
Cost of turbine and generator units estimated with Saini and Singal (2008) equations <b>= R 435 million</b>			

\*A currency conversion rate of R13.70 per Euro was used, as on 10 December 2014.

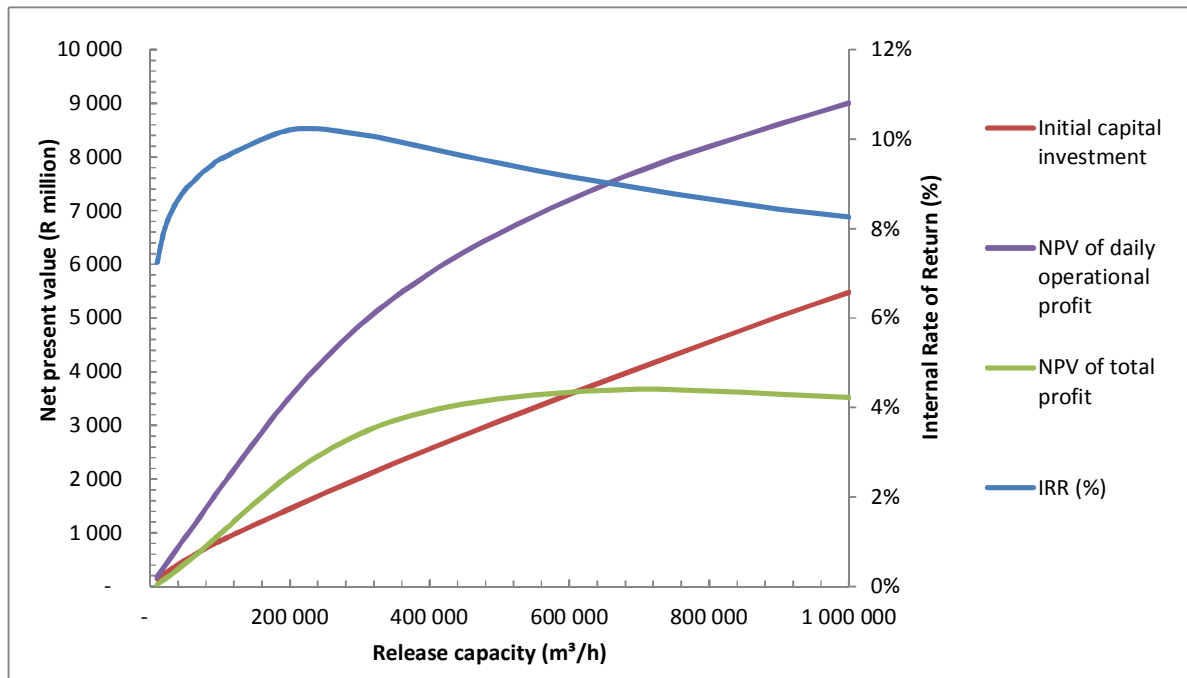


Figure 4-27: Profit and IRR for various release rates

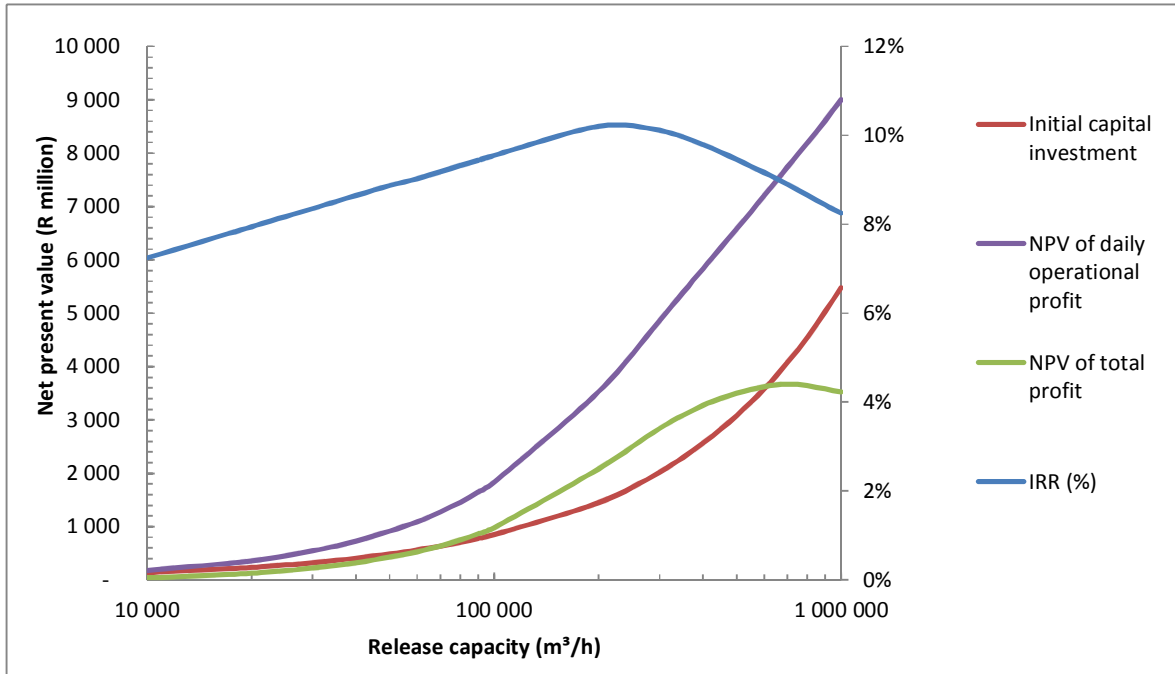


Figure 4-28: Profit and IRR for various release rates (plotted on a log scale)

### 4.2.3 Reliability analysis

Statistical analysis of the calculated data provides an indication of the reliability of the pump storage scheme to generate peak demand period electricity.

The orange curve in Figure 4-29 shows the reliability of the plant being able to produce a certain amount of peak period electricity on a weekday (top horizontal axis). The system reliability only reflects the availability of water on the TSF and does not account for factors like equipment breakdowns etc. The calculations show that 90% of the time (calculated over the last 50 years of the rainfall record) the plant will produce at least 330 MWh per weekday (during the 5 peak consumption hours). In other words the plant will be 90% reliable to provide 330 MWh on a weekday. There is a 78% chance that the plant will be able to produce 390 MWh on a weekday. For the remaining 22% of the time the volume of water in the TSF pond is not enough to operate the system at full capacity for the entire 5 hours of peak consumption. This is also reflected by the histogram in Figure 4-30 which shows the distribution of weekday peak power generation. It shows that the system is operating at or near capacity for nearly 80% of the peak consumption time.

The blue curve in Figure 4-29 shows the reliability of the plant being able to generate a certain amount of daily operational profit (bottom horizontal axis). There is a 90% chance that the plant

will produce at least R120 000 (in net present monetary value) on a weekday. There is a 25% chance that the plant will produce at least R200 000 and a 23% chance that the plant will produce at least R620 000. This flat section of the blue curve (between R200 000 and R620 000) is due to the fact that the probability of generating a daily income between those two values is low (2%). The probability of generating less than R200 000 on any given day is rather high (75%, during the nine low demand season months in a year), whilst the probability of generating more than R620 000 is 23% (approximately corresponding with the 3 months in a year that it is high demand season between June and August, i.e. 25% of the time). This is discussed in greater detail below.

The histogram in Figure 4-31 presents the distribution of daily operational profit on week days (when the pump storage scheme is operational during peak consumption periods, see Figure 3-4). It can be seen that the daily operational profit is wide spread, showing two distinct groupings. The first grouping is narrow, below R0.2 million daily operational profit. This occurs during the low demand season (from September to May each year) when the differential between peak and off-peak tariffs is low (compared to that during the high demand season). The low demand season includes the regular rainy season (usually occurring between October and February each year), meaning that during the rainy season there is enough water in the system for it to operate at capacity for the entire 5 peak hours on a weekday.

The second grouping (above R0.6 million) shows a wide distribution of daily operational profit and this takes place during the high demand season (from June to August each year) when the differential between peak and off-peak tariffs is high. This takes place during the dry winter months, and hence the production is a function of the volume of water available in the system, (which is a function of the cumulative rainfall from the previous rainy seasons), hence the wide spread of the high profit end of the histogram.

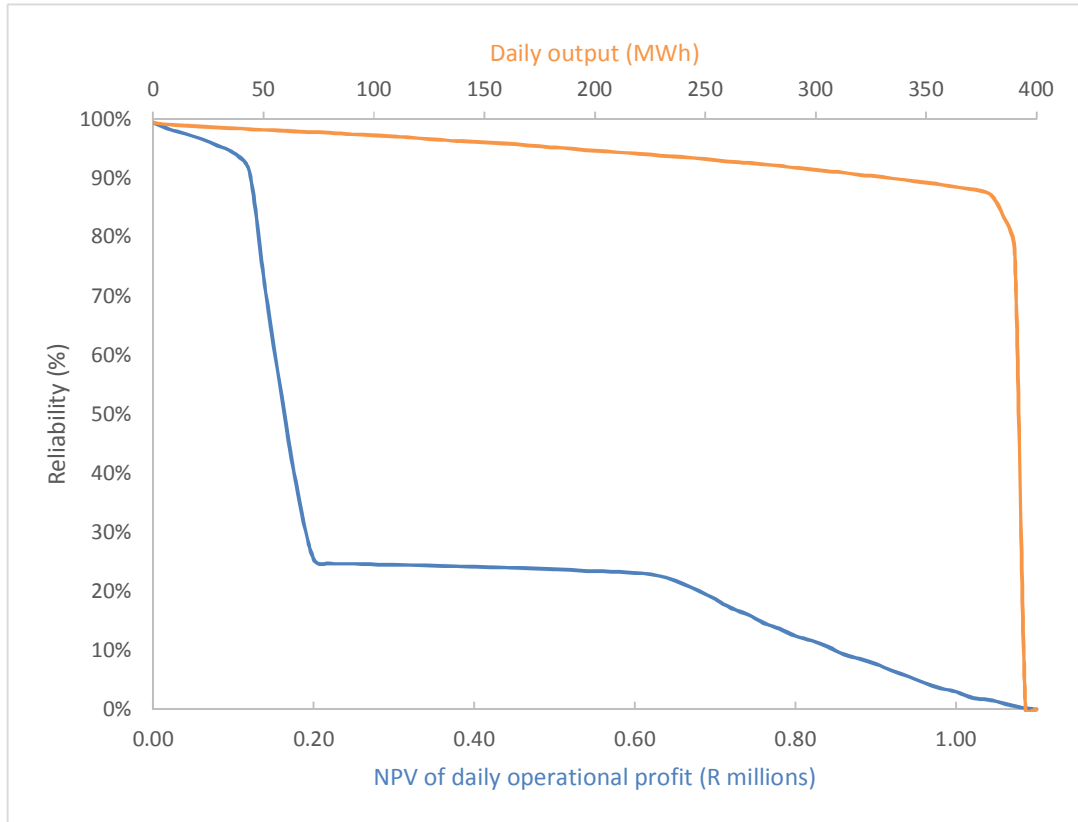


Figure 4-29: Reliability of daily electricity generation and associated daily operational profit

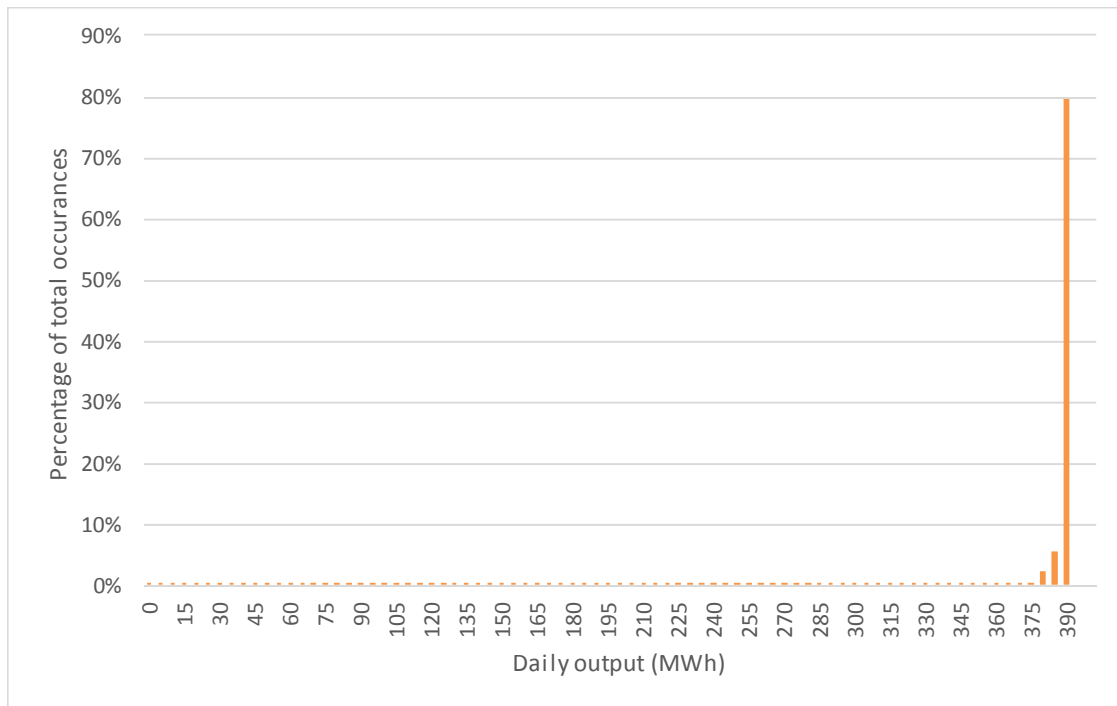


Figure 4-30: Distribution of daily electricity production during the peak hours of week days

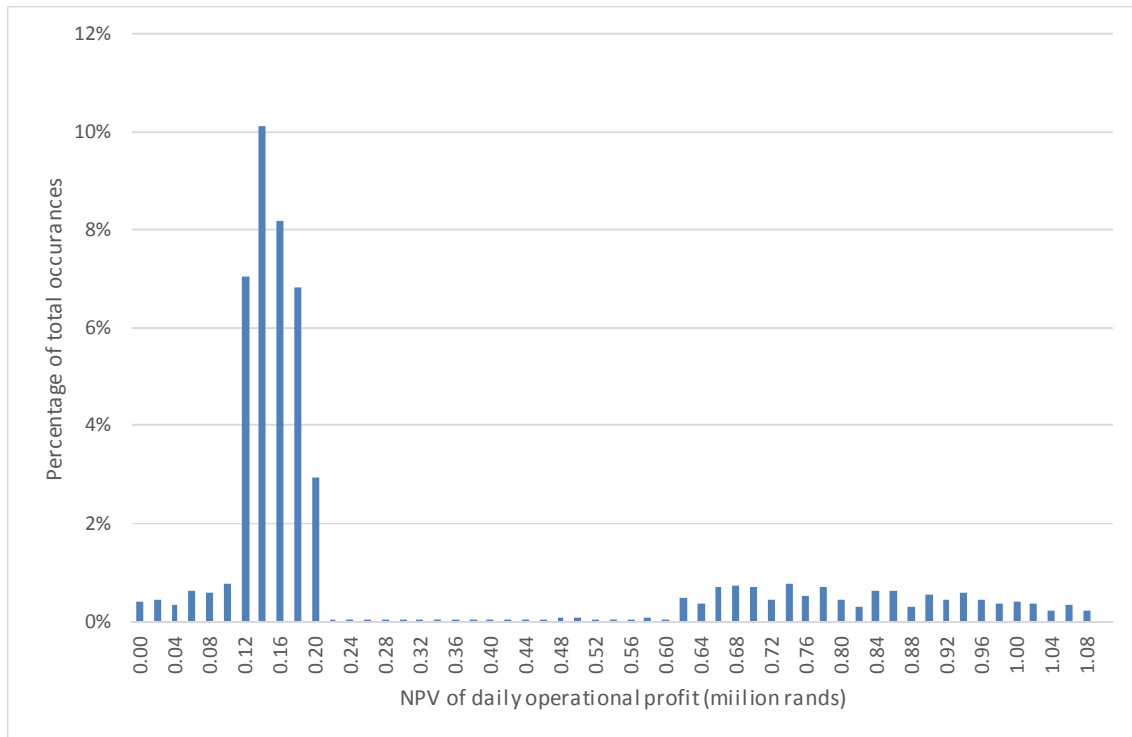


Figure 4-31: Distribution of daily operational profit on week days

#### 4.2.4 Sensitivity analysis results

The sensitivity of the pump storage scheme to a change in release rate was assessed in Section 4.2.2. The following section presents the results of a number of sensitivity analyses conducted on some of the other assumed parameters that may influence the performance (i.e. overall efficiency) and financial feasibility of the pump storage scheme development. Parameters were varied (each within its expected range) to determine the sensitivity of the IRR (over a 50 year lifetime) and overall efficiency of the scheme to a change in the following assumed parameters (whilst keeping all other variables constant):

- Total TSF catchment area
- Flow velocity in the outlet pipe
- Total static head
- Turbine efficiency
- Pump efficiency
- Eskom Megaflex tariff structure
- High demand season release rate

The overall efficiency percentage provides an indication of the conversion of off-peak electricity converted to electricity generated for peak period consumption.

#### 4.2.4.1 Total TSF catchment area

The total TSF catchment area contributing rainfall runoff to the system was assumed to be 1 500 ha in Section 3.6.1.1. The effect on the IRR and overall efficiency due to a change in the total TSF catchment area is shown in Figure 4-32. The red curve shows that the IRR increases with an increase in catchment area simply because a larger catchment area will increase the volume of runoff water available for electricity generation and hence results in a higher IRR. It can be seen that the IRR will exceed the current South African inflation rate of 6.3% if the catchment is larger than 180 ha and will exceed the current prime interest rate of 9.25% if the catchment is larger than 870 ha.

The blue curve shows the size of the catchment area has minimal effect on the overall efficiency of the system (how much electricity is generated from every unit of electricity consumed), with an almost negligible decrease in overall efficiency with an increase in catchment area. This provides a first indication of the feasibility of implementing a similar development on TSFs with smaller catchments. Unless the TSF catchment is larger than 180 ha (and at least 140 m high) it is unlikely that the development of a pump storage scheme after its closure will exceed the current South African inflation.

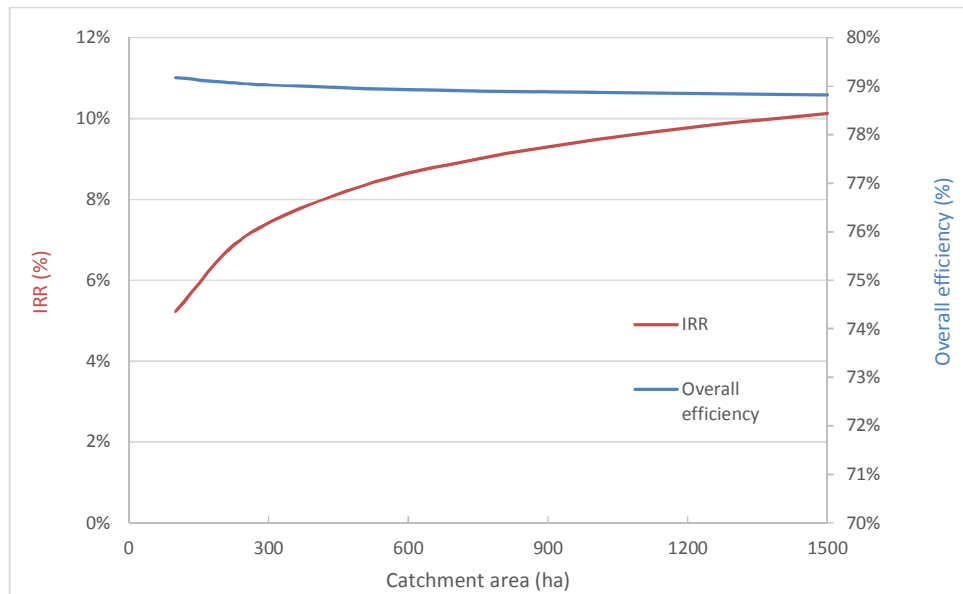


Figure 4-32: Sensitivity of the IRR and overall efficiency to a change in catchment area contributing to rainfall runoff

#### 4.2.4.2 Outlet pipe flow velocity

The flow velocity in outlet pipe (during the release of water to the turbine) was assumed to be 3 m/s in Section 3.6.3, upon recommendation by Van Dijk (2014), in order to minimise friction and local losses in the outlet pipeline. The effect on the IRR and overall system efficiency due to a change in the outlet pipe flow velocity is shown in Figure 4-33. The red curve shows that the IRR decreases with an increase in flow velocity, this is due to an increase in energy (friction and local) losses in the outlet pipe, which results in lower electricity generation and higher electricity consumption during pumping. However, it can still be seen that as long as the flow velocity is kept below 10 m/s, the IRR will exceed both the current inflation rate (of 6.3%) and below 8 m/s to exceed the current prime interest rate of 9.25%.

The blue curve shows the overall efficiency of the system decreases quite drastically when the flow velocity in the outlet pipe is increased. Again, it is due to the lower electricity generation and higher electricity consumption during pumping.

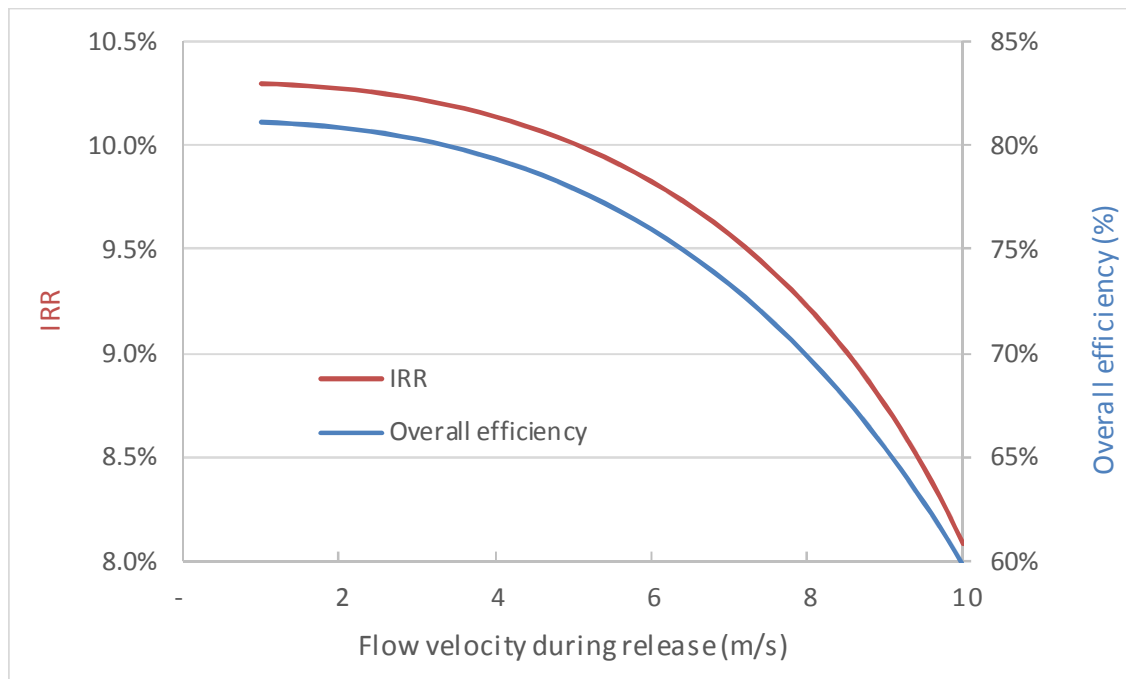


Figure 4-33: Sensitivity of the IRR and overall efficiency to a change in flow velocity during release

#### 4.2.4.3 Total static head

The total static head, i.e. total height of the facility was assumed to be 140 m in Section 3.6.3. The effect that the total height of the facility has on the IRR and overall efficiency is shown in Figure 4-34. The red curve shows that the IRR increases with an increase in TSF height. It can be seen that the IRR will exceed the current inflation rate of 6.3% if the TSF is higher than 40 m and will exceed the current prime interest rate of 9.25% if the TSF is higher than 100 m.

The blue curve shows the overall efficiency of the system increases quite drastically when the height of the TSF increases. This provides a first indication of the feasibility of implementing a similar development on TSFs with a lower final height in excess of 40 m.

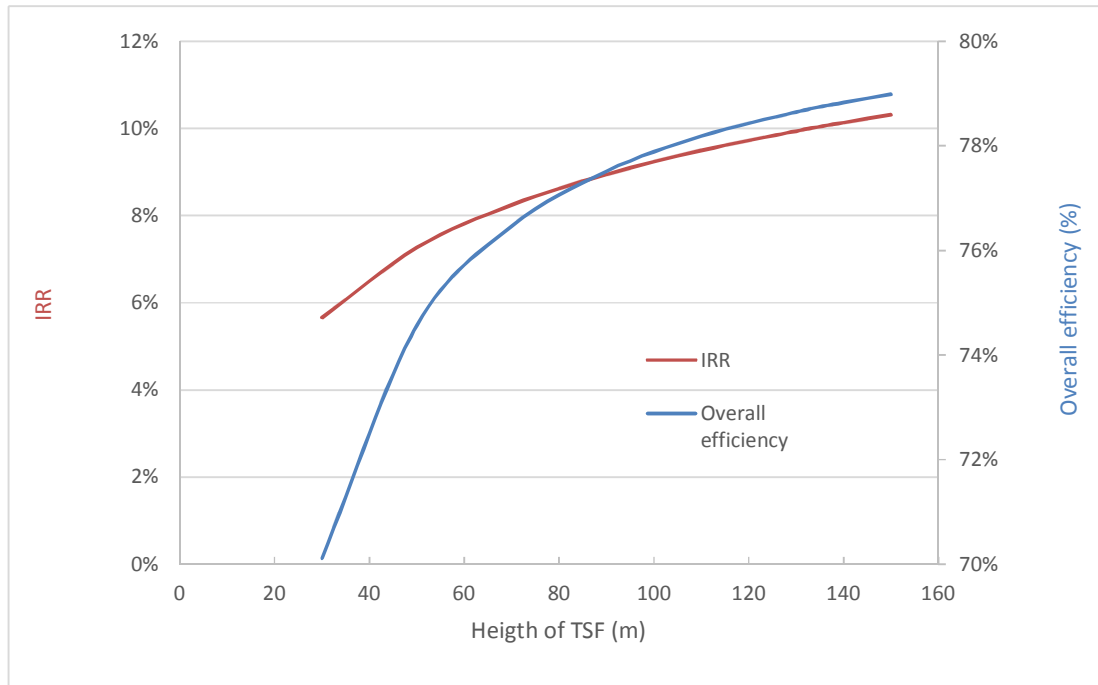


Figure 4-34: Sensitivity of the IRR and overall efficiency to a change in final height of the facility

#### 4.2.4.4 Turbine efficiency

The turbine efficiency was assumed to be 90% in Section 3.6.3. The effect that a potential decrease in turbine efficiency might have on the IRR and overall efficiency is shown in Figure 4-35. The turbine efficiency may be expected to reduce gradually over time due to wear. The red curve shows that the IRR increases with an increase in turbine efficiency. It can be seen that the IRR will exceed the current prime interest rate of 9.25% as long as the turbine has an average efficiency of above 77%.

The blue curve in Figure 4-35 (straight line) shows the overall efficiency of the system increases linearly by 0.89% for every 1.0% increase in turbine efficiency. This is expected due to the fact that the electricity generated ( $E_T$ ) is directly proportional to the efficiency of the turbine ( $\eta_T$ ) ( $E_T \propto \eta_T$ , see Section 2.6.3) and the overall system efficiency is directly proportional to the electricity generated ( $E_T$ ) (see Section 3.6.9). Hence, overall system efficiency has to be directly proportional to the turbine efficiency ( $\eta_T$ ) and therefore the straight blue line.

The non-linearity of the red IRR curve is due to the different tariffs applied by Eskom during the low and high demand seasons respectively.  $\eta_T$  is assumed to be constant throughout the life of the plant,  $E_T \propto \eta_T$ , but the tariff with which  $E_T$  is multiplied to determine the IRR is not a constant, therefore the red IRR curve is not linear.

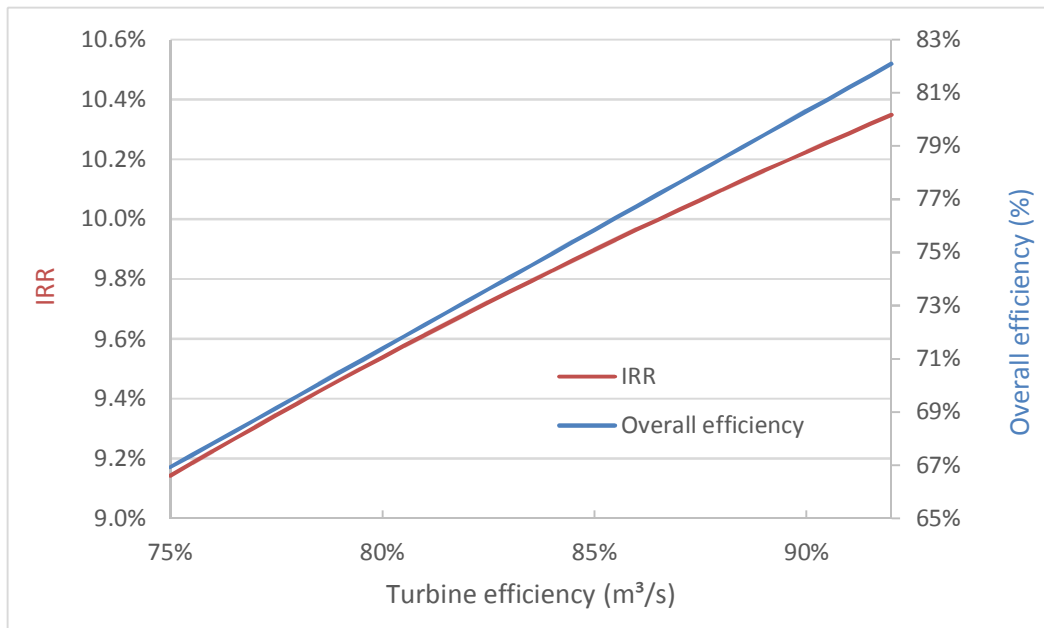


Figure 4-35: Sensitivity of the IRR and overall efficiency to a change in turbine efficiency

#### 4.2.4.5 Pump efficiency

It was assumed in Section 3.6.4 that the pump(s) will be engineered to have an efficiency of at least 90%. The effect that a potential decrease in pump efficiency might have on the IRR and overall efficiency is shown in Figure 4-36. The red curve shows that the IRR increases with an increase in turbine efficiency. It can be seen that the IRR will exceed the current prime interest rate of 9.25% even if the average pump efficiency is as low as 75%.

The blue curve (straight line) shows the overall efficiency of the system increases linearly by 0.87% for every 1.0% increase in pumping efficiency. This is expected due to the fact that the electricity consumed ( $E_p$ ) is indirectly proportional to the efficiency of the pump ( $\eta_p$ ) ( $E_p \propto \frac{1}{\eta_p}$ , see Section 2.6.4) and the overall system efficiency is indirectly proportional to the electricity consumed ( $E_p$ ) (see Section 3.6.9). Hence, overall system efficiency has to be directly proportional to the pump efficiency ( $Overall\ system\ efficiency \propto \frac{1}{E_p} \propto \eta_p$ ) and therefore the straight line.

The non-linearity of the red IRR curve is due to the different tariffs applied by Eskom during the low and high demand seasons respectively.  $\eta_p$  is assumed to be constant throughout the life of the plant,  $E_p \propto \frac{1}{\eta_p}$ , but the tariff with which  $E_p$  is multiplied to determine the IRR is not a constant, therefore the red IRR curve is not linear.

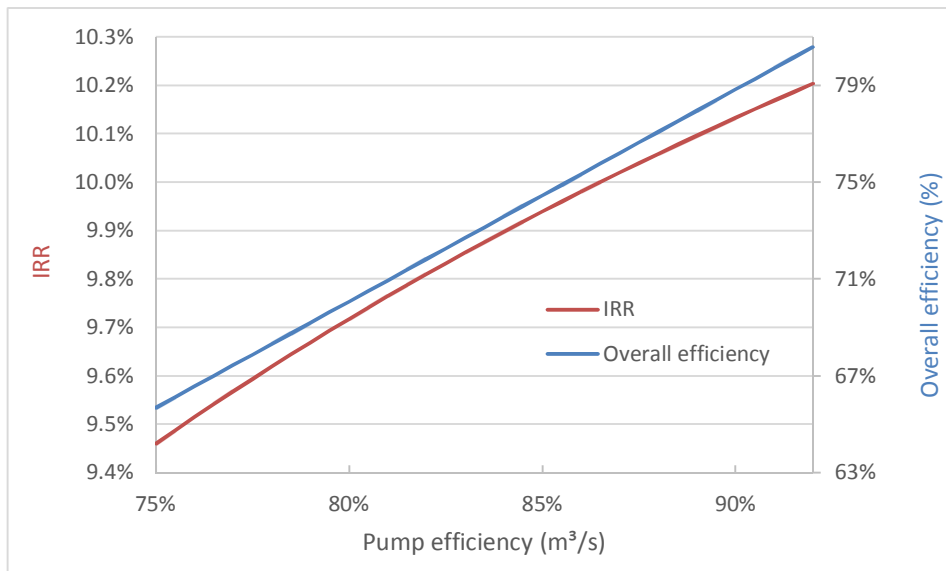


Figure 4-36: Sensitivity of the IRR and overall efficiency to a change in pump efficiency

#### 4.2.4.6 Eskom Megaflex tariff structure

The Eskom Megaflex tariff structure (Eskom, 2014f) illustrated in Figure 3-4 was used throughout this study. The effect that a potential decrease or increase in the differential between the peak and off-peak rates might have on the IRR and overall efficiency is shown in Figure 4-37. The red curve shows that the IRR increases with an increase in the differential. It can be seen that the IRR is negative if the differential is less than 15% of what it is currently. As long as the differential remains at least 50% of what it is currently, the IRR will exceed the current inflation

rate of 6.3%. The IRR of the development will exceed the current prime interest rate of 9.25%, as long as the differential remain above 85% of what it is currently.

The blue curve is shown as a straight horizontal line, which indicates that the overall efficiency is not influenced by a change in the tariff structure, as expected.

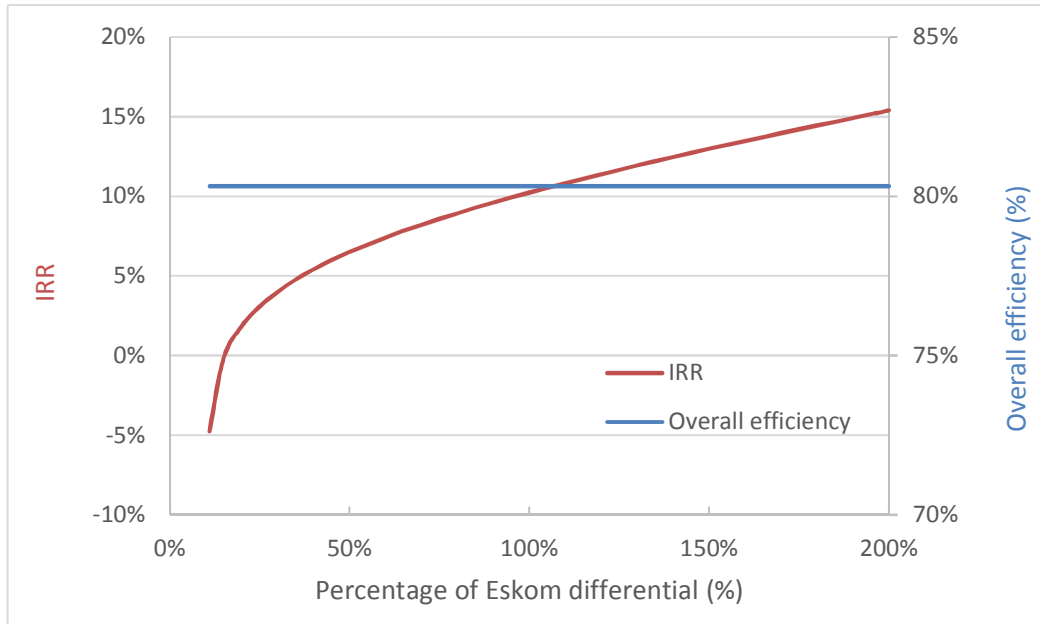


Figure 4-37: Sensitivity of the IRR and overall efficiency to a change in Eskom peak/off-peak tariff differential

#### 4.2.4.7 High demand season release rate

Due to the significant difference between the high and low demand season rates (provided in Figure 3-4), an assessment was done to determine whether the IRR would increase if the release rate ( $Q_T$ ) is increased during the high demand season.

The IRR was calculated for various low demand season release rates ( $Q_T$ ) and increased during the high demand seasons by 50% or 100% ( $1.5 \times Q_T$  and  $2 \times Q_T$  respectively). The results are displayed in Figure 4-38. It can be seen that the purple ( $1 \times Q_T$ ) curve has a higher peak than the green curve ( $2 \times Q_T$ ). The reason for this is that the initial capital investment required for larger release capacity is more than the profit that can be gained from it. Generating more electricity during the high demand season and underutilising the system during the low demand season, results in a lower IRR. Hence it can be concluded that increasing the release rate during the high demand season does not result in any financial benefit.

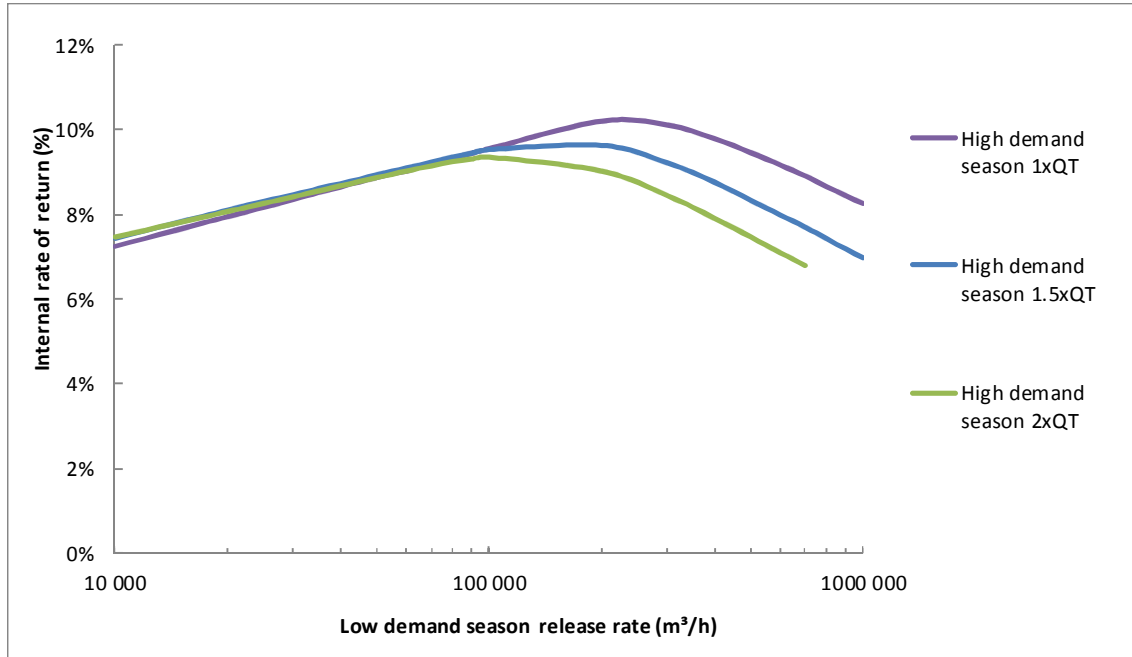


Figure 4-38: Sensitivity of the IRR to change in high demand season release rate

#### 4.2.4.8 Summary of sensitivity analysis for the pump storage scheme

From the above sensitivity analyses the following can be concluded about the IRR of the pump storage scheme:

- TSF catchment area larger than 180 ha will exceed the current inflation rate.
- TSF catchment area larger than 870 ha will exceed the current prime interest rate.
- Flow velocity below 10 m/s it will exceed the current prime interest rate.
- TSF higher than 40 m will exceed the current inflation rate.
- TSF higher than 100 m will exceed the current prime interest rate.
- Turbine efficiency above 77% will exceed the current prime interest rate.
- Pump efficiency above 75% will exceed the current prime interest rate.
- If the Megaflex tariff differential is above 50% of what it is currently, the IRR will exceed the current inflation rate.
- If the Megaflex tariff differential is above 85% of what it is currently, the IRR will exceed the current prime interest rate.
- There is no financial benefit for increasing the release rate during the high demand season.

As mentioned in Section 3.6.9, all sensitivity analyses were *only* done for the “no lining” option, as opposed to the lined TSF option which follows. However, it is deemed that the trends (not necessarily the magnitudes) will be the same for the lined basin option.

#### 4.2.5 Determining the effect of lining the TSF basin

As mentioned in Section 3.6.10, it was identified that by improving the runoff from the catchment and limiting the seepage from the TSF pond, more water will be available for electricity generation. The proposal is to line the TSF basin with an impermeable barrier system, such as high density polyethylene (HDPE).

The water balance simulation and financial analysis were repeated. The volume of water available for power generation in the TSF pond is shown by the red curve in Figure 4-39 if an impermeable lining system is introduced. It can be seen that the pond volume is significantly more than that in Figure 4-26 (represented by the blue graph in Figure 4-39), resulting in significantly larger generation potential. The pond volume (if the basin is lined) varies between about 7 and 20 million cubic meters of water available to generate electricity. Previously (without lining) the pond volume varied between 1 and 6 million cubic meters.

The results of the optimisation of the IRR were plotted in Figure 4-40 and Figure 4-41 on a natural and log scale respectively. It can be seen that the net profit (green curve) peaks at around 5 million m<sup>3</sup>/h (or 1 400 m<sup>3</sup>/s). It can also be seen that the IRR reaches a maximum of 10.14% if the pump storage scheme has a release capacity of 1.4 million m<sup>3</sup>/h (390 m<sup>3</sup>/s). That is a release rate *six* times higher than that of the unlined option. The IRR of 10.14% is only marginally less than the 10.27% calculated for the un-lined option. However, the infrastructure required to accommodate the sheer volume of water to be transported for the lined TSF basin to the lower reservoir (in order to release water at 1.4 million m<sup>3</sup>/h, to achieve an IRR of 10.14%) might deem it impractical.

Table 4-6 provides the details of the pump storage scheme system with a capacity to release 1.4 million m<sup>3</sup> of water per hour.

In order to convey water at such a high rate, large hydraulic structures are required. In fact, to maintain an ideal flow velocity of 3 m/s, a 13 m diameter pipe has to be installed. However, this is not practical and it might be better to split it up into 27 x 2.5 m diameter pipes, each with its own 18 MW turbine. Such a system is considered impractical due to the structural requirements to accommodate the pipes and their respective inlet structures.

Table 4-6: Particulars of a system with a release capacity of 1 400 000 m<sup>3</sup>/h

Parameter	Result
Release capacity of outlet pipes	1 400 000 m <sup>3</sup> /h (optimum at 1 437 181 m <sup>3</sup> /h)
Single “representative” outlet pipe size	13 m (at assumed flow rate of 3m/s)
Generation capacity	478 MW
Electricity generation on a weekday	2 392 MWh (during 5 peak hours)
Total production over 50 year life	28.7 TWh
Required pumping power input	380 MW
Electricity consumption on a weekday	3 041 MWh (during 8 off-peak hours)
Total consumption over 50 year life	36.4 TWh
Overall system efficiency ( $E_T/E_P$ )	78.8%
Required lower reservoir volume	7 820 000 m <sup>3</sup>
Percentage of peak time operating at capacity*	57%
Initial capital investment required	R 9 918 million
Cost of electromechanical equipment ( $C_{EM}$ )	R 2 149 million (22% of total cost)
Cost of civil works equipment ( $C_{CW}$ )	R 2 423 million (25% of total cost)
Cost of lower reservoir construction ( $C_{LR}$ )	R 2 737 million (28% of total cost)
Cost of TSF lining system	R 2 475 million (25% of total cost)
Annual cost of maintenance and operation ( $C_{MO}$ )	R 135 million
NPV of cumulative operational profit	R 23 544 million
NPV of net profit over 50 year project life	R 13 626 million
IRR over 50 year project life	10.14%

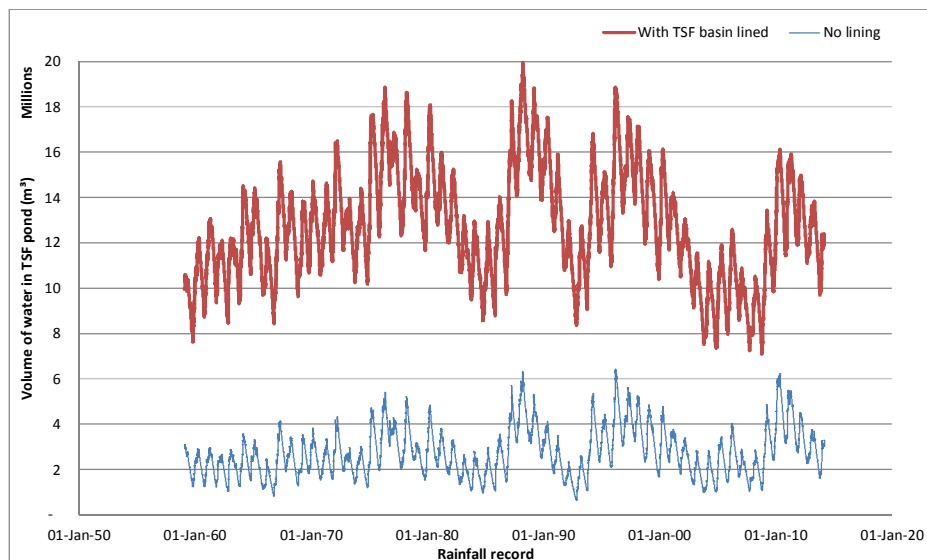


Figure 4-39: Volume of water in the lined TSF pond available for power generation

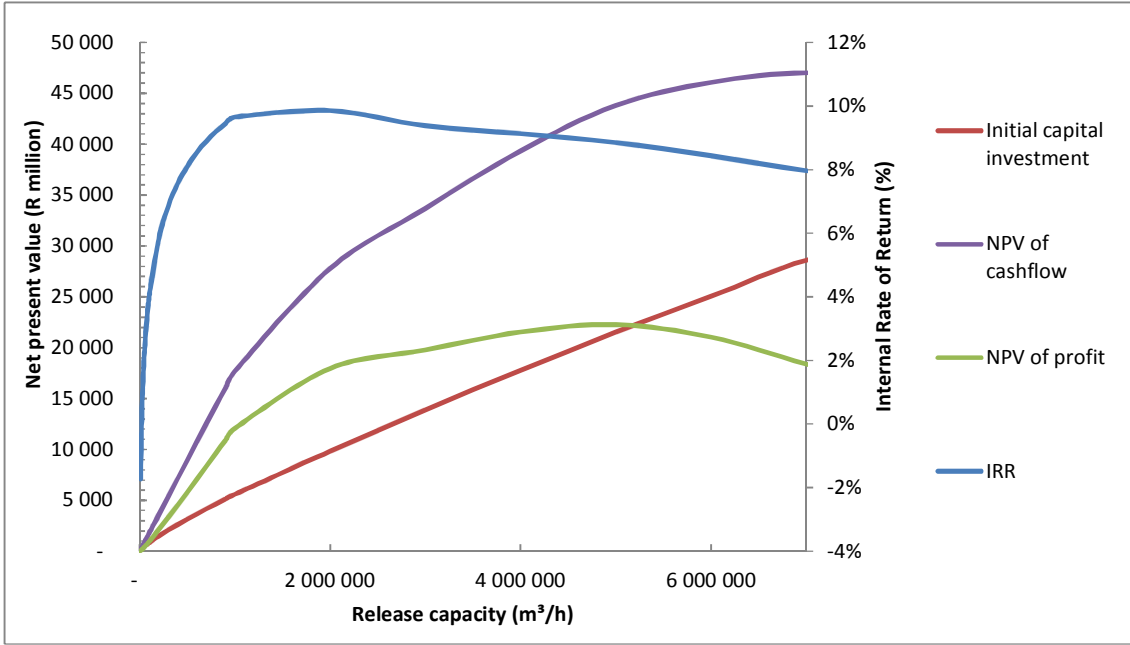


Figure 4-40: Profit and IRR for various release rates when the TSF basin is lined

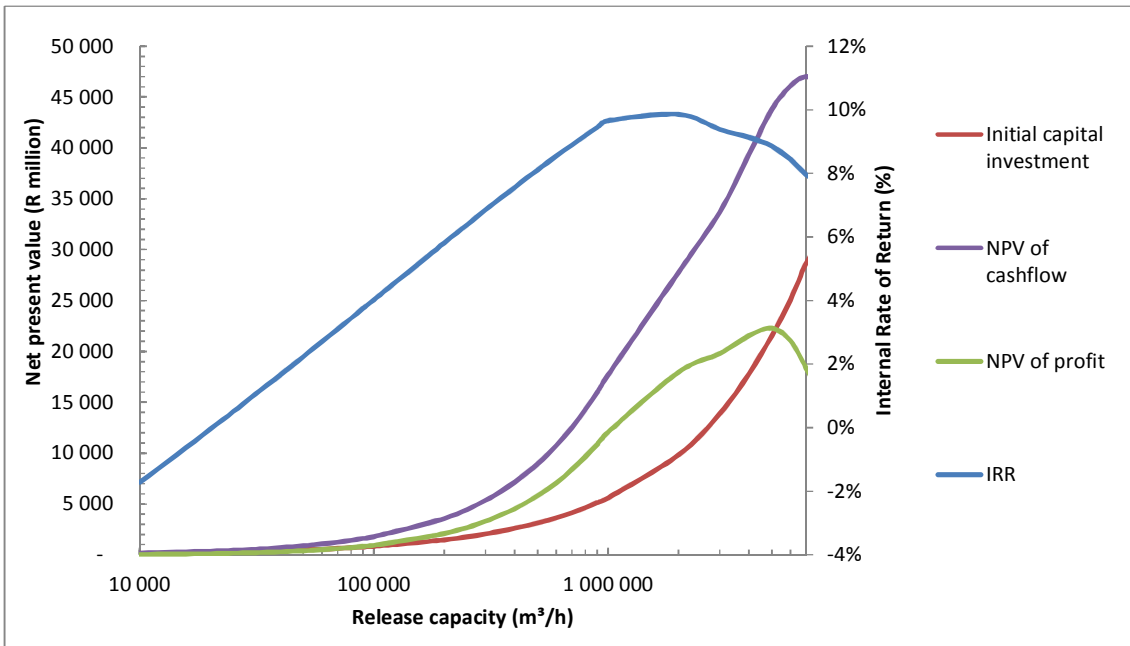


Figure 4-41: Profit and IRR for various release rates when the TSF basin is lined (plotted on a log scale)

### 4.3 COMBINATION OF SOLAR PV AND PUMP STORAGE SCHEME OPTIONS

This section presents the results of the analysis to determine the financial feasibility of combining the solar PV and pump storage scheme options as summarised in Table 3-6. The following results are discussed:

- Combination 1 - The optimal release rate of the pump storage scheme (from a financial feasibility point of view) when used in a combined system if solar PV electricity is used to pump the water from the lower to the top reservoir.
- Combination 2 - The financial feasibility of combining the two options on the same site, while keeping them independent of one another, i.e. selling the PV electricity and not using it to pump water back.
- Combination 3 - The financial feasibility of combining the two options for the system to be completely independent from Eskom, i.e. using the PV electricity to pump water back for later release.

#### 4.3.1 Combination 1 - Optimising the release rate of the pump storage scheme in a combined system

By following the procedure described in Section 3.7.1 the optimal release rate was determined for the pump storage scheme to be equal to 0 m<sup>3</sup>/s, which will generate an IRR of 10.70%. Therefore it was concluded that the highest IRR is achieved when the pump storage scheme is not constructed at all, i.e. only the solar PV plant is constructed. The solar PV plant is predicted to produce 37.7 TWh of electricity over a 50 year life.

This result is to be expected, because the solar PV generated electricity is worth more per kilowatt-hour if it is independently fed into the grid (at standard tariffs during generation, see Figure 3-4), than if it is used to replace the surplus electricity obtained from the grid during the green off-peak periods (see Figure 3-4). It can be concluded that 10.70% is the maximum IRR that can be achieved with either the solar PV or the pump storage scheme option or any combination thereof.

It can therefore be concluded that from a financial feasibility perspective it is best to implement only the solar PV option. Therefore all other results (discussed in Section 4.1.7) applicable to the independent solar PV option are also applicable to this optimal combination, i.e. a system comprising of only a PV system and no pump storage scheme.

However, if practical implications such as a demand for uninterrupted electricity supply are taken into account, it might be necessary to combine the systems regardless of the financial implication,

even though it will result in an IRR of less than 10.70%. Therefore the following section discusses the financial implications of operating both the solar PV and pump storage scheme (as optimised in Sections 4.1 and 4.2) on the same site.

#### **4.3.2 Combination 2 - Financial feasibility of a combined solar PV and pump storage scheme option on the same site**

The methodology described in Section 3.7.2 was followed to determine that an IRR of 10.61% can be achieved if the two systems are operated independently on the same ERGO site (meaning the pump storage scheme uses surplus Eskom electricity to pump the water back to the upper reservoir, as opposed to using the Solar PV power). As mentioned in Section 3.7.2 the result was expected to be lower than 10.70%. It is however, close to the 10.70% (calculated in Section 4.3.1) if only the solar PV option is implemented, as the result is dominated by the difference in generation capacities of the two systems. The solar PV plant is predicted to produce 37.7 TWh or (89%) of the total 42.5 TWh combined plant production over a 50 year life.

A better balance of generation capacity might be possible if the TSF basin is lined with an impermeable barrier system, as discussed in Sections 3.6.10 and 4.2.5. This is due to fact that a lined TSF basin will contain significantly more water than if it is unlined and hence, the water resource available for the pump storage scheme is larger if the basin is lined. However, it will result in other engineering problems, such as:

- Constructing the 27 outlet structures as discussed in Section 4.2.5.
- Constructing the lining system and foundations for the solar PV structures, which will result is considerable additional costs.

#### **4.3.3 Combination 3 - Assessing financial feasibility of a combined solar PV and pump storage scheme to be independent of Eskom's surplus electricity supply**

The methodology described in Section 3.7.3 was followed to determine that the IRR of a system solely relying on solar PV electricity for pumping of water to the upper reservoir is 10.32%. This combination is completely independent of an external electricity source, as it does not rely on surplus electricity available in the grid for pumping water to the upper reservoir.

Table 4-7 below summarises the results and capacities of the combinations investigated.

Table 4-7: Summary of results for combinations investigated

<b>Parameter</b>	<b>Combination 1</b>	<b>Combination 2</b>	<b>Combination 3</b>
Power supply for pumping	PV power / Eskom surplus	Eskom surplus	PV power
<b>Solar PV plant</b>			
Optimum azimuth angle of solar panels	16.3° East of North	16.3° East of North	16.3° East of North
Optimum tilt angle of solar panels	27.6° with the horizontal	27.6° with the horizontal	27.6° with the horizontal
Number of solar panels in plant	1 926 000	1 926 000	1 926 000
Rated solar plant output	471.9 MWp	471.9 MWp	471.9 MWp
Cumulative production over 50 year life	37.7 TWh	37.7 TWh	37.7 TWh
<b>Pump storage scheme</b>			
Release capacity of outlet pipes	Not constructed	230 000 m <sup>3</sup> /h	230 000 m <sup>3</sup> /h
Generation capacity		78.2 MW	78.2 MW
Cumulative production over 50 year life		4.76 TWh	4.76 TWh
Required pumping power input		60.6 MW	60.6 MW
Cumulative consumption over 50 year life		5.93 TWh	5.93 TWh
<b>Combined</b>			
Total generation capacity of system	471.9 MWp	550.1 MWp	550.1 MWp
Cumulative production over 50 year life	37.7 TWh	42.46 TWh	36.53 TWh
Cumulative consumption over 50 year life	-	5.93 TWh	-
Total construction cost	R 10.4 billion	R 12.0 billion	R 12.0 billion
IRR at 50 years	10.70 %	10.61 %	10.32 %

## 5 CONCLUSIONS

This chapter summarises the conclusions of the study.

### 5.1 SOLAR PHOTO VOLTAIC POWER GENERATION

This section presents the conclusions from the results regarding the Solar PV electricity generation plant discussed in Section 4.1. It also presents a number of recommendations for further work.

- The solar resource calculations presented proves to accurately model the NASA (2014) data.
- The optimal IRR over the 50 year life of a solar plant at the ERGO site can be achieved if the azimuth angle of the solar panels are set to 16.3° East of North, as this angle takes advantage of the morning peak tariff bracket imposed by Eskom. The optimal tilt angle of the solar panels should be set to 27.6° with the horizontal to take advantage of the high demand season rates imposed by Eskom during the winter months.
- Based on the combination of the abovementioned optimal azimuth and tilt angles an IRR of 10.7% can be achieved over the 50 year life of a solar plant on top of the ERGO TSF.
- The largest achievable solar PV plant will consist of a total of 1 926 000 Yingli Solar's YGE 60Cell 40mm Series 245 W panels, with an efficiency of 15%. The rated minimum power output is 472 MWp. Under ideal circumstances (clear sky conditions) the plant can reach 500 MW of electricity production.
- The plant's expected electricity generation over the 50 year life period is 37.7TWh. Construction of the plant will cost in the order of R10.4 billion (2015 value).
- It can be concluded that covering the top of the ERGO TSF with solar panels will result in an IRR that will not only exceed the current inflation rate, but also the current prime interest rate of 9.25% and it therefore appears a viable investment.
- The sensitivity analysis results show that the IRR is not significantly influenced by the *expected* change in the panel performance (based on Yingli Solar's YGE 60Cell 40mm Series panels) or the expected degradation rate of the plant's performance assumed beyond the 25 year life of the plant. It also shows that the IRR is not influenced by the available area, which suggests that the project can be implemented in phases and that Solar PV might even be a feasible post closure land use option for smaller facilities across Johannesburg, as long as economy of scale costs apply. The sensitivity analysis shows that if the decrease in solar PV unit cost observed over the last decade continues, the IRR

may significantly increase, making it an even more attractive post closure land use option.

There are, however, a number of constraints:

- The plant only produces electricity when the sun shines, which is not necessarily when the electricity is needed most. Hence, in combination with an energy storage solution such as a pump storage scheme, such a combined system might present an ideal solution.
- For the purpose of the study it was assumed that the plant operates 100% of the daylight time (no maintenance or down time has been taken into account). This should be considered if the concept is further refined.
- The evacuation of the electricity from the site is a possible constraint. The evacuation of power is a function of the extent of the grid network and the availability of infrastructure close to the site. If a 400 MW solar plant is constructed and the nearby substation has less capacity, the costs associated with the upgrade of the substation should form part of the feasibility study. For the purpose of this study it was assumed that, because these facilities are located close to the consumers, the available infrastructure would be sufficient and therefore no additional costs were allocated for upgrading the grid infrastructure. Further work would include assessing various TSFs and the grid infrastructure available in the area to evacuate the electricity to the consumer, as well as liaison with the authorities for the necessary permissions.

## 5.2 PUMP STORAGE SCHEME

This section presents the conclusions from the study of the pump storage scheme discussed in Section 4.2.

- The volume of water stored on the ERGO TSF pond is predicted to vary between about 1 and 6 million cubic meters, which is conceptually available to generate electricity.
- A pump storage scheme can reach a maximum IRR of 10.27% based on a release capacity of 230 000 m<sup>3</sup>/h (63.8 m<sup>3</sup>/s).
- The above assumes a catchment area of 1 500 ha, a static head (final height of TSF) of 140 m, an ideal flow velocity in the outlet pipelines of 3 m/s and constant turbine and pumping efficiencies of 90% respectively.
- The plant will have a generation capacity of 78.2 MW.
- The plant's expected electricity generation over the 50 year life period is 4.76 TWh.
- The plant's expected electricity consumption over the 50 year life period is 5.93 TWh,

- The plant's overall system efficiency is 80.3%, i.e. the plant consumes more electricity than it produces. Therefore it represents a method of electricity storage, not a means of net positive electricity generation.
- Construction of the plant will cost in the order of R1.6 billion, which results in an IRR of 10.27% over 50 years.
- Four 2.6m diameter outlet pipes will have to be constructed, with a suitable inlet structure, each with its own 20 MW turbine.
- The empirically predicted cost of the electromechanical component compares well with the indicative prices obtained from three European turbine manufacturers.
- The development will require a lower reservoir with a capacity of 1 334 000 m<sup>3</sup> with a suitable lining system.
- Converting the ERGO TSF to a pump storage scheme will result in an IRR that will not only exceed the current South African inflation rate, but also the current prime interest rate of 9.25% and may pose an attractive investment. However, technical challenges associated with construction of such infrastructure in and on tailings may be considerable.
- A number of sensitivity analyses (keeping all other variables constant) showed that:
  - With a TSF catchment area larger than 180 ha the IRR will exceed the current inflation rate.
  - With a TSF catchment area larger than 870 ha the IRR will exceed the current prime interest rate.
  - In order to limit friction and secondary losses the flow velocity in the outlet pipe should be limited to below 10 m/s for the IRR to exceed the current prime interest rate. Such flows are however not technically sustainable.
  - The return from a pump storage scheme on a TSF with a height exceeding 40 m will exceed the current inflation rate (assuming a catchment area of at least 1500 ha).
  - The return from a pump storage scheme on a TSF higher than 100 m will exceed the current prime interest rate (assuming a catchment area of at least 1500 ha).
  - With a turbine efficiency above 77% the IRR will exceed the current prime interest rate.
  - Pump efficiency above 75% will exceed the current prime interest rate.
  - If the Megaflex tariff differential between peak and off-peak rates is above 50% of what it is currently, the IRR will exceed the current inflation rate.
  - If the Megaflex tariff differential is above 85% of what it is currently, the IRR will exceed the current prime interest rate.

- There is no financial benefit for increasing the release rate during the high demand season. The reason is that the initial capital investment required for larger release capacity is more than the profit that can be gained from it.
- Lining the TSF catchment with an impermeable barrier increases the volume water in the ERGO TSF available for electricity generation. A lined TSF pond will store between 7 and 20 million cubic meters of water, but at prohibitive additional expense.
- Developing a pump storage scheme on a lined TSF can yield an IRR of 10.14% if it has a release capacity of 1.4 million m<sup>3</sup>/h (390 m<sup>3</sup>/s). However, the infrastructure required to accommodate the sheer volume of water to be transported for the lined TSF basin to the lower reservoir might deem it impractical.
- To maintain the ideal operational flow velocity of 3 m/s, 27 x 2.5 m diameter outlet pipes, each with its own 18MW turbine, will have to be constructed in addition to a 7 820 000 m<sup>3</sup> suitably lined lower reservoir. Such a system is considered impractical due to the structural requirements and costs.

Some of the practical aspects of the development of the pump storage scheme option include:

- A suitable location for the construction of the lower reservoir has not yet been identified at the ERGO TSF. Provisional costs have merely been allowed for the construction of a lower reservoir to serve this purpose, including for earthworks. Alternatively, the TSF adjacent to the ERGO TSF can be used for lower storage reservoir. This will lead to a decrease in generating capacity as the static head will be less than the assumed 140m. A separate study in this regard will have to be conducted.
- Sloughing of the tailings due the rapid draw down of water from the TSF pond may be a possible drawback of this option and it is a challenge that will have to be addressed and properly engineered.
- The possibility of TSF instability due to the storage of such a large volume of water (especially when the TSF is lined) will have to be analysed and was not considered in this study.
- The inlet structure to the outlet pipelines will require careful consideration and engineering to enable such a large volume of water to be taken in by the outlet structure. It is recommended that part of the outlet works be constructed during the operational life of the dam as it gains in height which will considerably save on excavation costs.

### 5.3 COMBINATION OF SOLAR PV AND PUMP STORAGE SCHEME

This section presents the conclusions regarding a combination of Solar PV and pump storage scheme as discussed in Section 4.3. There are distinct advantages and disadvantages to each of the previous two post closure land use options discussed, including:

- The Solar PV system provides clean renewable electricity, between sunrise and sunset. Its most significant disadvantage is that the time of electricity generation does not coincide with the time of peak demand.
- In contrast, the pump storage scheme is a method of electricity storage, which provides electricity whenever it is switched on (provided there is water in the upper reservoir available for release). Its disadvantage is that it consumes more electricity than it produces.
- From the above it can be seen that there is potential benefit if the above options are combined, namely net positive electricity production and electricity at demand.
- From a financial perspective the highest possible IRR of 10.7% is achieved if only the solar PV plant is constructed. No combination of the solar PV and pump storage scheme can exceed that.
- However, due to practical reasons it might be beneficial to combine the solar PV system and the pump storage scheme on the same site.
  - Independently operating the solar PV and pump storage scheme on the same site results in an IRR of 10.61% (reliant on surplus grid electricity for pumping).
  - Operating the pump storage scheme solely dependent on solar PV electricity results in an IRR of 10.32%.
  - Both the above combinations result in IRR values less than the 10.70% of the solar PV option, and both exceeding the 10.27% achieved by implementing only the pump storage scheme.
- All of the above combinations exceed the current inflation rate and the current prime interest rate of 6.3% and 9.25% respectively, as mentioned in Section 3.3.2.

## 5.4 SUMMARY

From the conclusions reached in Section 5.1 to 5.3, it can be concluded that a Solar PV plant on top of the ERGO TSF will achieve the highest possible IRR of 10.70% and a power generation capacity of 471.9 MWp. Developing a pump storage scheme at the ERGO TSF can achieve an IRR of 10.27% and generation capacity of 78.2 MW. Combining the two options independently on the same site will result in an IRR of 10.61% and a combined generation capacity of 550 MW. If the combined system is required to be independent of the surplus electricity available in the grid an IRR of 10.32% and a combined peak generation capacity of 550 MW is achievable.

From a financial and technical perspective it is considered to be most beneficial to implement *only* the solar PV plant on top of the ERGO TSF. Construction of a pump storage scheme on TSF as referred to in this report is considered to be a challenging undertaking and seeing that its generation capacity is only 17% of that of the solar PV facility on the same site, it is probably not the optimal solution for utilisation of a TSF. The construction cost may also exceed that predicted using the empirical relations used in this study as construction on tailings is likely to be more challenging than conventional sites. In contrast, solar panels are light weight and can easily be installed in large numbers on tailings dams associated with little engineering challenges.

It should be noted that the ERGO TSF is one of the largest TSFs in the world, therefore not all studies will be equally feasible, but it provides a positive indication that renewable energy generation provides a feasible post closure land use option for the ERGO TSF.

## 6 LIST OF REFERENCES

Alvarado-Ancienta, C.A. 2009. Estimating E&M powerhouse costs. *Water Power Magazine*.

Barr, D.I.H. 1975. Two additional methods of direct solution of the Colebrook-White function. *Proceedings of Institution of Civil Engineers*, 59, pp. 827.

Blight, G.E. 2007. Wind erosion of tailings dams and mitigation of the dust nuisance. *The Journal of the South African Institute of Mining and Metallurgy*, February 2007, pp 99-107.

Breeze, P. 2005. *Power Generation Technologies* ISBN 978-0-7506-6313-7. Elsevier Ltd.

Butler, H. and Bentel G. M. 2011. Mine relinquishment – processes and learnings. *Mine Closure 2011. Proceedings of the Sixth International Conference on Mine Closure*, Alberta, Canada.

Carter R. A. 2009. Nevada Mine Plans to convert geothermal heat to high voltage. *Alternative Energy Magazine*. <[www.e-mj.com](http://www.e-mj.com)>

Chadwick, A., Morfett, J. and Borthwick, M. 2004. *Hydraulics in civil and environmental engineering*. Fourth Edition. Spon Press. London and New York.

Chamber of Mines of South Africa. 1996. *Guidelines for Environmental Protection Volume 1/1979 (Revised 1983 and 1995). The Engineering Design, Operation and Closure of Metalliferous, Diamond and Coal Residue Deposits*.

Copeland, A. 2014. Do all TSF's leak and need to be lined? Discussion Paper. 5th International Mining and Industrial Waste Management Conference. The Geotechnical and Environmental divisions of the South African Institution of Civil Engineering. Rustenburg, 10 to 12 March 2014.

CSIR. 2005. *Guidelines for human Settlement Planning and Design, Volume 2*. Compiled under the patronage of the Department of Housing by CSIR Building and Construction Technology. ISBN 0-7988-5498-7

Dailymail. 2014. Watch world's largest solar power plant built – Huge farm generates energy 160 000 homes using nine million panels <<http://www.dailymail.co.uk/sciencetech/article-2853208/Watch-world-s-largest-solar-farm-generates-energy-160-000-homes-using-nine-million-panels.html>> 30 December 2014

Department of Mineral Resources. 2013. Media Release Minerals Resources Minister urges partnership with West Rand Community on illegal mining. Department of Mineral Resources, Republic of South Africa, 26 September 2013.

Department of Water and Sanitation. 2012. Water Resource Planning System Series. Feasibility for a Long term solution to address the Acid Mine Drainage associated with the East, Central and West Rand Underground Mining Basins. Report No.5.2.Assessment of the water quantity and quality of the Witwatersrand Mine Voids. Formerly known as Department of Water Affairs.

Department of Water and Sanitation. 2014. Approved Domestic and Industrial – Raw water tariffs 2014/15 < <https://www.dwaf.gov.za/Projects/WARMS/Revenue/WRI%20D&I.pdf>>. Formerly known as Department of Water Affairs.

Department of Water and Sanitation. 1998. Minimum Requirements for Waste Disposal by Landfill. Second Edition. ISBN 0620-22993-4. Formerly known as Department of Water Affairs.

Department of Water and Sanitation. 2007. Free basic water Implementation Strategy 2007: Consolidating and maintaining Version 4, April 2007. Formerly known as Department of Water Affairs.

Dames, B. 2014. Eskom CEO presentation titled “State of the Power System Quarterly Update ‘Pre-Winter’”, presented by Brian Dames.

Ekurhuleni Metropolitan Municipality. 2014. IDP, Budget and SDBIP 2014/15 – 2016/17 Tariff Schedules

Eskom. 2011. Eskom’s generation plant mix COP 17. Produced by Generation Communication GX 0001 Revision 12 Source: Eskom Holdings Limited Integrated Report 2011 <[www.eskom.co.za](http://www.eskom.co.za)>

Eskom. 2013a. Concentrating Solar Power (CSP) Produced by: Generation Communication RW 0003 Revision 4. <[www.eskom.co.za](http://www.eskom.co.za)>

Eskom. 2013b. Eskom and Agence Française de Développement committed to sign a €100 million loan agreement for the funding of the 100 MW concentrating solar power plant. Eskom media statement. <[www.eskom.co.za](http://www.eskom.co.za)>

Eskom. 2013c. Ingula Pumped Storage Scheme. Corporate Affairs Division: Generation Communication HY 0003 Revision 8, 2013. <[www.eskom.co.za](http://www.eskom.co.za)>

Eskom. 2013d. Klipheuwel wind energy facility. Produced by: Generation Communication RW 0002 Revision 8. <[www.eskom.co.za](http://www.eskom.co.za)>

Eskom. 2013e. Solar Energy – Photovoltaic Solar Power Generation. Produced by: Letabo Visitors Centre. Generation Stakeholder Management and Communication. Generation Communication RW 0004 Revision 4. <[www.eskom.co.za](http://www.eskom.co.za)>

- Eskom, 2013f. Solar water heating rebate programme. COP17 Fact sheet. <[www.eskom.co.za](http://www.eskom.co.za)>
- Eskom. 2014a. Base and Peak Load Electricity. Produced by: Generation Communication GX 0003 Revision 9. <[www.eskom.co.za](http://www.eskom.co.za)>
- Eskom. 2014b. Coal in South Africa. Produced by: Generation Communication CO 0007 Revision 12. <[www.eskom.co.za](http://www.eskom.co.za)>
- Eskom. 2014c. Company information. <[http://www.eskom.co.za/OurCompany/Company\\_Information/Pages/Company\\_Information.aspx](http://www.eskom.co.za/OurCompany/Company_Information/Pages/Company_Information.aspx)>
- Eskom. 2014d. Hydro Electricity in South Africa: Generation Communication HY 0006 Revision 3, 2014. <[www.eskom.co.za](http://www.eskom.co.za)>
- Eskom. 2014e. Pumped Storage Hydroelectric Schemes and Water Transfer. Generation Communication HY 0001 Revision 6, 2014. <[www.eskom.co.za](http://www.eskom.co.za)>
- Eskom. 2014f. Schedule of Standard Prices. <[www.eskom.co.za/tariffs](http://www.eskom.co.za/tariffs)>
- Fraser Alexander Tailings Pty Ltd. 2014. Cone penetrometer testing. Brakpan Tailings Dam, South Africa. Project Management International. Ref. 14-034-PMI-RPT REV A.
- Fritz Wagener and Associates. 2013. Water Balance Report for Conventional Deposition at Mispah Tailings Complex. Vaal River Operations. Report No.: FWA 01/13/305.
- Global-Hydro. 2014. Email correspondence with Peter Falkner, including an offer for Francis turbines from Global Hydro, a turbine manufacturer in Austria.
- GreentechMedia. 2014. 550 Megawatts AC to be exact. <<http://www.greentechmedia.com/articles/read/550-megawatt-AC-to-be-exact>> 30 December 2014
- Gulde C., Wagner A., Koch E., De Boer K. and Martin P. 2011. Brown to green – developing a solar project and cover study on a mine tailings facility. Mine Closure 2011.
- Handley, J.R.F. 2004. Historic Overview of the Witwatersrand Goldfields. Handley, Howick.
- Jones, G.M., Bosserman II, B.E., Sanks, R.L. and Tchobanoglous, G. 2008. Pumping Station Design. Revised Third Edition. Butterworth-Heinemann ISBN 9781856175135
- Kearney, L. 2012. Mining and minerals in South Africa. Brand South Africa, viewed on 11 June 2014. <[www.southafrica.info/business/economy/sectors/mining.htm](http://www.southafrica.info/business/economy/sectors/mining.htm)>
- Kleynhans, L. 2014. Personal communication with Mr. Louis Kleynhans, a horticultural expert for DRD who is responsible for the rehabilitation of their remined sites.

Masters, G.M. 2004. Renewable and efficient electric power systems. John Wiley and Sons Inc. Publication. ISBN 0-471-28060-7

Midgley, D.C., Pitman, W.V. and Middleton, B.J. 1995. Surface Water Resources of South Africa 1990 (WR90), Volume 2

NASA. 2014. Surface meteorology and Solar Energy - A renewable energy resource web site (release 6.0) sponsored by NASA's Applied Science Program in the Science Mission Directorate and developed by POWER: Prediction of Worldwide Energy Resource Project. 22 March 2014, < <https://eosweb.larc.nasa.gov/sse/>>.

National Renewable Energy Laboratory. 2014. Best Research-Cell Efficiencies. <[http://www.nrel.gov/ncpv/images/efficiency\\_chart.jpg](http://www.nrel.gov/ncpv/images/efficiency_chart.jpg)>

PBA International SA. 2011, Mispah Conversion Water balance. Hydrological assessment addendum report Rev 1. May 2011 deposition scenario and pump assessment.

PV Magazine, 2014. World's largest solar plant in operation <[http://www.m.pv-magazine.com/news/details/beitrag/worlds-largest-solar-plant-in-operation\\_100017288](http://www.m.pv-magazine.com/news/details/beitrag/worlds-largest-solar-plant-in-operation_100017288)> 30 December 2014

South African National Roads Agency Limited. 2007. Drainage Manual 5th Edition.

South African Reserve Bank. 2014. <[www.resbank.co.za/Research/Rates/Pages/SelectedHistoricalExchangeAndInterestRates.aspx](http://www.resbank.co.za/Research/Rates/Pages/SelectedHistoricalExchangeAndInterestRates.aspx)> Accessed on 18 December 2014.

South African Weather Service. 2014. Weather data provided for research study.

Saini, R. and Singal, S. 2008. Cost analysis of low head dam-toe small hydropower plants based on number of generating units. Energy for Sustainable Development, Volume 12, Issue 3.

SolarEff. 2014. Email correspondence and personal conversations with Mr. Jaco Botha and Mr. Coen Fourie, representatives of SolarEff, a solar energy equipment supplier.

South African Government News Agency. 2009. Nersa announces renewable energy feed-in tariffs. <[www.sanews.gov.za/south-africa/nersa-announces-renewable-energy-feed-tariffs](http://www.sanews.gov.za/south-africa/nersa-announces-renewable-energy-feed-tariffs)>

Statistics South Africa. 2014. Consumer Price Index July 2014, Statistical release P0141

Statistics South Africa. 2011. <<http://census2011.adrianfrith.com/place/797>>

Trading Economics. 2014. <<http://www.tradingeconomics.com/south-africa/inflation-cpi>>

Valiantzas, J. D. 2013. Simplified forms for the standardized FoA-56 Penman-Monteith reference evapotranspiration using limited weather data, Journal of Hydrology 505.

- Van Dijk, M. 2014. Personal communication regarding the pump storage scheme concept.
- Van Eeden, S.J., Jacobsz, S.W., Rust, E. and Rust, M. 2014. Feasibility of a pump storage scheme development on a dormant Tailings Storage Facility. Proceeding of Hydro 2014 Conference, Cernobbio, Italy, 13 to 15 October 2014.
- Van Vuuren, S.J., Blersch, C.L. and Van Dijk, M. 2011. Modelling the feasibility of retrofitting hydropower to existing South African dams. Water SA Vol. 37 No. 5 WRC 40-year Celebration Special Edition.
- Van Wyk, S. J., Hattingh, J. and Human, C. 2014. Scientific Dust Management on a Tailings Storage Facility: A Case Study. 5th International Mining and Industrial Waste Management Conference. The Geotechnical and Environmental divisions of the South African Institution of Civil Engineering. Rustenburg, 10 to 12 March 2014.
- Voith. 2014. Email correspondence with Hannes Hornung, including an indicative cost estimate for a pump-turbines from Voith, a global turbine supplier.
- Wasserkraft. 2014. Email correspondence with Gunther Scharrer, including an offer for Francis turbines from Wasserkraft, a turbine manufacturer in Austria.
- Winde, F. and Stoch, E.J. 2010. Threats and opportunities for post-closure development in dolomitic gold mining areas of the West Rand and Far West Rand (South Africa) – A Hydraulic view Part 1: Mining legacy and future threats. Water SA Vol. 36 1 January 2010.
- Whitbread-Abrutat, P.H. and Coppin N. J. 2011. Exploring alternative energy options for mine sites. Mine Closure 2011. Proceedings of the Sixth International Conference on Mine Closure, Alberta, Canada.
- Yingli Solar. 2012. YGE 60 Cell 40mm series product brochure. DS\_YGE60Cell-29b\_40mm\_EU\_EN\_201211\_v02.20. <yinglisolar.com>
- Zweibel, K. 1990. Harnessing Solar Power. The Photovoltaics Challenge. Plenum Press, New York and London. ISBN 0-306-43564-0

**APPENDIX A – SUMMARY OF WEATHER DATA**

## SUMMARY OF WEATHER DATA USED

As mentioned in Section 3.6.1, the determination of the water resource available for power generation with a pump storage scheme is a function of the weather data.

Weather data was kindly provided with compliments by the South African Weather Service (SAWS, 2014) for research purposes. The following weather data was received.

Various weather stations surrounding the ERGO TSF were selected. Including, the Johannesburg International airport (also known as the Oliver Tambo International Airport), Nigel, Springs and Vereeniging weather stations. Table A-1 summarises the length of record that was obtained from the SAWS (2014). The satellite image in Figure A-1 shows the locations of the respective weather stations relative to the ERGO TSF site being investigated. It can be seen that the Nigel and Springs sites are located the closest to the ERGO TSF, approximately 16 km, and would therefore provide the most representative data. The Nigel weather station only records rainfall and the Springs station has a significantly shorter record than that available at ORTIA. Hence the Airport site data was predominantly used. The Vereeniging station was included to have weather stations all around the site.

Table A-1: Weather data (SAWS, 2014)

Weather station	ORTIA	Nigel	Springs	Vereeniging
Weather record available since	1956	1989	1993	1991
Length of record (years)	58	25	21	23
Maximum Temperature				
Maximum recorded temperature (°C)	35.4		37.4	36.8
Average maximum daily temperature (°C)	22.1		23.5	24.6
Minimum temperature				
Minimum recorded temperature (°C)	-8.2		-10.1	-8.4
Average minimum daily temperature (°C)	10.1		8.4	9.1
Rainfall				
Highest 24hour rainfall event recorded (mm)	188	67	129	106

Mean Annual Precipitation (mm)	697	513	581	736
Wind				
Highest recorded wind speed (m/s)	16.0		11.1	17.9
Average daily wind speed (m/s)	3.3		1.4	2.3
Humidity				
Average humidity (%)	62.7		78.3	68.4

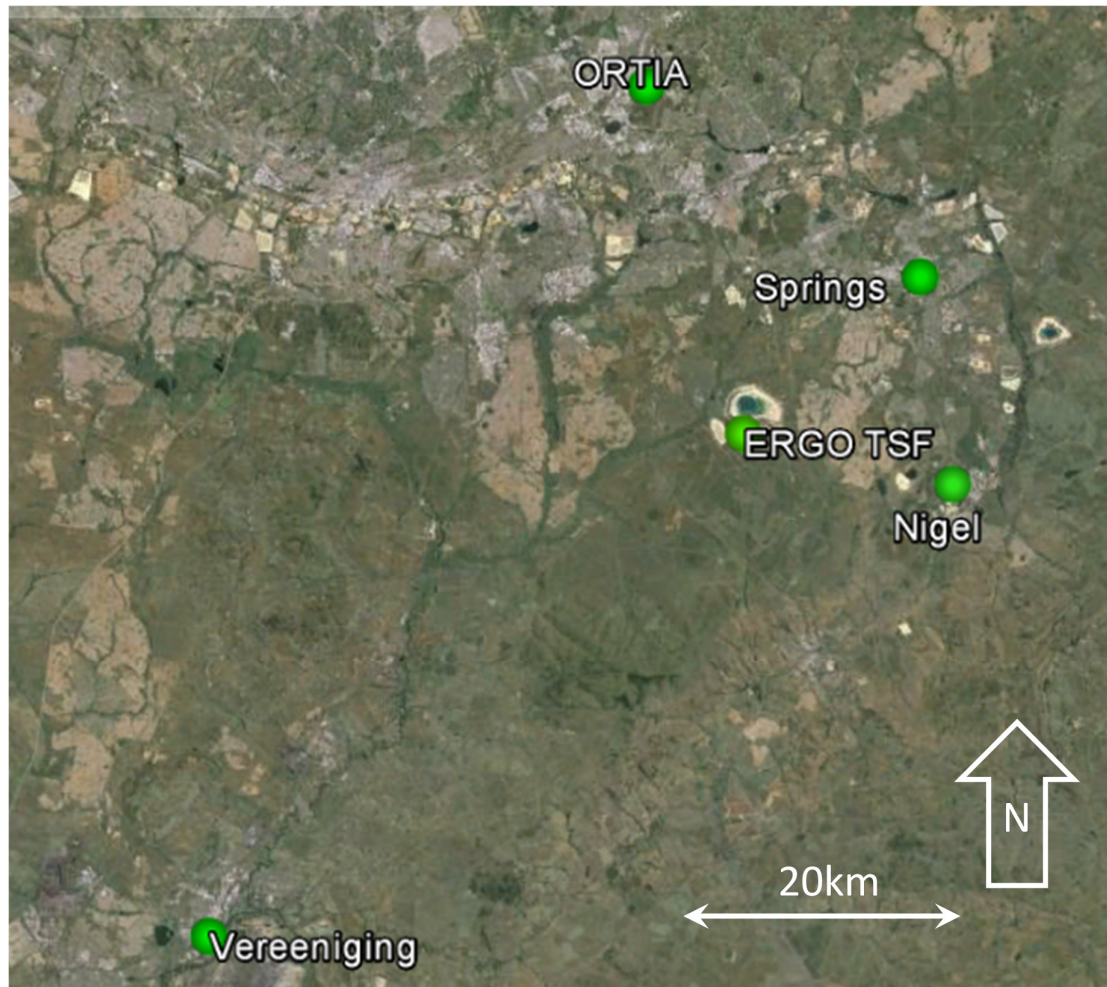


Figure A-6-1: Locations of the respective weather stations relative to the ERGO TSF (Google Earth Copyright Acknowledged)